IDENTIFICATION OF NOVEL REGULATORS OF NUMB ALTERNATIVE SPLICING

by

Dushyandi Rajendran

A thesis submitted in conformity with the requirements
for the degree of Master of Science
Department of Medical Biophysics
University of Toronto

Identification of Novel Regulators of Numb Alternative Splicing

Dushyandi Rajendran

Master of Science
Department of Medical Biophysics
University of Toronto
2014

Alternative splicing (AS) is a post-transcriptional mechanism resulting in the production of multiple mRNA and protein isoforms from a single gene. The endocytic adaptor protein Numb undergoes AS of exon 9 (E9) to produce two developmentally regulated isoforms: E9-included products are expressed in progenitors while E9-excluded products are expressed in differentiated cells. A global analysis of AS events in multiple cancers identified a shift in Numb transcript and protein expression from the E9-excluded to the E9-included isoform, suggesting that misregulation of the mechanisms that control E9 inclusion may play a role in tumorigenesis. Here we describe a potential mechanism by which the splicing regulators PTBP1 and ASF/SF2 and the MAPK/ERK signalling pathway contribute to cancer development by regulating the observed Numb AS switch. We also found evidence of a functional role for the Numb AS switch in cancer, through alterations in Notch signalling target gene expression due to MAPK/ERK suppression.

ACKNOWLEDGEMENTS

Firstly I would like to sincerely thank my supervisor, Dr. Jane McGlade, for taking a chance on me and taking me into her lab. Her mentorship, guidance and support was extremely valuable to me during my time as a graduate student, and her never-ending patience with me in both good times and bad is very much appreciated.

I would also like to thank the members of my committee, Dr. Annie Huang and Dr. Dwayne Barber, who were extremely supportive about my work on this project. My committee meetings were always true tests in determining my ability to think like a scientist.

I would like to thank all members of the McGlade lab, who supported me through my experiments and lent an ear whenever I needed someone to talk to. I will miss hearing all the funny stories you have shared with me over the years.

I also wish to acknowledge the labs of Dr. Huang, Dr. Gelareh Zadeh, Dr. Vuk Stambolic, and Dr. Jim Woodgett, as well as members of the SickKids Brain Tumour Research Centre for assistance with experiments and reagents.

Finally, I wish to express my thanks to my friends both in and out of grad school, as well as my family, who have acted as a wonderful support team outside of the lab and kept me relatively sane.

TABLE OF CONTENTS

CHAPTER 3: RESULTS

CHAPTER 4: DISCUSSION AND FUTURE DIRECTIONS

LIST OF TABLES

LIST OF FIGURES

LIST OF SYMBOLS AND ABBREVIATIONS

a.a.	amino acid
ActD	Actinomycin D
aPKC	atypical protein kinase C
APP	amyloid precursor protein
AS	alternative splicing
ASF/SF2	serine/arginine-rich splicing factor 1
atRA	all-trans retinoic acid
BAC	bacterial artificial chromosome
bp	base pair
C-terminal	carboxyl-terminal
Chr	chromosome
DNA	deoxyribonucleic acid
DPF	aspartic acid-proline-phenylalanine
E9	Exon 9 (of Numb gene)
EGFR	epidermal growth factor receptor
EMT	epithelial-mesenchymal transition
ESE	exonic splicing enhancer
ESS	exonic splicing silencer
GTPase	guanosine triphosphate hydrolase enzyme
hnRNP	heterogeneous nuclear ribonucleoprotein
HRAS	GTPase transforming protein p21
IgG	immunoglobulin G
ISE	intronic splicing enhancer
ISS	intronic splicing suppressor
kbp	kilo-base pair
kDa	kilodalton
KH	K homology domain
MAPK/ERK	mitogen-activated protein kinase/extracellular signal-regulated kinase
MEK	MAP kinse kinase
MEKK	MAP kinase kinase kinase
mRNA	messenger mRNA
Numb+E9	Numb mRNA transcript including exon 9
NumbΔE9	Numb mRNA transcript excluding exon 9

N-terminal	amino-terminal
NPF	asaparagine-proline-phenylalanine
NSCLC	non-small cell lung cancer
nt	nucleotide
p72	denotes molecular weight of a protein, in this case 72 kilodaltons (kDa)
Par	partitioning defective
PCR	polymerase chain reaction
PI3K	phosphoinositide 3-kinase
PIP3	phosphatidylinositol-3,4,5-triphosphate
pre-mRNA	precursor-mRNA
PRR	proline-rich region
PTBP1	polypyrimidine tract-binding protein
PTEN	phosphate and tensin homolog
PTB	phosphotyrosine-binding
qPCR	quantitative polymerase chain reaction
RIP	RNA-protein immunoprecipitation
RNA	ribonucleic acid
RNP	ribonucleoprotein
RRM	RNP-type RNA-recognition motif
RT	reverse transcription
RTK	receptor tyrosine kinase
Sam68	Src-associated in mitosis 68kDa protein
SF1	splicing factor 1
SH2	src homology 2 domain
SH3	src homology 3 domain
shRNA	short hairpin RNA
siRNA	small interfering RNA
snRNP	small nuclear RNP
SR	serine-arginine rich protein
STAR	signal transduction activator of RNA
UTR	untranslated region
Wnt	Wingless-related integration site

CHAPTER 1: INTRODUCTION

1.1 Overview of RNA Processing

In order to survive, cells must maintain a level of homeostasis between major functions of proliferation, differentiation, and apoptosis (Blaustein, Pelisch, & Srebrow, 2007). An inability to do so impairs cellular function and results in the progression of diseases such as cancer (Bissell & Labarge, 2005; Blaustein et al., 2007). Homeostasis is maintained through complex regulatory networks dependent on specific gene and protein expression patterns. In the past, these expression patterns were thought to arise from a model known as the "Central Dogma", which describes the flow of information from DNA to protein via unstable protein-coding RNAs, known as messenger RNAs (mRNAs) (Ward & Cooper, 2010). However, recent evidence has shown that this model is fairly simplistic. In fact, this model can now only be seen as a "framework" on which complex networks of mechanisms that regulate transcription and translation are layered (Ward & Cooper, 2010). Post-transcriptional regulation of gene expression has been of particular interest in recent years due to extensive evidence pointing towards misregulation in cancer.

1.1.1. *Splicing and Processing of Precursor Messenger RNA*

RNA is formed in the nucleus through a process known as transcription, which involves the conversion of a DNA sequence to an RNA sequence with the assistance of transcription factors and enzymes. The product that is immediately formed from this conversion is known as a precursor-mRNA (pre-mRNA). The pre-mRNA undergoes processing to form a mature mRNA, which is then exported to the cytoplasm and translated using ribosomes to produce a protein (Z. Zhang & Stamm, 2011). There are two major events that take place during processing of pre-mRNA: (1) the addition of a 5' cap and an

approximately 200 nucleotide poly-adenosine (poly-A) tail to the 3' end of the transcription termination site (Ward & Cooper, 2010), and (2) splicing, which involves both the selective removal and degradation of non-coding sequences known as introns (Z. Zhang & Stamm, 2011), and the joining together of coding regions known as exons (Figure 1.1A, above) (Blaustein et al., 2007; Z. Zhang & Stamm, 2011). Splicing of the pre-mRNA involves a protein complex known as the spliceosome (Ward & Cooper, 2010), and RNA-binding proteins that complex with RNAs to form ribonucleotide protein (RNP) complexes (Cooper, Wan, & Dreyfuss, 2009). Mutations that alter pre-mRNA sequences or RNP formation have both been shown to promote disease (Cooper et al., 2009).

1.1.2 *Mechanism of Constitutive Splicing*

The spliceosome is a large protein complex that consists of five small nuclear RNPs (snRNPS) and additional proteins that assist with recognizing and binding to consensus sequences known as splice sites, within the pre-mRNA where splicing required for forming the mature mRNA occurs (Chen & Manley, 2009). These sequences include: (1) a 5' donor splice site that is immediately downstream of the 5' flanking exon, and starts with the sequence “GU” in the intron, (2) a 3' acceptor site that is immediately upstream of the 3' flanking exon, and ends with the sequence “AG” in the intron, (3) a polypyrimidine tract which can be found near the acceptor site upstream of the “AG” sequence in the intron, and (4) a 7-nucleotide branch point sequence within the intron to be spliced (Figure 1.1A, below) (Blaustein et al., 2007). Spliceosome assembly occurs when the snRNP U1 binds to the 5' splice site and splicing factor 1 (SF1) binds to the branch point, forming an *E' complex*. Binding of the snRNP U2 auxiliary factor (U2AF, consisting of a heterodimer of U2AF65 and U2AF35) to the 3' splicing site forms the *E complex*. Replacement of SF1 with the snRNP U2 on the branch point forms the ATP-dependent prespliceosome *A complex*.

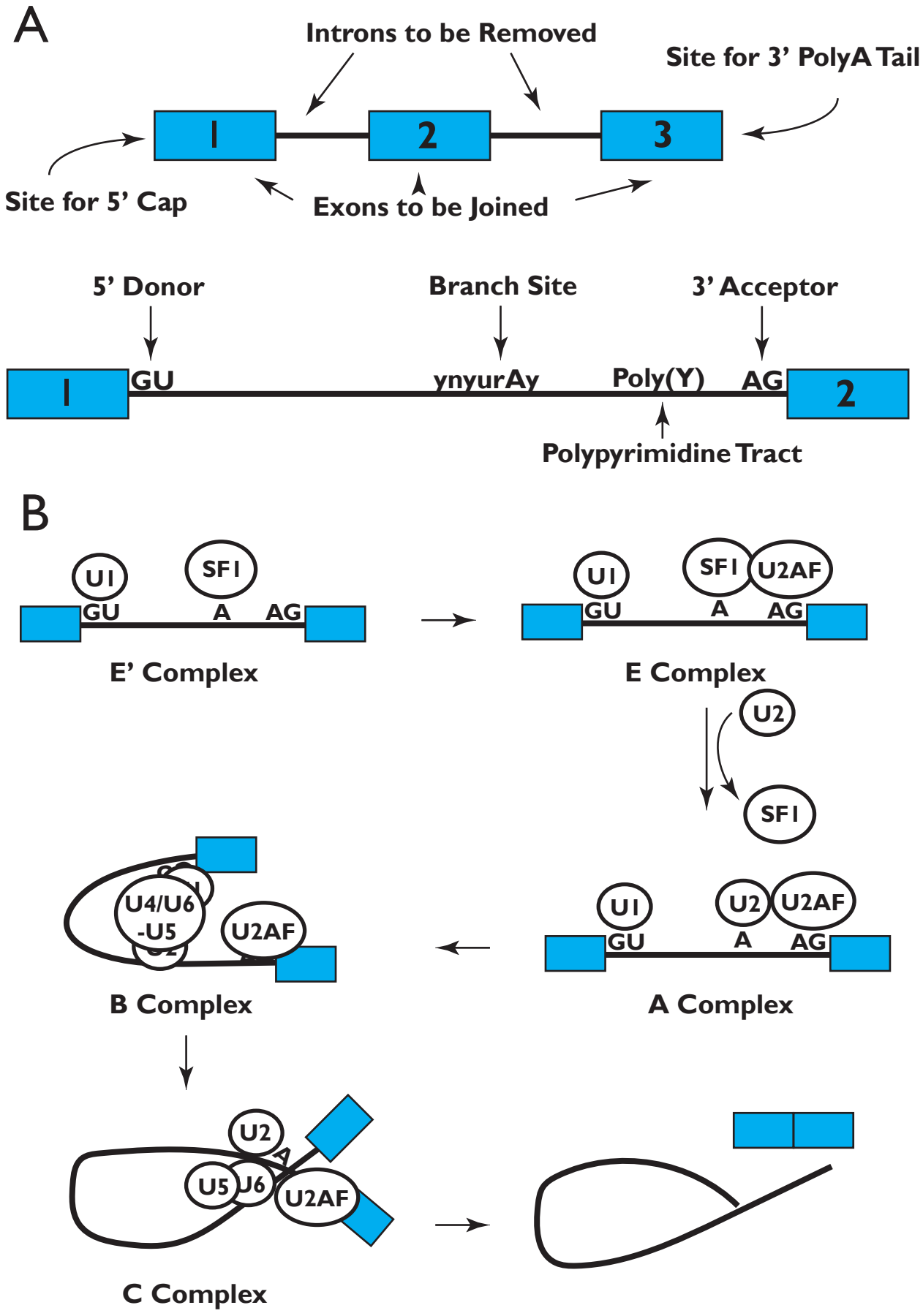
A
Introns to be Removed
Site for 3' PolyA Tail
1
2
3
Site for 5' Cap
Exons to be Joined
5' Donor
Branch Site
3' Acceptor
1
GU
ynyurAy
Poly(Y)
AG
2
Polypyrimidine Tract
B
U1
SF1
GU
A
AG
E' Complex
U1
SF1
U2AF
GU
A
AG
E Complex
U2
SF1
U4/U6
-U5
U2AF
B Complex
U1
U2
U2AF
GU
A
AG
A Complex
U2
U5
U6
U2AF
C Complex

Figure 1.1

Figure 1.1. Structure and organization of precursor mRNA (pre-mRNA).

(A) Above: structure of pre-mRNA and sites involved in RNA processing, including the 5' cap site and the 3' poly-adenylation site. The boxes are exons, while the black lines are introns, which are typically spliced out during pre-mRNA processing. Below: components of pre-mRNA required for splicing: the 5' donor site, the branch site (containing a highly conserved adenosine), the polypyrimidine tract, and the 3' acceptor site.

(B) Spliceosome assembly occurs when the snRNP U1 binds to the 5' splice site and splicing factor 1 (SF1) binds to the branch point, forming an E' complex. Binding of the snRNP U2 auxiliary factor (U2AF, consisting of a heterodimer of U2AF65 and U2AF35) to the 3' splicing site forms the E complex. Replacement of SF1 with the snRNP U2 on the branch point forms the prespliceosome A complex. Subsequent recruitment of a complex of proteins consisting of U4, U5, and U6 to the 5' splice site produces the B complex, which induces a series of conformational changes in the pre-mRNA, forming the active spliceosome, the C complex. Two transesterification reactions subsequently occur, resulting in the ligation of the flanking exons, and the release of the intron (Blaustein et al., 2007; Chen & Manley, 2009).

Subsequent recruitment of a complex of proteins consisting of U4, U5, and U6 to the 5' splice site produces the B complex, which induces a series of conformational changes in the pre-mRNA, forming the active spliceosome, the C complex. Two transesterification reactions subsequently occur, resulting in the ligation of the flanking exons, and the release of the intron (Figure 1.1B) (Blaustein et al., 2007; Chen & Manley, 2009; Schroeder, Barta, & Semrad, 2004; Ward & Cooper, 2010).

1.1.3 *Alternative Splicing*

The many tasks that can be consecutively conducted by a typical human cell can be attributed to a highly complex proteome. In order to produce a diverse range of proteins from only 20,000-25,000 genes, cells utilize a mechanism known as alternative splicing. In basic terms, alternative splicing is the selective inclusion or exclusion of exons in a pre-mRNA through alternative selection of splice sites (David & Manley, 2010). This results in the ability of a single gene to produce multiple mRNA products and, therefore, multiple protein products with potentially varying functions (Ghigna, Valacca, & Biamonti, 2008). It is believed that at least 90% of human genes are alternatively spliced (Ward & Cooper, 2010), and that 70-90% of alternatively spliced mRNAs produce distinct protein products (Shin & Manley, 2004). The scope of alternative splicing regulation and its role in enhancing protein diversity points to the conclusion that mutations or misregulation in the alternative splicing machinery by intrinsic or exogenous factors can alter cell function and contribute to disease.

1.1.4 *Mechanism of Alternative Splicing*

The occurrence of an alternative splicing event is highly dependent on both the "splicing code" made up by defined consensus sequences in the pre-mRNA and the stoichiometry of a multitude of trans-acting RNA-binding proteins, known as splicing factors, that regulate spliceosome assembly (Cooper et al., 2009). Splicing factors recognize

specific motifs in the pre-mRNA, and alter the behaviour of spliceosome activity to manipulate selective exon inclusion (enhancement) or exclusion (silencing). These cis-acting motifs are short (~10 nucleotide; Blaustein et al., 2007) sequences in the pre-mRNA that can be located either in the exon of interest (exonic splicing enhancers and silencers, otherwise known as ESEs and ESSs) or in the flanking intronic region (intronic splicing enhancers and silencers, otherwise known as ISEs and ISSs) (Figure 1.2A) (Cooper et al., 2009).

There are several known patterns by which alternative splicing can occur. A cassette exon is a single exon that can be selectively included or excluded, producing two possible mRNA isoforms. Mutually exclusive exons are two adjacent exons, where each exon can be selectively included or excluded, producing at least three possible mRNA isoforms. Alternative 5' and 3' splice sites allow for the selective alternative splicing based on an additional 5' or 3' splice site within an exon. Intron retention involves the selective inclusion or exclusion of an intronic region flanking a pair of exons (Figure 1.2B) (Blaustein et al., 2007; Ghigna et al., 2008).

1.2 Regulation of Alternative Splicing by Splicing Factors

As mentioned previously, a spliceosome complex's ability to determine splice sites for alternative splicing is dependent on additional protein regulators, known as splicing factors, that recognize and interact with exonic and intronic cis-sequence elements (ESEs, ESSs, ISEs, and ISSs) (Chen & Manley, 2009). Two of the most common classes of splicing factors are serine-arginine rich (SR) proteins and heterogeneous nuclear ribonucleoprotein (hnRNP) proteins (Cooper et al., 2009), which are characterized by their protein domain structure. SR proteins are nuclear proteins that generally positively affect spliceosome assembly to promote constitutive splicing, resulting in exon inclusion. In contrast, hnRNP proteins

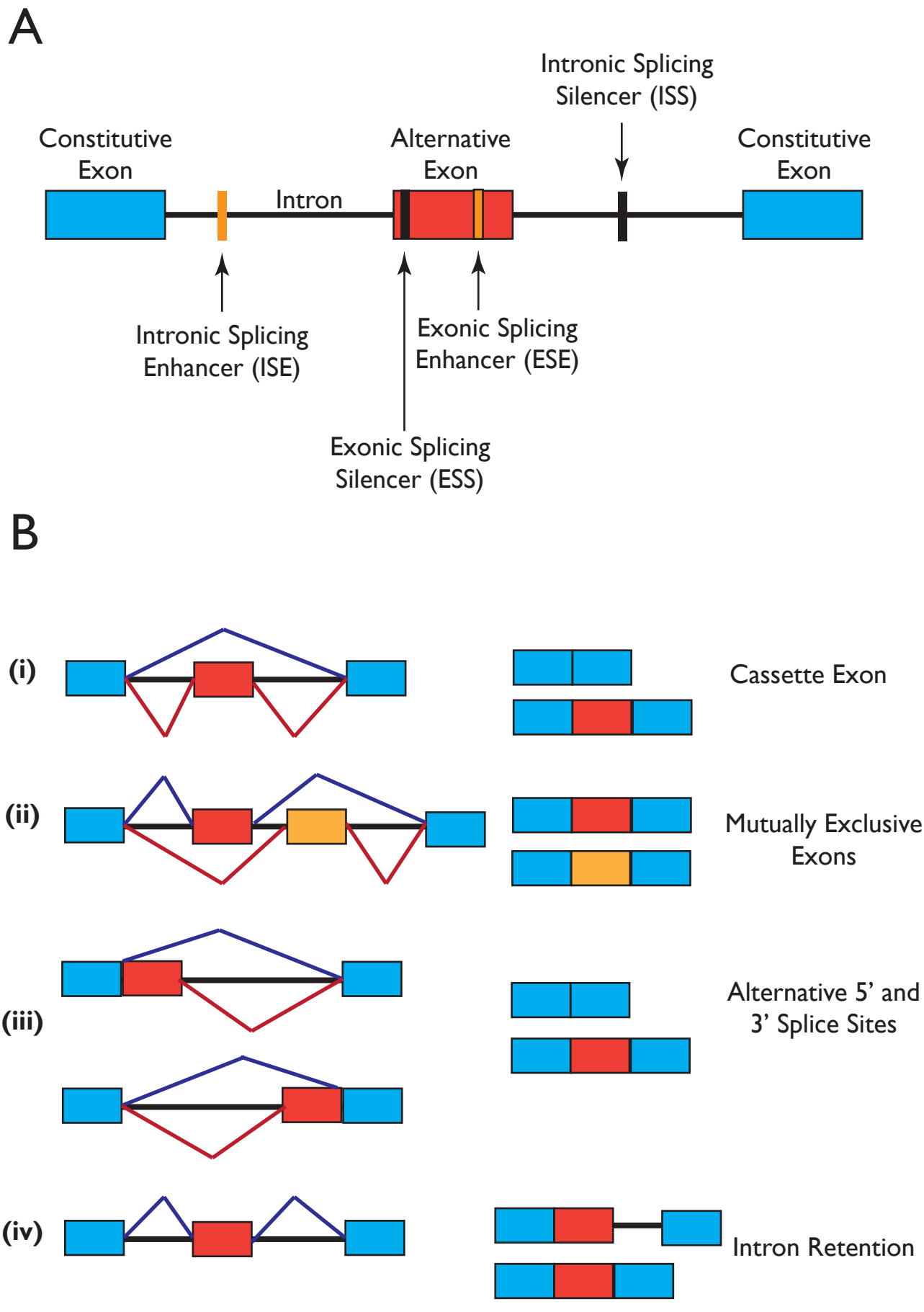
A
Intronic Splicing
Silencer (ISS)
Constitutive
Exon
Alternative
Exon
Constitutive
Exon
Intron
Intronic Splicing
Enhancer (ISE)
Exonic Splicing
Enhancer (ESE)
Exonic Splicing
Silencer (ESS)
B
(i)
Cassette Exon
(ii)
Mutually Exclusive
Exons
(iii)
Alternative 5' and
3' Splice Sites
(iv)
Intron Retention

Figure 1.2

Figure 1.2. Mechanism of alternative splicing.

(A) Structure of pre-mRNA, indicating cis-acting motifs that are required for selective exon inclusion (enhancement) or exclusion (silencing). Sites found within the alternative exon include exon splicing enhancer (ESE) and silencer (ESS) sites. Sites found within the flanking introns include intronic splicing enhancer (ISE) or intronic splicing silencer (ISS) sites.

(B) Examples of common alternative splicing patterns. Common alternative splicing patterns include (i) splicing of cassette exons, (ii) splicing of mutually exclusive exons, (iii) splicing at alternative 5' and 3' splice sites, and (iv) intron retention (Blaustein et al., 2007; Li, Lee, & Black, 2007).

generally negatively affect spliceosome assembly, resulting in exon exclusion (Blaustein et al., 2007; Cooper et al., 2009).

Most SR and hnRNP proteins are ubiquitously expressed; however, there are some notable examples, such as the hnRNP protein PTBP2, which has tissue-specific functions. In addition, the function of both classes of splicing factors in regulating alternative splicing is highly dependent on their post-translational modifications, localization in the cell, and their stoichiometry, which is dependent on the activity of upstream regulators that activate or inhibit the function of the splicing factors. Finally, both SR and hnRNP proteins have been shown to regulate both exon inclusion and exclusion in a position-dependent manner, depending on whether they bind upstream or downstream of an alternative exon (examples include the hnRNP proteins NOVA1 (Ule et al., 2006), and FOX2 (Yeo et al., 2009)). All of these factors reveal the complex nature of how alternative splicing events are regulated.

1.2.1 *SR Family Proteins*

SR family proteins are evolutionarily conserved proteins that consist of at least eighteen members (Chen & Manley, 2009; Shin & Manley, 2004). A typical SR protein consists of one or two amino-terminal (N-terminal) RNP-type RNA-recognition motif (RRM) domains, which allows the protein to recognize cis-sequences on the pre-mRNA. In addition, SR proteins contain a region enriched in repetitive arginine-serine dipeptides, known as the RS domain, which allows them to interact with either a pre-mRNA or other proteins containing an RS domain (Blaustein et al., 2007; Shin & Manley, 2004). The dipeptide sequences in the RS domain can be phosphorylated, which can potentially modify the activity of the SR protein by altering its cellular distribution and its ability to interact with other proteins or a pre-mRNA (Blaustein et al., 2007).

SR proteins play a large role in both constitutive and alternative splicing (Blaustein et

al., 2007). SR proteins help regulate splice site selection through interactions with snRNPs. For example, SR proteins that bind to ESE sites in an alternative exon can promote U2AF binding to the 3' splice site upstream of the exon or the U1 snRNP binding to the 5' splice site downstream of the exon (Chen & Manley, 2009). SR proteins can also interact with other splicing activators through its RS domain to form splicing complexes to stabilize the spliceosome and promote its function (Chen & Manley, 2009). Therefore, SR proteins are capable of regulating alternative splicing in both a pre-mRNA sequence-dependent and -independent manner (Shin & Manley, 2004).

The function of SR proteins has been shown to be highly regulated by extensive phosphorylation and dephosphorylation events on residues in the RS domain. This can affect its ability to interact with both pre-mRNA and other RS domain-containing proteins (Chen & Manley, 2009). A well-established example is SRp40, which is dephosphorylated by serine-threonine protein phosphatases, activating it and promoting its ability to regulate exon inclusion in the pre-mRNAs of several genes including glutamate receptor, ionotropic AMPA2 (Chen & Manley, 2009; Komatsu, Kominami, Arahata, & Tsukahara, 1999). Another well-known example is ASF/SF2 (also known as SRSF1), which has been found to be phosphorylated by serine-threonine protein kinases such as SRPK1, which activates ASF/SF2 and promotes its ability to regulate exon inclusion in the pre-mRNAs of the Rac1 gene (Gonçalves et al., 2014).

SR proteins can function antagonistically towards each other. For example, SR proteins ASF/SF2 and Srp20 have been shown to antagonistically regulate alternative splicing of exon 3b in the Rac1 pre-mRNA, with ASF/SF2 acting as an enhancer and SRp20 acting as a silencer (Gonçalves, Matos, & Jordan, 2009).

1.2.2 *hnRNP Family Proteins*

There are at least 20-30 characterized proteins in the hnRNP protein family (Carpenter et al., 2006; Pino et al., 2003). All hnRNP proteins are known to contain at least one N-terminal RRM domain, which allows them to interact with DNA or RNA sequence elements (Carpenter et al., 2006). In addition, some hnRNP proteins contain additional domains such as KH domains (50 amino acid-length sequence with peptide repeats of Ile-Gly-X2-Gly-X2-Ile) essential for RNA binding, and RGG motifs (25 amino acid regions with Arg-Gly-Gly repeats) that mediate protein-protein interactions and cellular localization (Carpenter et al., 2006).

Like SR proteins, hnRNP proteins are capable of regulating both constitutive and alternative splicing. Typically, hnRNP proteins inhibit splice site recognition in order to silence alternative exons, though there are exceptions. One way by which this can be achieved is by binding close to splicing sites, preventing snRNP protein or SR proteins from binding to enhancer sites (Chen & Manley, 2009). For example, PTBP1 (also known as hnRNP1 or PTB), is an ubiquitously expressed polypyrimidine tract-binding protein that binds to sequences with a high number of polypyrimidine nucleotides, such as the polypyrimidine tract within the 3' splice site, and may block U2AF from binding to the tract (Chen & Manley, 2009; Saulière, Sureau, Expert-Bezançon, & Marie, 2006).

Another way by which hnRNP proteins can inhibit splice site recognition is through multimerization of the hnRNP protein around the alternative exon. For example, PTBP1 has been shown to bind both upstream and downstream of the N1 exon in the Src pre-mRNA; mutation of one site alters PTBP1's ability to bind to the other site (Chen & Manley, 2009; Spellman & Smith, 2006).

Unlike SR proteins, hnRNP proteins are more structurally diverse, allowing for them

to play a role in a wide range of cellular functions. Due to this structural diversity, the guidelines for classifying hnRNP proteins are not very strict (Busch & Hertel, 2012). One well-known example of these "non-canonical" hnRNP proteins is Src-associated in mitosis 68kDa protein (Sam68), an ubiquitously expressed member of the Signal-Transduction and RNA (STAR) family of proteins (Michelle, Barbier, & Chabot, 2012). Unlike typical hnRNP proteins, Sam68 contains a RNA-binding domain flanked by proline-rich and tyrosine-rich motifs that allow it to interact with protein SH3 and SH2 domains (Bielli, Busà, Paronetto, & Sette, 2011). Sam68 has been shown to regulate a large number of alternative splicing events implicated in development and cancer. Its function is regulated through post-translational modifications by signal transduction pathways (Bielli et al., 2011).

1.3 Regulation of Alternative Splicing by Growth Factor Signalling Pathways

Gene and protein expression is highly regulated by extracellular signals that activate networks of signalling pathways within a cell. There is some evidence that signal transduction pathway networks can play a major role in regulating pre-mRNA alternative splicing, particularly in the cancer context. One way that signalling pathways may act on alternative splicing regulation of a given pre-mRNA is by modifying the activity of splicing factors through transcriptional, translational or post-translational changes. However, relatively little is known about the relationship between signal transduction pathways and the splicing factors they act on.

1.3.1 *MAPK/ERK Signalling*

The mitogen-activated protein kinase/extracellular signal-regulated kinase (MAPK/ERK) signalling pathway consists of a cascade of protein kinases that is triggered by a receptor located at the cell surface and activated by growth factors or cytokines (Siegfried,

Bonomi, Ghigna, & Karni, 2013).

MAPK/ERK signalling occurs as a series of phosphorylation events that results in the activation pathways that promote cell growth, survival, differentiation and migration (Dhillon, Hagan, Rath, & Kolch, 2007; Yang, Sharrocks, & Whitmarsh, 2013). For example, ligand-mediated activation of receptor tyrosine kinases results in the loading of Ras, a small GTPase, with GTP (Dhillon et al., 2007). GTP-bound Ras then recruits and activates the kinase Raf, which then phosphorylates and activates the kinases MEK1 and MEK2, which subsequently phosphorylate and activate ERK1 and ERK2 (Figure 1.3A). Activated ERK1 and ERK2 then go on to promote the activation of various cell pathways involved in cell growth, particularly through transcriptional regulation of downstream target genes (Dhillon et al., 2007). Interestingly, in some conditions, ERK1/2 activation has been correlated with increased transcription of splicing regulatory proteins (Gazel, Nijhawan, Walsh, & Blumenberg, 2008).

MAPK/ERK signalling has been implicated in the regulation of alternative splicing. One well-established example is the regulation of the SR protein Sam68, and its function in alternative splicing of CD44 in T lymphocytes (Figure 1.3B). The CD44 gene encodes a cell-surface glycoprotein involved in functions such as cell migration and proliferation (Lynch, 2007). The CD44 pre-mRNA consists of ten variable exons that are included in the mature RNA upon T lymphocyte stimulation via the MAPK/ERK signalling pathway (Matter, Herrlich, & Konig, 2002). Inclusion of variable exon v5, however, has been shown to be associated with tumour progression in addition to T lymphocyte activation (Sherman et al., 1996). The regulation of inclusion of exon v5 by Sam68 is activated by direct phosphorylation of serine and threonine sites in Sam68 by ERK, promoting its interaction with an ESE in CD44 v5, and resulting in v5 splicing enhancement (Lynch, 2007; Matter et

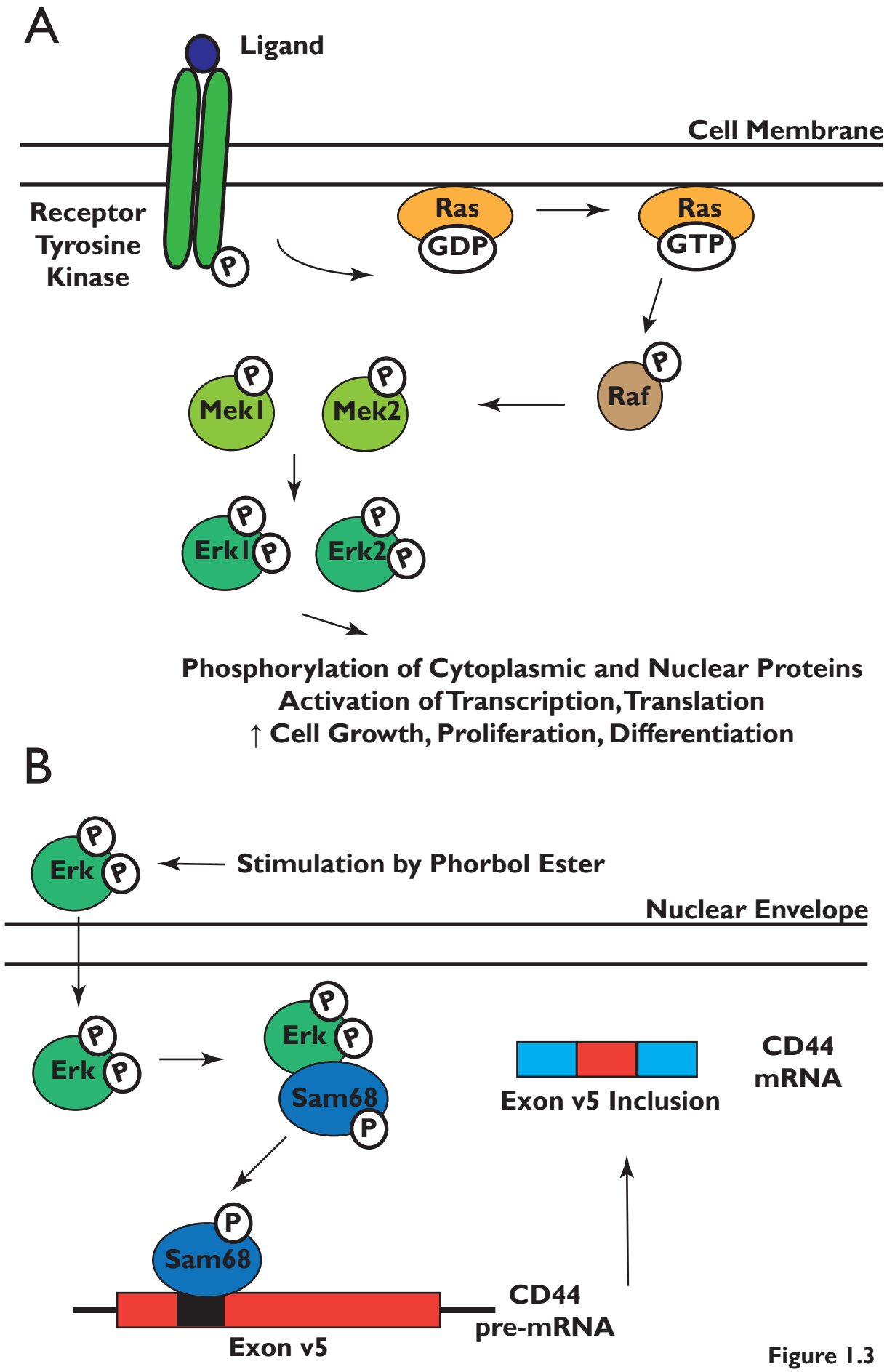
A
Ligand
Cell Membrane
Receptor
Tyrosine
Kinase
P
Ras
GDP
Ras
GTP
Raf
P
Mek1
Mek2
Erk1
Erk2
Phosphorylation of Cytoplasmic and Nuclear Proteins
Activation of Transcription, Translation
↑ Cell Growth, Proliferation, Differentiation
B
Erk
Stimulation by Phorbol Ester
Nuclear Envelope
Sam68
CD44
mRNA
Exon v5 Inclusion
CD44
pre-mRNA
Exon v5

Figure 1.3

Figure 1.3. Mechanism of mitogen-activated protein kinase/extracellular signal-regulated kinase (MAPK/Erk) signalling, and its role in regulation of alternative splicing.

(A) Overview of the MAPK/Erk signalling pathway. The pathway is triggered by activation of a receptor tyrosine kinase (RTK) at the cell surface by extrinsic growth factors or cytokine ligands, resulting in the phosphorylation of the RTK at tyrosine residues. Activation of docking proteins that interact with the RTK results in the removal of GDP from the small GTPase Ras by a guanine nucleotide exchange factor. Ras is then loaded with GTP, activating it and triggering a signal cascade involving phosphorylation and subsequent kinase activity of Raf kinase, Mek1 and Mek2 kinases, and Erk1 and Erk2 kinases. Erk phosphorylation induces its kinase activity, and phosphorylated Erk activates pathways correlated with increased cell proliferation, differentiation, and migration. This can be done by the phosphorylation of cytoplasmic proteins, or by the translocation to the nucleus and activation of nuclear proteins, such as transcription factors.

(B) An example of the regulation of CD44 exon v5 alternative splicing by MAPK/Erk signalling in T lymphocytes. Activation of MAPK/Erk signalling by phorbol ester stimulation results in the phosphorylation of Sam68 by phosphorylated Erk1/2. Sam68 subsequently interacts directly with an ESS site in exon v5, resulting in exon inclusion (David & Manley, 2010; Lynch, 2007; Matter et al., 2002; Paronetto, Achsel, Massiello, Chalfant, & Sette, 2007; Shin & Manley, 2004).

al., 2002) and promoting a tumorigenic phenotype.

1.3.2 *PI3K/Akt Signalling*

Phosphoinositide 3-kinase (PI3K) is another starting point for a major signalling cascade that promotes cell survival, growth, and migration. Activation of PI3K results in the formation of phosphatidylinositol-3,4,5-triphosphate (PIP3), which then regulates the recruitment and activation of the kinase Akt, which subsequently regulates downstream events through phosphorylation (Figure 1.4A) (Luo, Manning, & Cantley, 2003; Siegfried et al., 2013).

There is evidence of the PI3K/Akt pathway regulating the activity of SR and hnRNP proteins either directly or through other kinases. Akt can phosphorylate both SR and hnRNP proteins that contain multiple RXRXX(S/T) Akt phosphorylation consensus motifs (Naro & Sette, 2013). One recent study showed that PI3K/Akt pathway activation and subsequent Akt-dependent phosphorylation of the splicing regulator hnRNP L increases its activity and its affinity for exon 3 in the pre-mRNA of the pro-apoptotic gene caspase-9. This results in exon 3 exclusion and produces an anti-apoptotic isoform of caspase-9 that promotes cell survival (Vu et al., 2013) (Figure 1.4B). In addition, PI3K/Akt signalling has been shown to be correlated with upregulated ASF/SF2 expression in colorectal cancer, promoting its function as a splicing enhancer of the Rac1 pre-mRNA, producing an alternative splice variant known as Rac1b that promotes tumour cell viability (Gonçalves et al., 2009).

1.4 Alternative Splicing and Cancer

Alternative splicing has been frequently shown to be misregulated in cancer, either as a result of mutations within the pre-mRNA that alters splice site selection, or as a result of changes in expression or activity of the splicing factors that regulate alternative splicing

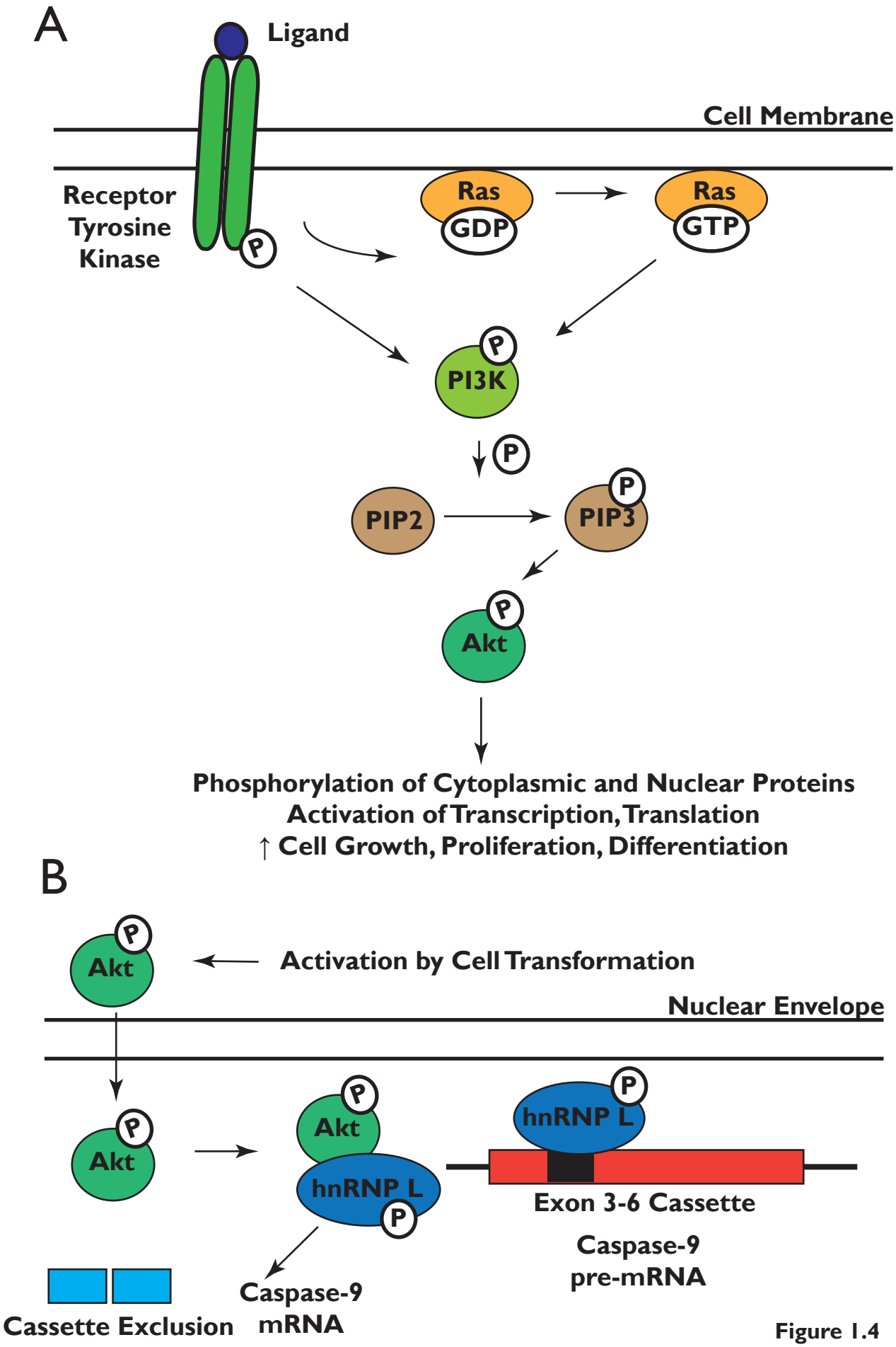
A
Ligand
Cell Membrane
Receptor
Tyrosine
Kinase
P
Ras
GDP
Ras
GTP
P
PI3K
P
PIP2
PIP3
P
Akt
P
Phosphorylation of Cytoplasmic and Nuclear Proteins
Activation of Transcription, Translation
↑ Cell Growth, Proliferation, Differentiation
B
Akt
P
Activation by Cell Transformation
Nuclear Envelope
Akt
P
Akt
P
hnRNP L
P
hnRNP L
P
Exon 3-6 Cassette
Caspase-9
pre-mRNA
Caspase-9
mRNA
Cassette Exclusion

Figure 1.4

Figure 1.4. Mechanism of phosphoinositide 3-kinase (PI3K)/Protein Kinase B (Akt) signalling, and its role in regulating alternative splicing.

(A) PI3K is activated by receptor tyrosine kinase (RTK) activation at the cell membrane by extrinsic growth factors or cytokines. PI3K subsequently catalyzes the formation of phosphatidylinositol-3,4,5-triphosphate (PIP3), which then regulates the recruitment and activation of the kinase Akt, which subsequently regulates downstream events through phosphorylation. PI3K can also be activated directly by activated Ras. (B) An example of the regulation of alternative splicing by PI3K/Akt signalling. Increased Akt activation during transformation in lung cancer results in phosphorylated Akt phosphorylating the splicing factor hnRNP L. hnRNP L is thus able to bind directly to an exon 3-6 cassette exon in the caspase-9 pre-mRNA, promoting exon exclusion (Vu et al., 2013).

events (Ward & Cooper, 2010). Based on what is known about the regulation of splicing factor expression, activity and localization by signal transduction pathways, it can be understood that alterations in these signalling pathways can affect the alternative splicing events, contributing to a splicing profile that promotes tumorigenesis.

1.4.1 *Signalling Pathways Altered in Cancer*

The MAPK/ERK and PI3K/Akt signalling pathways are two major pathways that have been shown to be aberrantly activated in many cancers. RTK and Ras activating mutations can give rise to both MAPK/ERK and PI3K/Akt pathway activation. Over-expression of the RTK epidermal growth factor receptor (EGFR) has been shown to occur in more than 50% of carcinomas, while Ras activating mutations are found in about 30% of cancers, particularly in melanomas, lung adenocarcinoma, pancreatic carcinomas, and colon cancers (Dhillon et al., 2007; Friday & Adjei, 2008).

Additional mutations of kinases downstream of Ras have been shown to aberrantly activate ERK signalling. For example, B-Raf activating mutations are among some of the most common in cancer, most frequently occurring in melanomas, thyroid and colon carcinomas (Santarpia, Lippman, & El-Naggar, 2012). Mutations in MEK and ERK are largely absent in human cancers (Friday & Adjei, 2008). However, activated ERK signalling in cancer promotes activation of pathways regulating cellular growth, proliferation, and migration (Santarpia et al., 2012).

Mutations have also been shown to aberrantly activate PI3K/Akt signalling. For example, inactivating mutations in PTEN, the gene that codes for a phosphatase of PIP3, results in the increased activation of PI3K signalling (Engelman, 2009). Also, there are many identified somatic mutations of the subunits that make up PI3K, that constitutively activate PI3K signalling. For example, mutations in the gene that codes for the p110 catalytic subunit

of PI3K have been found to occur in 30% of epithelial cancers, including breast, colon and prostate (Engelman, 2009).

Increased Akt activation in cancers has also been shown to occur due to over-activation of mutated RTKs, resulting in constitutive activation of Akt (Altomare & Testa, 2005). Amplified Akt has also been described in ovarian, breast and colon cancers (Luo et al., 2003). Activated Akt is well known to act on downstream pathways that promote cell survival, through activities like the inactivation of pro-apoptotic factors and antagonizing cell cycle control. In addition, it has been shown to promote cell migration, tumour invasion and metastasis (Altomare & Testa, 2005).

1.4.2 *Cancer-Associated Changes in Alternative Splicing*

The expression of several splicing factors have been shown to be either upregulated or downregulated in tumors. For example, the splicing factor SPF45 is upregulated in many cancer types, including lung, breast, colon, ovary and bladder cancer (Grosso, Martins, & Carmo-Fonseca, 2008; Grosso, Gomes, et al., 2008; Sampath et al., 2003), while PTBP1 is over-expressed in breast cancer (He et al., 2014), ovarian cancer (He et al., 2007) and glioblastoma (Cheung, Corley, Fuller, McCutcheon, & Cote, 2006). SF2/ASF, which has been recognized as a proto-oncogene, is over-expressed in several types of cancers, including colon, thyroid, breast and lung, due to ASF/SF2 gene expression upregulation (Karni et al., 2007).

MAPK/ERK and Akt signalling pathways have been implicated in modifying the expression and activity of splicing factors in cancer, thus disrupting normal alternative splicing events in a way predicted to promote tumour development. For example, in colorectal cancer, activation of Akt is correlated with upregulated ASF/SF2 expression, promoting its function as a splicing enhancer of the Rac1 pre-mRNA. This leads to the

production of a splice variant, Rac1b, that promotes epithelial-mesenchymal transition (EMT) and Wnt/β-catenin signalling (Gonçalves et al., 2009).

1.5 The Adaptor Protein Numb.

Mammalian Numb is an endocytic adaptor protein (Santolini et al., 2000) expressed in both developing and adult tissues. Numb was first identified as an intrinsic regulator of cell fate determination during *Drosophila melanogaster* embryonic development (Uemura et al., 1989), where it asymmetrically localizes to one daughter cell to drive unique cell fate (Rhyu, Jan, & Jan, 1994). The Numb gene is evolutionarily conserved, and the protein Numb has been shown to share common functions across vertebrates such as mouse (Shen, Zhong, Jan, & Temple, 2002) and chicken (Wakamatsu, Maynard, Jones, & Weston, 1999), and invertebrates such as *Drosophila* and *Caenorhabditis elegans*. Numb has been shown to be vital for mammalian development: mice that are homozygous for a loss-of-function numb allele die at approximately embryonic day 11.5 and show major defects with neural tube development, from which the central nervous system (CNS) normally derives (W Zhong et al., 2000; Zilian et al., 2001).

In vertebrates, the NUMB gene is alternatively spliced to produce four unique mRNA and protein variants through alternative splicing (Dho, French, Woods, & McGlade, 1999; Karaczyn et al., 2010; Licatalosi et al., 2012; Verdi et al., 1999). In addition to acting as a cell-fate determinant during asymmetric cell division, Numb also plays major roles in cell proliferation and migration, endocytosis, and tumorigenesis.

The human Numb gene is located on chromosome 14 (NCBI build 36.1), while the mouse Numb gene is located on chromosome 12 (GRC mouse build 38). The human Numb gene consists of thirteen exons (Figure 1.5A, above), of which the first three make up the 5'

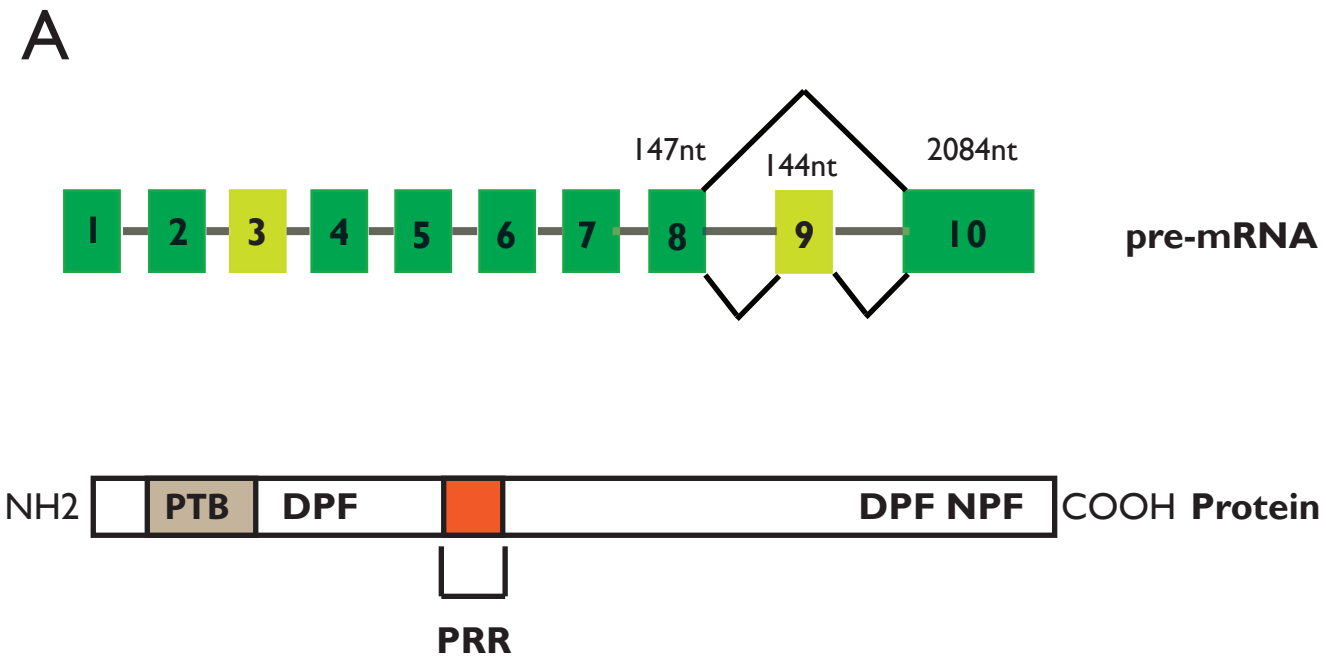
A
147nt
144nt
2084nt
1
2
3
4
5
6
7
8
9
10
pre-mRNA
NH2
PTB
DPF
DPF NPF
COOH
Protein
PRR

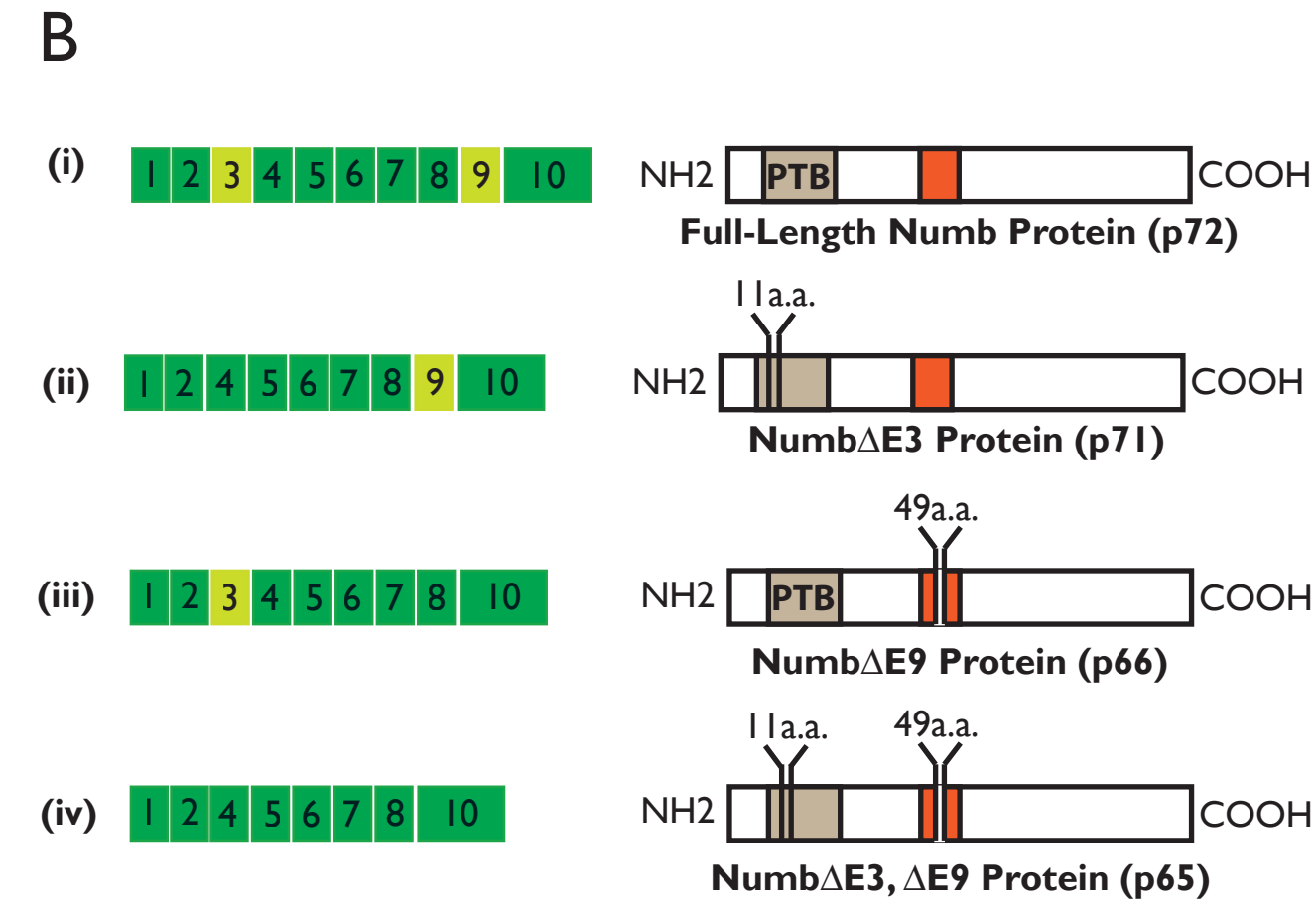
B
(i)
1 2 3 4 5 6 7 8 9 10
NH2
PTB
COOH
Full-Length Numb Protein (p72)
(ii)
11a.a.
1 2 4 5 6 7 8 9 10
NH2
COOH
NumbΔE3 Protein (p71)
(iii)
49a.a.
1 2 3 4 5 6 7 8 10
NH2
PTB
COOH
NumbΔE9 Protein (p66)
(iv)
11a.a.
49a.a.
1 2 4 5 6 7 8 10
NH2
COOH
NumbΔE3, ΔE9 Protein (p65)

Figure 1.5

Figure 1.5. Structure of Numb and its four alternative splice variants.

(A) Above, the structure of Numb precursor-mRNA, with exon 9 depicted as an alternative cassette exon. Below, the structure of full-length Numb protein, which contains an animo-terminal phosphotyrosine-binding domain, a proline-rich region, two aspartic acid-proline-phenylalanine motifs, and an asparagine-proline-phenylalanine motif.

(B) The four splice variants of Numb. Splice variants are formed from the alternative splicing of cassette exons 3 and 9. (i) Full-length Numb (p72), where both exons 3 and 9 are included. (ii) Exclusion of exon 3 produces the p71 Numb protein variant. (iii) Exclusion of exon 9 produces the p66 Numb protein variant. (iv) Exclusion of both exons 3 and 9 produces the p65 Numb protein variant.

untranslated region (5' UTR). The Numb protein includes an amino-terminal phosphotyrosine-binding (PTB) domain, a proline-rich region (PRR), two aspartic acid-proline-phenylalanine (DPF) motifs, and an asparagine-proline-phenylalanine (NPF) motif (Figure 1.5A, below).

1.6 Functions of Mammalian Numb

Numb regulates diverse functions in the cell associated with cell fate, cell polarity, endocytosis, membrane trafficking, and proteolytic degradation. The main cellular functions of Numb will be described below.

1.6.1 *Polarized Distribution of Numb and Functions in in Asymmetrical Cell Division, Migration, and Junction Formation*

Numb is a major player in a developmental mechanism known as asymmetric cell division, which involves the differential segregation of cell fate determinants in two daughter cells from a single precursor parent cell (Knoblich, 2008). Numb was the first cell fate determinant to be found to asymmetrically segregate during precursor cell division (Knoblich, 2008; Rhyu et al., 1994). In *Drosophila,* the absence of Numb was found to result in the inability of precursor cells to differentiate into neurons (Uemura et al., 1989).

Asymmetric cell division is regulated by a highly conserved complex of proteins containing the proteins Par3, Par6, and atypical protein kinase C (aPKC); collectively they form the partitioning defective, or Par, complex (Henrique & Schweisguth, 2003). In developing epithelial cells, the Par complex localizes in the apical region of the cell, opposite of the basally localized Numb, and plays a role in directing localization of cell fate determinants like Numb, and positioning mitotic spindles during mitosis (Casanova, 2007; Knoblich, 2008).

Numb polarity is maintained in the cell by aPKC, which phosphorylates it at two conserved serine residues S7 and S295. This results in the distribution of Numb to the basolateral membrane, while the apical membrane is devoid of Numb. When these residues are mutated, Numb symmetrically distributes around the cell membrane (Dho, Trejo, Siderovski, & McGlade, 2006; Smith et al., 2007). These studies confirm that Numb distribution is maintained by cellular polarity in a aPKC-dependent manner, in both Drosophila and mammalian cells.

The polarized distribution of Numb allows it to regulate cell migration and adhesion. In progenitor radial glial cells, cadherin junctions, which are required for maintaining epithelial cell polarity, localize at the apical end of the cells to maintain cell-cell adhesion. Numb was found to also localize in this region, and Numb knock-out resulted in a loss of cell polarity and the disruption of cell adhesion through a loss in cadherin localization (Rasin et al., 2007). Numb was also demonstrated to promote directional cell migration through the regulation of integrin endocytosis at the leading edge (Nishimura & Kaibuchi, 2007). The depletion of Numb in MDCK canine kidney cells is also correlated with a change in distribution of cadherin from the basal to the apicolateral membrane, which indicates that Numb is important for maintaining cell polarity. They also saw weakened cell-cell adhesion, contributing to enhanced cell migration (Wang, Sandiford, Wu, & Li, 2009).

A study by Lau and McGlade (2011), however, found that depletion of Numb in MDCK cells had no effect on the localization of basolateral or apical markers, indicating that Numb depletion does not affect MDCK cell polarity. However, in the absence of Numb, cadherin was depleted from the cell membrane and internalized more quickly, correlating with destabilization of of cadherin-mediated junctions, a decrease in cell-cell adhesion and increased hepatocyte-induced cell migration (Lau & McGlade, 2011).

1.6.2 *Role of Numb in Endocytosis and Endosomal Trafficking*

Numb was first linked to endocytosis through the identification of the interaction between the EH domain of the endocytic protein epidermal growth factor receptor substrate (Eps15) and Numb's NPF motif (Salcini et al., 1997). Numb was shown to localize in endosomes, clathrin-coated pits, and vesicles (Santolini et al., 2000). The DPF motif of the c-terminal end of Numb has also been shown to interact with α-adaptin, a component of the AP2 adaptor complex (Santolini et al., 2000).

Numb acts as a negative inhibitor of Notch function. Numb has been shown to regulate the internalization and recycling of the transmembrane receptor Notch in a ligand-independent manner. The Notch receptor is constitutively internalized from the plasma membrane into endocytic vesicles, after which it can be sorted into late endosomes for lysosomal degradation or recycled back to the cellular membrane. Over-expression of Numb promoted sorting of the Notch receptor through late endosomes, while knockdown of Numb promoted enhanced recycling of Notch receptor to the cell membrane (McGill, Dho, Weinmaster, & McGlade, 2009). These studies show that Numb inhibits Notch by regulating its degradation through endosomal sorting events.

Numb also plays a role in the endocytosis of integrin receptors (Nishimura & Kaibuchi, 2007). Numb promotes directional cell migration through the regulation of integrin endocytosis at the leading edge, though this is impaired when Numb is phosphorylated by aPKC (Nishimura & Kaibuchi, 2007).

1.6.3 *Role of Numb in Regulation of p53 Ubiquitylation and Degradation*

p53 is a tumour suppressor protein and transcription factor that promotes expression of genes that regulate cell senescence, apoptosis and growth inhibition in the presence of cellular stress such as hypoxia and oncogene activation (Carter & Vousden, 2008). Mutations

of p53 have been detected in approximately 50% of human cancers (Colaluca et al., 2008), highlighting the protein's role as a "master regulator" of major cellular functions (Farnebo, Bykov, & Wiman, 2010).

p53 is targeted for proteosomal degradation through ubiquitylation by the E3 ubiquitin ligase and oncoprotein MDM2, thus inhibiting its transcriptional function (Colaluca et al., 2008). The Numb protein has also been shown to be a substrate of ubiquitylation by MDM2 (Colaluca et al., 2008; Yogosawa, Miyauchi, Honda, Tanaka, & Yasuda, 2003), and is capable of forming a tricomplex with MDM2 and p53. Numb binding to MDM2 leads to the maintenance of p53 stability by inhibiting ubiquitylation by MDM2 and subsequent degradation. A recent study found that the interaction between Numb and p53 could be altered by methylation of two lysine sites in the Numb PTB domain by the lysine methyltransferase Set8. This results in the separation of Numb and p53 and the subsequent ubiquitination and proteasomal degradation of p53 (Dhami et al., 2013).

1.7 Alternative Splicing of Numb

Coding exons 3 (E3) and 9 (E9) in the Numb pre-mRNA have been shown to undergo alternative splicing, each acting as a cassette exon during the splicing process. E3 corresponds to an 11-amino acid region within the PTB domain, while E9 corresponds to a 49-amino acid region in the central region of the protein. Selective exclusion of the two exons produce four possible transcript and protein products: (1) Numb+E3+E9 transcript (p72 protein isoform), (2) NumbΔE3+E9 (p71 isoform), (3) Numb+E3ΔE9 (p66 isoform), and (4) NumbΔE3ΔE9 (p65 isoform) (Figure 1.5B).

1.7.1 *Differential Expression of Numb Splice Variants*

Several early studies suggest that Numb splice variants may play different and important roles in development. Dho et al. (1999) utilized Western blotting with numb

isoform-specific antibodies to establish that different tissues had varying expression levels of the four Numb protein isoforms. For example, the adult brain and lung were found to express high amounts of the p66 and p65 isoforms and almost no expression of the p72 or p71 isoforms. In addition, Numb isoform expression was shown to be altered during differentiation. When mouse embryonal carcinoma p19 cells, which express predominantly the p72 isoform, were induced with all-trans retinoic acid to differentiate into neurons, expression of the p72 isoform was downregulated, and upregulated p66 expression was observed. This suggests a change in Numb alternative splicing during differentiation (Dho et al., 1999).

Similarly, Verdi et al. (1999) confirmed the differential expression of Numb mRNA isoforms during neuronal development. They showed that the Numb+E9 mRNA transcript is poorly expressed in adult tissues, though expression of the NumbΔE9 isoform was highly expressed across multiple tissues. In addition, the Numb+E9 isoform was highly expressed in fetal brain tissue, and progressively decreased in expression as the brain developed (Verdi et al., 1999). A study by Revil et al. (2010) involved the use of a splicing-sensitive exon microarray to identify alternative splicing events during embryonal development in the mouse. The authors identified Numb as one of seventeen validated AS candidates during embryonal development, and identified a switch towards E9 exclusion in Numb transcripts, as early as embryonic day E8.5 (Revil, Gaffney, Dias, Majewski, & Jerome-Majewska, 2010).

Retinal development has also been associated with a switch in E9 alternative splicing. A study by Dooley et al. (2003) found that expression of the rat transcript corresponding to the human Numb+E9 transcript was highest at embryonic days E12 to E14, but decreased at later stages of development. However, expression of the rat transcript corresponding to the

human NumbΔE9 transcript was consistently high, peaking at embryonic day E14 (Dooley, James, McGlade, & Ahmad, 2003). This trend was similar to the developing pancreas, where expression of the protein corresponding to the human p72 isoform was expressed in high levels in progenitor cells but downregulated during differentiation (Yoshida, Tokunaga, Nakao, & Okano, 2003). The results from these studies suggest that alternative splicing of exon 9 in Numb is developmentally regulated, with exon 9-included transcript and protein variants expressed at high levels in progenitor cells, and these transcript and protein variants decreasing during cellular differentiation.

There is no evidence of developmental regulation of E3 splicing. For example, a study by Kim et al. (2013) found that, during the development of the chick neural tube, there was no alteration in exon 3 inclusion levels at the mRNA level (Kim, Nam, Mukouyama, & Kawamoto, 2013). However, it is evident that expression of E3 is differentially expressed across tissues. For example, Dho et al. (1999) found that there was poor expression of both E3-included and E3-excluded protein isoforms in developing embryo, but high amounts of the E3-excluded protein isoforms in the lung and brain.

1.72 *Differential Function of Numb Protein Variants*

To date, a limited number of studies have attempted to compare the functions of Numb isoforms. Studies by the McGlade laboratory on the role of Numb on cell polarity, adhesion and endocytosis focus on the p66 isoform due to its abundant expression in most mammalian cells (McGill et al., 2009). However, other studies do not specify which isoforms of Numb have been studied. These discrepancies make it difficult to determine if there are any differential functions of Numb protein variants.

This differential regulation of exon 9 alternative splicing appears to have a functional effect. Several studies indicate that the p72 isoform may promote cellular proliferation in

both cultured cells and stem cells. Over-expression of rat p71 and p72 isoforms in MONC-1 multipotential neural crest cells was found to promote cellular proliferation, while over-expression of rat p65 and p66 isoforms drove cells towards a neuronal fate (Verdi et al., 1999). Dooley et al. (2003) similarly found that high expression of the p72 isoform in progenitor retinal cells was correlated with rapid expansion due to increased proliferation, while increasing expression of the p66 isoform correlated with cell fate determination of embryonic retinal cells, starting at around embryonic day E14 (Dooley et al., 2003). These results demonstrate that alternative splicing of Numb exon 9 promotes either cell proliferation or differentiation.

Less is known about the role of the PRR in Numb protein function. A study conducted by Krieger et al. (2013) used affinity purification-mass spectrometry on Flag-tagged Numb p72 and p66 immunoprecipitates to identify the protein-protein interactions for each isoform. The authors found that, though there were no protein-protein interactions unique to either isoform, the p72 isoform was found to associate with greater amounts of Eps15 and AP-2 complex components compared to the p66 isoform. This was confirmed using proximity ligation assays and selected reaction monitoring mass spectrometry.

The PTB domain is highly conserved across both vertebrate and non-vertebrate Numb (Verdi et al., 1996; Zhong, Feder, Jiang, Jan, & Jan, 1996). The lysine-rich insert in the PTB domain, which can be found in the p72 and p66 isoforms, has been found to have unique functions. The PTB domain in p72 and p66 has also been shown to interact with the PDZ domain-containing protein LNX, an E3 ubiquitin ligase which ubiquitinates both isoforms, in order to be targeted for degradation (Nie et al., 2002). Though all four Numb protein isoforms are capable of binding to LNX, the interaction between a PDZ domain in LNX and the PTB insert in Numb targets only the p72 and p66 isoforms specifically for ubiquitination

and degradation (Nie, Li, & McGlade, 2004). The PTB insert also plays a role in isoform localization. Inclusion of the PTB insert promotes PTB binding to phospholipids and subsequent localization of Numb to the cortical membrane. The absence of this insert relegates Numb to the cytoplasm (Dho et al., 2006).

Another study by Kyriazis et al. (2008) found that, when neuronal cells expressed a Numb isoform lacking the PTB insert, there was an increase in internalization of amyloid precursor protein (APP), pointing towards a mechanism in APP trafficking regulated by Numb (Kyriazis et al., 2008).

A study by Jiang et al. (2012) found that high expression of the PTB insert-containing Numb p72 isoform promoted the activity of a Skp1-Cullin-F-box ubiquitin ligase in glioblastoma, resulting in increased internalization and degradation of Notch and increasing cellular proliferation (Jiang et al., 2012).

1.8 Regulation of Alternative Splicing in Numb

One of the first studies that analyzed the regulation Numb E9 alternative splicing event was conducted by Zhang et al. (2010), who used Bayesian networks to statistically model the target genes of hnRNP-like splicing regulators Nova1 in the mouse brain. Their data revealed that there was combinatorial regulation between Nova1 and another hnRNP-like factor Fox2 for many alternative splicing events in the mouse brain. Numb was identified to be regulated by both Nova1 and Fox2: over-expression of each factor promoted Numb E9 exclusion, in an additive manner (Zhang et al., 2010). However, it remains to be seen what signalling mechanisms regulate Numb E9 alternative splicing, and whether these splicing factors act as conduits between the signalling pathways and the Numb splicing event.

1.9 Numb Isoform Expression in Cancer

Pece et al. (2004) used breast adenocarcinoma to determine that Numb protein expression was frequently altered in breast cancer tumour tissue samples compared to normal control tissue. Using immunohistochemistry, they found that, in about 55% of tumor samples observed, Numb staining was present in less than 50% of cells. They also determined that there was an inverse correlation between total Numb expression status and disease severity. They found that there were no mutations in the Numb cDNA that could be attributed to changes in expression in cancer, and that Numb downregulation was correlated to tumor progression and colony-forming ability through increased activation of Notch pathway targets (Pece et al., 2004). Similar conclusions were made by Stylianou, Clarke, & Brennan (2006).

Westhoff et al. (2009) conducted a similar study to observe the role of Notch signalling in non-small cell lung cancer (NSCLC), using lung adenocarcinoma and squamous cell carcinoma cell lines. They observed that there was a frequent loss of Numb expression in tumour samples compared to normal lung tissue. They established that a possible mechanism of Numb expression regulation in NSCLC was at the post-translational level, possibly through proteosomal degradation. Like in breast cancer, they also observed no change in the Numb coding sequence at the genomic level in NSCLC, and saw an inverse correlation between Numb downregulation and upregulation of Notch-1 receptor expression and Notch target mRNA expression. They concluded that Numb may act in a tumour suppressor-like manner. These studies, however, do not explore changes in Numb isoform expression (Westhoff et al., 2009).

A study by Di Marcotullio et al. (2006) showed that, compared with healthy adult cerebellar tissues, Numb expression was markedly decreased in medulloblastoma tumour

tissue. In addition, there was a significant upregulation in the tumour samples of Gli1, a transcription factor activated by the Hedghog signalling pathway. Numb was found to target Gli1 for ubiquitination and degradation through the recruitment of the E3 ubiquitin ligase Itch, resulting in downregulation of Hedgehog signalling and driving cells towards differentiation (Di Marcotullio et al., 2006).

Recent advancements in detection of alternative splicing events enabled researchers to study changes in alternative splicing in cancer. Langer et al. (2010) used a modified exon array data set obtained from NSCLC and normal lung tissue samples and found that there was a switch in Numb E9 alternative splicing from predominantly expression of the NumbΔE9 isoform in nomal adult lung tissue to significantly increased expression of the Numb+E9 isoform in lung adenocarcinoma. A similar trend was detected in squamous cell carcinoma but was not significant (Langer et al., 2010).

A study conducted by Misquitta-Ali et al. (2011) used quantitative alternative splicing microarray profiling in lung adenocarcinoma tissue and identified the switch in Numb alternative splicing towards increased E9 inclusion as the most frequent alternative splicing event in lung, colon and breast adenocarcinoma. This also correlated with expression of the E9-containing protein isoforms. However, though there was no change in total Numb transcript expression, there was less total Numb protein present in lung adenocarcinoma, poentially explaining why previous studies observed less Numb expression in lung and breast cancer. They determined that the relationship between the Numb isoforms and Notch signalling was isoform-dependent: over-expression of the p72 isoform significantly increased Notch targets Hey1 and Hey2, while over-expression of the p66 isoform did not affect Notch target expression, implying that the p66 isoform is involved in suppressing the Notch targets, but the p72 isoform inhibits this suppression through an unknown mechanism. Finally, they

found that cell proliferation in lung adenorcarcinoma was also isoform-dependent (Misquitta-Ali et al., 2011).

1.9.1 *Study Rationale and Hypothesis*

The differential role of Numb isoforms NumbΔE9 and Numb+E9 in regulating cell proliferation and Notch activation, which is correlated with tumorigenesis, suggests that Numb E9 alternative splicing has a functional role in development and cancer. The mechanism involved in Numb E9 alternative splicing are currently not clear, and the aim of this thesis is to identify potential signal transduction networks and their downstream splicing factor targets that regulate Numb E9 alternative splicing. I hypothesized that oncogenic and differentiation pathways regulate Numb E9 alternative splicing, and this splicing event is important for Numb function in both development and cancer.

CHAPTER 2: MATERIALS AND METHODS

2.1 PLASMIDS AND CLONING

2.1.1 Construction of Human Numb E9 Alternative Splicing Full-Length Reporter.

BAC DNA corresponding to human genomic sequence Chr14 72778081-72952456 (NCBI build 36.1/hg18) was cloned into a pBACe3.6 vector and provided as an agar stab (Empire Genomics, Cat. #RP11-76J16). DNA was isolated using a modified protocol from QIAGEN (Manual QP01, available at http://www.qiagen.com/resources/resourcedetail?id=ab7c2c09-8f47-403b-aaa6-18deef55e80e).

A 50µL PCR reaction was set up containing 40ng of the BAC plasmid, 3% DMSO solution, 1X HF Buffer, 0.2mM dNTPs, 0.5µM of each primer, 1U of Phusion DNA polymerase (New England Biolabs), and water. Thermocycler parameters were as follows: 98ºC for 30 seconds, followed by 30 cycles of 98ºC for 10 seconds, 60ºC for 30 seconds (30 seconds/kb elongation), and 72ºC for 3 minutes and 39 seconds. The reaction ended with a final elongation at 72ºC for 10 minutes. The primers used in this reaction (Table 1) flanked the human genomic region encompassed between exons 8 through 10, including the 3' UTR (Chr14: 72811671-72818966), resulting in the amplification of a 7296nt product. The PCR reaction was resolved in a 0.8% agarose gel, and the PCR product was purified from the gel by QIAEX gel extraction (Qiagen).

To polyadenylate the ends of the PCR product, 75ng of the purified product was incubated at 70ºC for 30 minutes in the presence of 10X Taq DNA polymerase buffer containing magnesium chloride (Roche), 0.2mM dATP (Roche), and 5U Taq DNA polymerase (Roche). The product was ligated into a pGEMT-Easy vector (Promega, kindly

Table 1. List of primers utilized for cloning of splicing reporters.

Construct	Forward (5'→3')	Reverse (5'→3')	Product Length (nt)	Annealing Temp (°C)
Full-length Numb Reporter	AAAAGCTTCTACCATGAACATTTA	TGCCAGAAGTAGAAGGGGAG	7296	60.0
Numb1kb Reporter	CGCGGATCCggagtgcagtggcgcaatctt	CGCCTCGAGGTCTCGAACTCCTGACCTCAG	1184	54.0
Del1Reporter	caccttaatttgaaattgttttcgtaggtacattcacctgactgacacagctcc	ggagctgtgtcagtcaggtgaatgtacctacgaaaacaatttcaaattaaggtg	5417	68.0
Del2 Reporter	gccagttagctgagtgggaactagggccatagagcttttataaaatacag	ctgtattttataaaagctctatggccctagttcccactcagctaactggc	5463	68.0
F1R1 Reporter	CCGCTCGAGcagtattattgttaacataatctgacctttgg	cgcggatccGGAATCTGTATTTTATAAAAGCTCTATGGG	841	50.0
F1R2 Reporter	CCGCTCGAGcagtattattgttaacataatctgacctttgg	cgcggatccGTAAGCAACTTATTTCTAGGAGGG	781	50.0
F2R1 Reporter	CCGCTCGAGcctacttcattatgccgaaggc	cgcggatccGGAATCTGTATTTTATAAAAGCTCTATGGG	726	50.0

provided by Dr. Daniela Rotin, Toronto) for one hour, and a fraction of the ligation reaction was transformed into competent DH5α E. coli. The bacteria was streaked onto an LB plate coated with 1000x diluted ampicillin and incubated at 37ºC overnight. A single colony was picked and grown in LB supplemented with ampicillin (diluted 1000X) overnight in a shaker (225 RPM, 37ºC). DNA was purified from the bacterial preparation using a DNA extraction kit (Qiagen).

The purified plasmid was digested with NotI at 37ºC to separate the insert from the vector. The reaction was resolved in an agarose gel and the insert was extracted and purified from the gel. The insert was ligated into a pcDNA3.1+ vector (Invitrogen) containing an N-terminal double-HA tag (constructed by lab), which was previously digested with NotI and treated with shrimp alkaline phsophatase (Fermentas). The ligation was set up in a 3:1 mol vector:mol insert ratio, in the presence of 1U of T4 DNA ligase (Fermentas) and 1X T4 DNA ligase buffer. The reaction was incubated overnight at 15ºC. Reactions were transformed into competent DH5α. DNA was propagated in the bacteria and purified as described above. The plasmid sequence was verified by 5'-sequencing (with T7: 5'-TAA TAC GAC TCA CTA TAG GG-3') and 3'-sequencing (with BGH: 5'-TAG AAG GCA CAG TCG AGG-3'), as well as by sequencing using primers that targeted exon 9.

2.1.2 Construction of Truncated (Numb1kb) Human Numb E9 Alternative Splicing Reporter.

A 50µL PCR reaction was set up using 10ng of the BAC plasmid, 1X ThermoPol Buffer, 0.2mM dNTPs, 0.25µM of each primer, 1U of Vent DNA polymerase (New England Biolabs), and water. Thermocycler parameters were as follows: 95ºC for 2 minutes, followed by 30 cycles of 95ºC for 30 seconds, 54ºC for 30 seconds, and 72ºC for 1 minute and 12 seconds (1 minute/kb elongation). The reaction ended with a final elongation at 72ºC for 5

minutes. The primers used in this reaction (Table 1) flanked the human genomic region including exon 9, 540nt of upstream intron, and 507nt of downstream intron. This region encompassed chromosome 14 from positions 72815237-72816420. The amplified product was 1184nt in length.

The PCR reaction was purified (Qiagen) and digested for seven hours at 37ºC with BamHI and XhoI. The insert was purified and ligated in a 1:6 vector:insert ratio with EoxnTrap pET01 vector, which was previously digested with XhoI and BamHI followed by SAP treatment. The reaction was set up as described above, and incubated overnight at room temperature. The reaction was transformed in competent DH5α. DNA was propagated in the bacteria and purified as described above. The plasmid sequence was verified using primers ConstEx Foward and Reverse, which each target the constitutive exons built-in into the vector (Table 3).

2.1.3 Mutagenesis of Truncated Numb Splicing Reporter.

Using the Numb1kb plasmid as a template, a series of deletions were made using the primers listed in Table 1. A schematic of the deletions is available in Figure 3.14.

For the F1R1, F2R1, and F1R2 constructs, 50μL PCR reactiosn were set up using 100ng of template, 0.25μM of each primer, 1X ThermoPol Buffer, 0.2mM dNTPs, and 1U of Vent DNA polymerase. Thermocycler parameters are as described in Section 2.1.2. The PCR reactions were digested overnight at 37ºC and resolved in an agarose gel. DNA was purified by gel extraction and ligated into a ExonTrap pet01 vector, which was previously digested with the same enzymes and treated with shrimp alkaline phosphatase (SAP). Ligation reactions were set up as previously described in Section 2.1.2. The reaction was transformed in competent DH5α. DNA was propagated in the bacteria and purified as described above. The plasmid sequences were verified using primers ConstEx Foward and Reverse (Table 3).

For the Del1 and Del2 constructs, PCR reactions were set up using a QuikChange II kit (Stratagene) containing 10ng of the Numb1kb template, 1X reaction buffer, 125ng of each primer, 0.2mM dNTPs and 2.5U of Pfu Turbo enzyme. Thermocycler parameters are as follows: 95ºC for 1 minute, followed by 18 cycles of 95ºC for 50 seconds, 60ºC for 50 seconds, and 68ºC for 1 minute/kb product length (5 min 26 seconds for Del1, and 5 min 28 seconds for Del2). A final elongation step of 68ºC for 7 minutes was also conducted. The reactions were incubated with 10U DpnI enzyme for 1 hour at 37ºC, prior to transformation. Reactions were transformed in competent DH5α E. Coli. DNA was propagated in the bacteria and purified as described above. The plasmid sequences were verified using primers ConstEx Foward and Reverse (Table 3).

For the Mut1 and Mut2 constructs, 50µL PCR reactions were set up using approximately 100ng of template, 0.25µM of each primer, 1X ThermoPol Buffer, 0.2mM dNTPs, and 1U of Vent DNA polymerase. The thermocycler parameters, as well as digestion, ligation, and transformation methodologies are as described in Section 2.1.2. The plasmid sequences were verified using primers ConstEx Foward and Reverse (Table 3).

2.1.4 Cloning of Splicing Factor cDNA.

An HA-tagged YBX1 construct in a pcDNA3.1 vector was kindly provided by Dr. Annie Huang (Hospital for Sick Children). Constructs for human full-length FOX2, NOVA1, MBNL1, ASF/SF2, PTBP1 and PTBP2 were obtained from the SPARC BioCenter (Hospital for Sick Children, Toronto). The inserts in each construt was amplified by PCR and ligated into 2HA-pcDNA3.1+ vectors. Primers used for cloning each plasmid are listed in Table 2.

A 50µL PCR reaction was set up for each construct using 50-150ng of DNA, 1X PCR Reaction buffer, 0.2mM dNTPs, 0.25µM of each primer, 1.25U of Taq DNA polymerase

Table 2. List of primers utilized for cloning of splicing factors.

Construct	Forward (5'→3')	Reverse (5'→3')	Product Length (nt)	Annealing Temp (°C)
FOX2	CG GGA TCC GAG AAA AAG AAA ATG GTA ACT CAG	CCGCTCGAGTCACTTCAGTAGGGGGCAA	1080	57.0
NOVA1	C CGC TCG AGG GCG GCA GCT CCC ATC CAG	TGC TC TAG AAC TCA ACC CAC TTT CTG AGG ATT GGC AG	1521	58.0
MBNL1	CG GGA TCC GGC CGT TGC TCC AGG GAG AAC	GC TC TAG ATT CTA CAT CTG GGT AAC ATA CTT GTG GC	1032	54.0
ASF/SF2	CGC GGA TCC tcg gga ggt ggt gtg att cgt	CCG GA ATT CCA tta tgt acg aga gcg aga tct g	744	57.0
PTBP1	CGCGGATCC gac ggc att gtc cca gat ata gc	CCGGAATTC CTA GAT GGT GGA CTT GGA GAA GGA	1671	55.0
PTBP2	CGC GGA TCC gac gga atc gtc act gag gtt gca	CCG GA ATT CCA tta aat tgt tga ctt gga gaa aga cac	1593	67.0

Table 3. List of primers utilized for semi-quantitative PCR.

Target	Forward (5'→3')	Reverse (5'→3')	Product Length (nt)	Annealing Temp (°C)
Endogenous Numb Isoforms	GAAGGGGAGGCAGAGAGC	GATGCTGGCTGGGAGATG	479 and 335	57.7
ConstEx (pET01)	GATCCGCTTCCTGCCCCTG	TGCCGGGCCACCTCCAGTG	-	59.0
Full-length reporter	TCCAGTGTGGTGGAATTCTG	GATGCTGGCTGGGAGATG	608 and 464	53.0
b-actin	AAGATCAAGATCATTGCTCCTC	GGGTGTAACGCAACTAAGTC	182	55.0
c-jun	GCATGAGGAACCGCATCGCTGCCTCCAAGT	CGCGCCAAGTCCTTCCCACTCGTGCACACT	411	63.1

(Roche), and water. Thermocycler parameters were as follows: 94ºC for 2 minutes, followed by 30 cycles of 94ºC for 30 seconds, the annealing temperature specific to each primer pair for 30 seconds (listed in Table 2), and 72ºC for a time specific to each primer pair (1 minute/kb elongation; times listed in Table 2). The reaction ended with a final elongation at 72ºC for 7 minutes. PCR reactions were digested at 37ºC overnight (FOX2: XhoI and BamHI, NOVA1: XhoI and XbaI, MBNL1: BamHI and XbaI, ASF/SF2: BamHI and EcoRI, PTBP1: BamHI and EcoRI, PTBP2: EcoRI only). For each reaction, 2HA-pcDNA3.1+ was digested in the same enzymes for the same time span, and then treated with SAP for 1 hour at 37ºC. All digestion reactions were resolved in an agarose gel and purified by gel extraction. Ligations were set up in a 1:5 mol vector: mol insert ratio. Reactions were set up as described in Section 2.1.2. The ligations were transformed in competent DH5α E. coli. DNA was propagated in the bacteria and purified as described above. The plasmid sequences were verified by 5'-sequencing with a T7 primer, and by 3'-sequencing with a BGH primer.

2.2 CELL CULTURE AND TRANSFECTION

2.2.1 Cell Culture.

Human HEK 293T (ATCC), MCF-7 (ATCC) and A549 (kindly provided by Dr. Michael Moran) cells were maintained in DMEM (Wisent) supplemented with 10% fetal bovine serum (FBS, Wisent). Murine p19 (ATCC) cells were maintained in AMEM (Wisent) supplemented with 7.5% fetal calf serum (CS, Wisent) and 2.5% FBS (Jones-Villeneuve, Rudnicki, Harris, & McBurney, 1983). All cells were grown in the absence of mycoplasma and incubated at 37ºC with 5% CO_2.

2.2.2 Transient Transfection.

Cells were grown to 70-80% confluence in 6-well plates (Nunc) and transfected with

1μg DNA 18-20 hours after seeding, using Lipofectamine 2000 (Invitrogen) and Opti-MEM I reduced serum medium (Life Technologies), according to manufacturers' directions. Cells were maintained in serum-supplemented medium during the transfection process. 24 hours post-transfection, cells were trypsinized, spun down and separated in half. Each half was lysed in the appropriate lysis buffer for either RNA or protein extraction.

For transfecting cells with siRNAs, cells were grown to 60-70% confluence in 6-well plates and transfected with 150pmol siRNA approximately 20 hours post-seeding, using Lipofectamine 2000 and Opti-MEM I, according to manufacturers' directions. 48 hours post-transfection, cells were trypsinized, spun down and separated in half. Each half was lysed in the appropriate lysis buffer for either total RNA or whole-cell protein lysate extraction.

2.2.3 Kinase Inhibition and Overexpression Assays.

The MEK inhibitor U0126 (Cell Signaling Technology) was prepared in 100% DMSO as a 10mM stock. The PI3 kinase inhibitor LY 294002 (Cell Signaling Technology) was also prepared in 100% DMSO as a 10mM stock. A549 and MCF-7 cells were grown to 70% confluence in 6-centimetre plates. 18-20 hours after seeding, the media was replaced with DMEM supplemented with 10% FBS and 20μM of DMSO, U0126, or LY 294002. Each experiment was performed in duplicate. The treated cells were lysed 48 hours post-treatment, and each replicate was lysed directly in RLT lysis buffer supplemented with β-mercaptoethanol (for total RNA extraction) or in RIPA lysis buffer with protease inhibitors (for whole-cell protein lysate collection).

Constructs for constitutively active MEKK-EE and MEK-EE, in pcDNA3.1 vectors, were kindly provided by Dr. Vuk Stambolic (Toronto). A constitutively active V12HRas construct, in a pcDNA3.1 vector, was kindly provided by Dr. Gelareh Zadeh (Toronto). HA-tagged kinase-dead Akt1 and HA-tagged constitutively active Akt were kindly provided by

Dr. James Woodgett (Toronto).

To transiently express constitutively active or kinase-dead kinase constructs, 1µg of each construct was transfected in HEK 293T cells, as described above. Cells were lysed 24 hours post-transfection, and total RNA and whole-cell protein lysate was extracted as described above.

2.2.4 Transcription Inhibition Assay.

Actinomycin D (from a species of *Streptomyces*) was obtained in a powder (Roche) and diluted to 1mg/mL in 100% ethanol. A549 cells grown to 70% confluence in 6-well plates were treated with 5µg/mL of actinomycin D in DMEM supplemented with 10% FBS. Cells were treated with actinomycin D for either 0, 3.5, 6.5, 8.5, and 26.5 hours, after which cells were trypsinized and spun down, and cytoplasmic RNA was isolated, as described above.

2.2.5 Differentiation of p19 cells into Neurons.

p19 cells were differentiated using all-trans retinoic acid (atRA, Sigma) using a protocol slightly modified from that previously described by Jones-Villeneuve et al. (1982). In short, cells were plated at a density of 10^5 cells/mL onto a 100mm bacteriological-grade Petri dish (Fisher Scientific) in the presence of $5x10^{-7}$M atRA (prepared in 100% ethanol to a concentration of 0.01M) in reduced-serum media (AMEM supplemented with 5% calf serum). After two days, the aggregated cells were removed from the plate and replated onto a new 100mm bacteriological-grade Petri dish in reduced-serum media in the presence of $5x10^{-7}$M atRA, for another three days. Cell aggregates were then plated onto 35mm tissue culture-grade dishes (Corning) for an additional five days. After five days, extensive neurite outgrowth can be observed. Due to the low number of cells used in each experiment, each experiment was performed in duplicate, and each replicate was lysed directly in RLT lysis

buffer with β-mercaptoethanol (for total RNA extraction) or in PLC lysis buffer with protease inhibitors (for protein lysate collection). RNA and protein was collected 0, 2, 5, 7, and 10 days after the commencement of differentiation.

2.3 Protein Isolation and Western Blotting

2.3.1 Protein Isolation.

Cells were washed three times with cold 1X PBS, lysed in either PLC lysis buffer (30 mM HEPES (pH 7.5), 150 mM NaCl, 1% Triton X-100, 10% glycerol, 1 mM EGTA, 1.5 mM $MgCl_2$) or radioimmunoprecipiation assay (RIPA) buffer (150mM NaCl, 50mM Tris (pH 8.0), 1% Triton X-100, 0.5% sodium deoxycholate, 0.1% SDS), supplemented with protease inhibitors (Roche cOmplete Protease Inhibitor Cocktail Tablet). Lysates were incubated at 4ºC for 15 minutes, then spun at full speed for 20 minutes at 4ºC in order to separate protein lysate from insoluble matter. Protein lysates were quantified using the Bradford protein assay (Bio-Rad).

2.3.2 Western Blotting.

Protein lysates (typically 25-30µg) were boiled in 2X Laemmli SDS sample buffer (4% SDS, 20% glycerol, 120mM Tris-HCl (pH 6.8), and bromophenol blue). Proteins were resolved in 10% SDS-polyacrylamide (SDS-PAGE) gels and transferred onto polyvinylidene difluoride membranes (PVDF) by wet transfer. The PVDF membrane was blocked in 1% BSA in 1X Tris-buffered saline with Tween-20 (TBS-T) for an hour at room temperature, on a shaker. Membranes were and immunoblotted with primary antibody (diluted in 1% BSA in TBS-T) overnight at 4°C, on a shaker. The membrane was then probed with secondary antibody conjugated with horseradish peroxidase (diluted in 3% milk in TBS-T) for an hour

at room temperature prior to treatment with Western Lightning Plus ECL (PerkinElmer). Membranes were exposed on HyBlot CL autoradiography film (Denville Scientific) and developed.

2.3.3 Antibodies.

The commercial primary antibodies used were mouse monoclonal anti-HA.11 (Covance, 1:1000), mouse monoclonal anti-α-tubulin (Sigma, 1:5000), rabbit polyclonal anti-phospho-p44/42 MAPK (Cell Signaling Technology, 1:1000), rabbit polyclonal anti-p44/p42 MAPK (NEB, 1:1000), rabbit polyclonal anti-phospho-Akt (Cell Signaling Technology, 1:1000), rabbit polyclonal anti-Akt (Cell Signaling Technology, 1:1000), mouse monoclonal PTPB1 (Novus, 1:1000), rabbit polyclonal SF2/ASF (Cell Signaling Technology, 1:1000).

The method of production of our rabbit polyclonal affinity purified anti-NbA antibody targeting the Numb p66 and p72 isoforms was previously described (Dho et al., 1999). Numb-specific antiserum was generated in rabbits immunized with a peptide corresponding to the sequence TTHPHQSPSLAKQQTFPQYE, conjugated to KLH. The crude serum was then affinity-purified using a GST-fusion protein for NbPTBi. To produce the rabbit polyclonal affinity purified anti-NbC antibody, targeting all Numb isoforms, Numb-specific antiserum was generated in rabbits immunized with a peptide corresponding to the last 15 amino acids of the carboxy terminal of Numb (Verdi et al., 1999). Both antibodies were used at a dilution of 1:500.

The secondary antibodies used were as follows: Protein A HRP (for Numb antibodies), Anti-Mouse HRP (for PTBP1, HA.11 and tubulin antibodies) and Anti-Rabbit HRP (for phosphorylated and total MAPK and Akt, as well as for SF2/ASF). All secondary

antibodies were used at a dilution of 1:10000.

2.3.4 Numb Immunoprecipitation

1 mg of lysate was brought up to a total volume of 1mL in PLC lysis buffer. Samples were incubated for 2-3 hours with 50µL of protein A sepharose beads and 1µg of NbA antibody, on a shaker at 4ºC. Beads were washed five times with PLC lysis buffer, resuspended in 30µL of 2X Laemmli buffer, and boiled.

2.4 RNA Isolation

2.4.1 Isolation of Total RNA.

Cells were suspended in RLT buffer (Qiagen) with 10µL/mL β-mercaptoethanol. Lysate was homogenized with a 23-gauge needle, and total RNA was isolated and purified with RNEasy Mini Kit silica columns (Qiagen), according to manufactuers' instructions. The quality of total RNA was measured by absorbance: samples with absorbance ratios A_{260}/A_{280} and A_{260}/A_{230} of at least 1.90 were deemed to be of high quality.

2.4.2 Isolation of Nuclear and Cytoplasmic RNA.

Cells were lysed in cold buffer RLN (50mM Tris-HCl (pH 8.0), 140mM NaCl, 1.5mM $MgCl_2$, 0.5% NP-40), supplemented with 1mM fresh DTT and 1000U/mL RNAse Inhibitor (Thermo Scientific). Lysate was incubated at 4°C for 5 minutes, and centrifuged at 4°C for 2 minutes at 300xg, in order to separate the cytosol from the nuclear compartments.

For cytoplasmic RNA extraction: The supernatant was collected and resuspended in Buffer RLT supplemented with β-mercaptoethanol. The sample was then resuspended in 100% ethanol prior to RNA extraction using the RNEasy Mini kit (Qiagen).

For nuclear RNA extraction: The pellet was washed in cold buffer RLN supplemented with DTT and RNAse inhibitor, and centrifuged at 4°C for 3 minutes at 300xg. The supernatant was discarded, while the pellet was resuspended in Buffer RLT supplemented

with β-mercaptoethanol and homogenized with a 23-gauge needle. RNA was extracted and purified using the RNEasy Mini kit, according to manufacturers' instructions.

The quality of both nuclear and cytoplasmic RNA was measured by absorbance, as described above (Chapter 2.4.1).

2.5 Semi-Quantitative PCR

1μg RNA was reverse-transcribed using the OmniScript Reverse Transcription kit (Qiagen) and 10μM oligo-dT primers, according to manufacturers' instructions. PCR reactions were subsequently conducted using 1/20 volume of the cDNA in a 50μL reaction using Taq DNA polymerase (Roche). PCR reactions involved a first denaturing of 94ºC for 2 minutes, then multiple cycles of denaturing, annealing and 72ºC elongation, before a final elongation at 72ºC for seven minutes. Transcript expression was conducted on a peltier thermocycler (MJ Research), using the primers and conditions listed in Table 1. PCR reactions were subsequently separated on 1.5% agarose gels pre-stained with RedSafe dye (Chembio). Images were documented as JPEG files and band intensities were quantified using ImageJ.

2.6 Quantitative PCR

RNA samples were reverse transcribed using QuantiTect Reverse Transcription kit (Qiagen) and a prepared mixture of random oligomers and oligo-dT primers, according to manufacturers' instructions. cDNA samples were diluted 15-fold, and 2μL was added to each 18μL real-time reaction in a 96-well clear PCR plate (Axygen). Each real-time reaction was set up with Platinum SYBR Green qPCR SuperMix-UDG (Invitrogen), using 5μM of each forward and reverse primer. Each reaction was set up in triplicate. The quantitative PCR

reactions were run on an Applied Biosystems StepOnePlus thermal cycler, using cycling conditions described by the manufacturer, and an annealing temperature of 60ºC. Reactions were normalized to either 18S or GAPDH expression. A list of primers used for quantitative PCR can be found in Table 2.

2.7 RNA IMMUNOPRECIPITATION (RIP) ASSAY

The protocol used for RNA immunoprecipitation was modified from Jain et al. (2011), Matsumiya et al. (2010), and Booy et al. (2012). Prior to starting the assay, all reagents were made up in RNAse-free and DNAse-free water, and filter-sterilized.

2.7.1 Cell Lysis

HEK 293T cells were grown on two 150mm tissue culture-grade plates, to 80-90% confluency. Cells were washed three times with cold PBS, and scraped off the plate into 10mL cold PBS using a cell scraper. The cells were collected into 15mL conical centrifuge tubes (Corning), and centrifuged at 4°C for 5 minutes, at 2500xg. The supernatant was aspirated and the pellets were resuspended in an equal volume (as measured by eye) of polysome lysis buffer (buffer PLB) (10 mM Hepes (pH 7.0), 100 mM KCl, 5 mM MgCl2, and 0.5% NP-40), supplemented with a protease inhibitor cocktail (Roche), 1mM DTT, and 100U/mL of RNAse inhibitor. Cells were left to swell on ice for five minutes. Cells were gently homogenized with a Dounce homogenizer approximately 15 times. The lysate was centrifuged twice at 4°C for 10 minutes at 12000xg, and the supernatant was collected each time. For each sample, protein quantification was conducted, in order to ensure the presence of protein complexes.

2.7.2 Coating of Sepharose Beads with Antibody

200µL of Protein G sepharose beads were washed three times in Buffer NT-2 (50mM

Table 4. List of human gene-targeting primers utilized for real-time PCR.

Target	Forward (5'→3')	Reverse (5'→3')	Product Length (nt)
SRSF1	CTCCAAGTGGAAGTTGGCAGGATT	ACACCAGTGCCATCTCGGTAAACA	91
PTBP1	AGGGGAAAAACCAGGCCTTC	GGGGTCACCGAGGTGTAGTA	82
Numb+E9 Isoform	CCCCTGATGCTGCTAACAAG	CCTGGAAGAGACCTGGAGAG	93
Total Numb Gene	ATGCAAGATGCCAAGAAAGC	AGGAGAGGTGGGAGAGGATG	99
GAPDH	TGCACCACCAACTGCTTAGC	GGCATGGACTGTGGTCATGAG	87
18S	CGCGGTTCTATTTTGTTGGTTT	TTCGCTCTGGTCCGTCTTG	120
Hes1	AGGCGGACATTCTGGAAATG	TCGTTCATGCACTCGCTGA	130
Hey1	CGGAGTTTGGGATTTCGGGA	AACCAGTCGAACTCGAAGCG	99
Hey2	AGATGCTTCAGGAACAGGG	CAAGAGCGTGTGCGTCAAAG	51

Table 5. List of murine gene-targeting primers utilized for real-time PCR.

Target	Forward (5'→3')	Reverse (5'→3')	Product Length (nt)
Numb+E9 Isoform	TCCCTGATGCTGCTAACAAG	CCTGGAAGAGACCTGGAGAG	93
Total Numb Gene	TTGCAAGATGCCAAGAAAGC	GGGAGAGGTGGGAGAGGATG	99
18S	CGCGGTTCTATTTTGTTGGTTT	TTCGCTCTGGTCCGTCTTG	120
Hes1	AGGCAGACATTCTGGAAATG	TCGTTCATGCACTCGCTGA	130
Hey2	AGATGCTCCAGGCTACAGGG	CAAGAGCATGGGCATCAAAG	51
Hey1	CGGAGTTTGGGGTTTCGGGA	GACCAGGCGAACGCGAAGCG	99

Tris-Hcl (pH 7.4), 150mM NaCl, 1mM MgCl2, and 0.05% NP-40) prior to incubation in 950µL of NT-2 supplemented with 5% BSA overnight on a shaker at 4°C, to produce a 20% bead slurry. The slurry mixture was divided into 3 300µL aliquots and diluted in 1mL of buffer NT-2 supplemented with BSA. For one of the aliquots, extra slurry was added so there were almost twice the volume of beads as there were in the other aliquots. 5µg of antibody (mouse IgG antibody for negative control, and mouse monoclonal anti-PTBP1 for both conditions) was added to each aliquot. For the aliquot with extra beads, 5µg of beads were added. Antibodies were incubated with the beads at 4°C for 2 hours on a shaker. Beads were then washed six times with cold NT-2 buffer.

2.7.3 Immunoprecipitation.

Beads coated in antibody were resuspended in 900µL NET-2 buffer (NT-2 buffer, 20mM EDTA (pH 8.0), 1mM DTT, and 100u/mL RNAse inhibitor). 100µL of lysate was added to the bead mixture, quickly mixed, and centrifuged. A 100µL aliquot was collected to act as a pre-IP input control. The remaining lysate was incubated with the beads at 4°C for 3 hours on a shaker. Beads were washed six times with cold NT-2. During the final wash, beads for each condition were separated into two aliquots.

2.7.4 Protein and Total RNA Extraction

For one of the aliquots, beads were boiled for seven minutes in 2X Laemmli buffer to strip the protein complexes from the beads. Boiled samples were resolved in a 10% SDS-PAGE and Western blotted for mouse monoclonal anti-PTBP1.

For the other aliquot, beads were resuspended in Buffer RLT supplemented with β-mercaptoethanol and incubated at room temperature for 5 minutes. Samples were centrifuged at full speed for 30 seconds at room temperature to pellet the beads, and the supernatant was collected. Input samples were also resuspended in RLT supplemented with β-

mercaptoethanol, and incubated at room temperature for 5 minutes. Total RNA was extracted with the Qiagen RNEasy Mini kit, according to manufacturers' instructions.

2.7.5 Reverse Transcription and Semi-Quantitative PCR

The entire volume of extracted RNA was reverse transcribed using the Omniscript reverse transcriptase enzyme, as described above (chapter 2.5). The resulting cDNA was amplified using Taq polymerase, as described above (chapter 2.5). The primers used targeted exons 8 and 10, respectively, in order to detect endogenous Numb. β-actin was used as a loading control. The PCR reactions were resolved in a 1.5% agarose gel.

2.8 IMMUNOHISTOCHEMISTRY

A549 cells were seeded to 70% confluency on glass cover slips in a 24-well plate. Approximately 24 hours after seeding, cells were treated with 20μM of either DMSO vehicle control or U0126, in DMEM supplemented with 10% FBS. 48 hours after treatment, cells were washed twice with 1X PBS and fixed 2% paraformaldehyde at room temperature for 30 minutes. Cells were washed five times with PBS and permeabilized 0.2% Triton X-100 in PBS for 10 minutes at room temperature. The cells were washed and blocked with 3% normal donkey serum in PBS for 30 minutes at room temperature. The cover slips were incubated overnight in mouse monoclonal anti-PTBP1 antibody diluted 1:500 in 3% donkey serum.

After washing the cover slips, they were incubated in cy3 donkey anti-mouse (red) antibody diluted 1:500 in 3% donkey serum for 30 minutes at 37ºC. Cover slips were incubated in DAPI for a few seconds in order to stain the nuclear compartment. Slides were observed with a confocal microscope.

2.9 DATA ANALYSIS

2.9.1 Semi-Quantitative PCR: Calculation of Numb Exon 9 Inclusion

Images of agarose gels were documented as JPEG files and analyzed with ImageJ. The image type was changed to 8-bit format and the image background was subtracted. For each lane, a box was drawn around both Numb splice isoforms. The band intensity was calculated for each band in each lane. Percent exon 9 inclusion was calculated by dividing the band intensity of the Numb+E9 isoform by the sum of the band intensities of both isoforms, and multiplying by 100%. Change in percent exon 9 inclusion was calculated by subtracting the percent inclusion value for each condition from the percent inclusion value for the control condition. Statistical significance was calculated using a paired t-test on the Δ %exon inclusion values ($p<0.05$).

2.9.2 Quantitative PCR: Calculation of Fold Change

Relative transcript expression was determined using the ΔΔCt method. For each group of technical replicates, the standard deviation was calculated, and any outliers were removed if the standard deviation exceeded 0.25. The mean Ct value for each target gene in each condition was subtracted from the mean Ct value for the endogenous gene in each condition, producing a normalized ΔCt value. The ΔCt value for each treatment was then subtracted form the control condition ΔCt value, producing the ΔΔCt value. Fold change was calculated as $2^{-\Delta\Delta Ct}$. Statistical significance was calculated on the ΔΔCt values using a paired t-test ($p<0.05$).

2.9.2 Quantitative PCR: Calculation of Splicing Index

In order to detect sensitive Numb E9 alternative splicing events, a splicing index value was calculated for expression of each splice variant relative to total Numb transcript expression, as previously described by Langer et al. (2010). In short, expression of both the

Numb+E9 transcript and total Numb transcript was detected for each condition and the ΔΔCt values for each target were calculated for each condition. Splicing index was calculated as $2^{-(\Delta\Delta Ct \text{ of Numb+E9} - \Delta\Delta Ct \text{ of Numb Gene})}$. Statistical significance was calculated on the splicing index values using a paired t-test ($p<0.05$).

CHAPTER 3: RESULTS

3.1 Numb Exon 9 is alternatively spliced in cancer and neuronal differentiation.

Evidence suggests differential expression of alternative splicing of Numb exon 9 (E9) across different tissues and in cancer (Dho, French, Woods, & McGlade, 1999; Misquitta-Ali et al., 2011). In order to assess this differential expression in cell lines, we immunoprecipitated Numb from whole cell protein lysates of HEK 293T (human embryonal kidney), SH-SY5Y (human neuroblastoma), A549 (human lung adenocarcinoma), IMR-32 (human neuroblastoma), and p19 (mouse embryonal carcinoma) cells, followed by immunoblotting with a Numb-specific antibody. Both Numb E9-included and -excluded isoforms p72 and p66 were detected. While HEK 293T, SH-SY5Y and IMR-32 cells predominantly expressed the p66 isoform, both A549 and p19 cells expressed predominantly the p72 isoform (Figure 3.1A).

Previous research conducted by our lab and others revealed that there is a switch from expression of predominantly the p72 isoform to the p66 isoform over the course of retinoic acid (RA)-induced differentiation of p19 cells (Bani-Yaghoub et al., 2007; Dho et al., 1999). We wanted to determine whether this change in protein isoform expression was also reflected at the transcript level. Suspended p19 cells were treated with all-trans RA for a five-day period before being replated onto tissue culture-grade plates and grown for an additional five days. Cells were harvested at 0, 2, 5, 7, and 10 days after initial RA treatment. By Western blotting, the change in Numb protein expression was confirmed. At day 0, undifferentiated p19 cells expressed the p72 isoform almost exclusively; however, by day 10, when the cells were fully differentiated, the p66 isoform was expressed almost exclusively (Figure 3.1B).

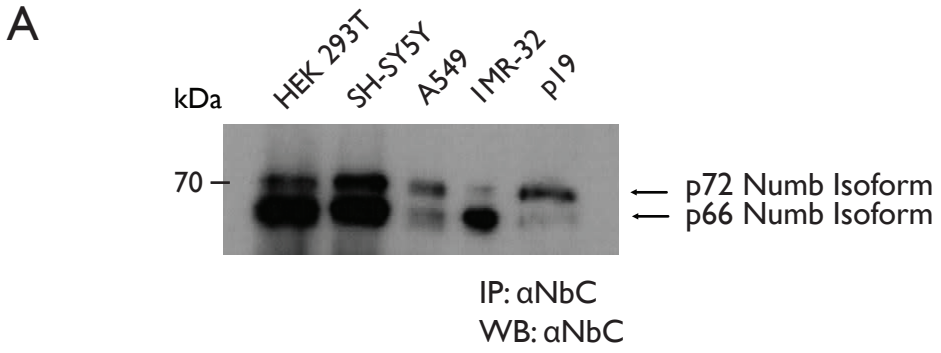
A
kDa
HEK 293T
SH-SY5Y
A549
IMR-32
P19
70
p72 Numb Isoform
p66 Numb Isoform
IP: αNbC
WB: αNbC

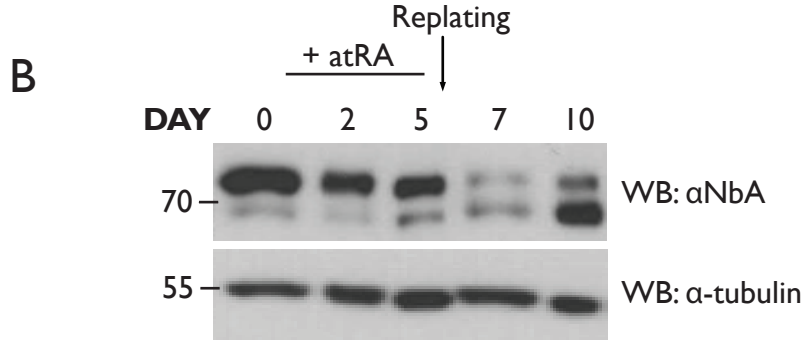
B
Replating
+ atRA
DAY
0
2
5
7
10
70
WB: αNbA
55
WB: α-tubulin

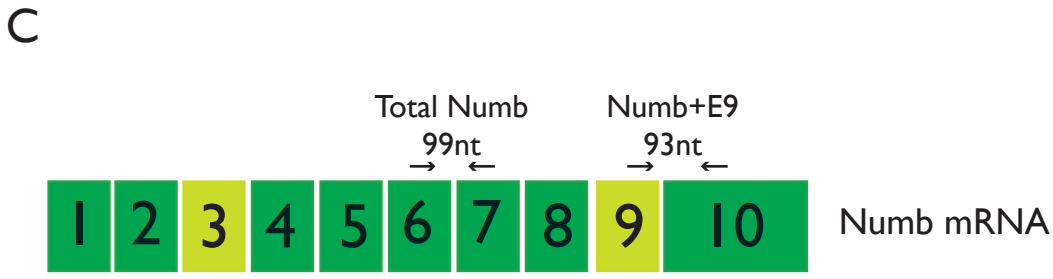
C
Total Numb
99nt
Numb+E9
93nt
1
2
3
4
5
6
7
8
9
10
Numb mRNA

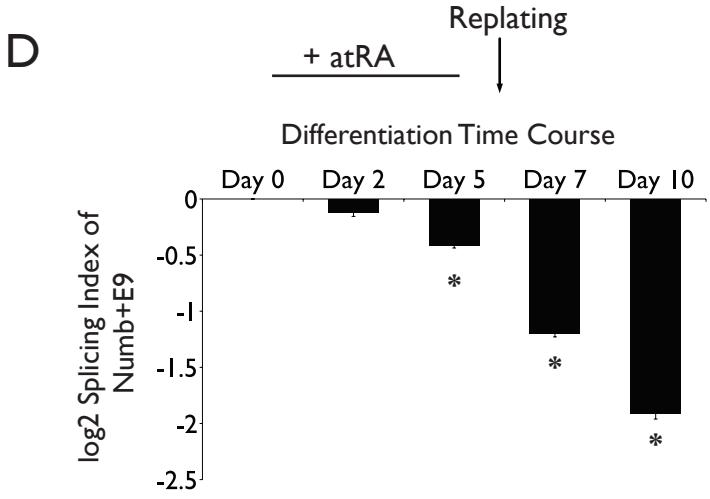
D
Replating
+ atRA
Differentiation Time Course
Day 0
Day 2
Day 5
Day 7
Day 10
log2 Splicing Index of Numb+E9
0
-0.5
-1
-1.5
-2
-2.5
*
*
*

Figure 3.1

Figure 3.1. The alternative splicing pattern of Numb exon 9 differs across cell lines as well as over the course of neuronal differentiation.

(A) Representative Western blot depicting expression of Numb protein variants p66 and p72 in several cell lines. Numb was immunoprecipitated from HEK 293T (human embryonal kidney), SH-SY5Y (human neuroblastoma), A549 (human lung adenocarcinoma), IMR-32 (human neuroblastoma), and p19 (mouse embryonal carcinoma) whole-cell protein lysates using αNbC antibody. The immunoprecipitates were then resolved in an SDS-PAGE gel, and Numb protein expression was detected by Western blotting with αNbC antibody.

(B) Representative Western blot depicting the detection of a Numb alternative splicing event over the course of p19 differentiation into neurons. p19 cells were treated with $5x10^{-7}$ M of all-trans retinoic acid (atRA) while in suspension, for five days, and were then grown in tissue culture-grade plates for an additional five days, where neurite outgrowth was observed. Whole-cell protein lysates were collected at days 0, 2, 5, 7, and 10, and resolved in a 10% SDS-PAGE gel. Numb protein expression was detected by Western blotting with αNbA antibody.

(C) Schematic of the primers used to detect the endogenous Numb E9 alternative splicing event during p19 differentiation. One pair of primers, which bind to sequences in the mouse ortholog of human Numb exons 9 and 10, respectively, was used to detect the presence of the Numb+E9 isoform. Another pair of primers, which bind to sequences in the mouse ortholog of human Numb exons 6 and 7, respectively, was used to detect the presence of all Numb isoforms. The primers were used for detection of the Numb E9 alternative splicing event through quantitative PCR (qPCR), as described in Chapter 2.

(D) log2 fold change expression of the Numb+E9 transcript relative to total Numb transcript

expression, also known as the splicing index (n=3, mean+SEM), over the course of p19 differentiation into neurons. p19 cells were differentiated into neurons as described in Figure 1B. At days 0, 2, 5, 7, and 10, total RNA was collected and transcribed, and the resulting cDNAs were processed through qPCR, using the primers described in Figure 1C to detect Numb+E9 and total Numb, and 18S as an endogenous control. A star (*) indicates statistical significance compared to undifferentiated cells ($p<0.05$). Calculation of the splicing index is described in Chapter 2 and in Langer et al. (2010).

To determine if alternative splicing of Numb accounted for the change in isoform expression, RNA was isolated from cells harvested 0, 2, 5, 7, and 10 days after the initiation of RA-induced differentiation. The RNA was then reverse-transcribed (RT) and the resulting cDNA used for quantitative PCR (qPCR) using primers optimized to detect the Numb+E9 isoform, total Numb transcript (Figure 3.1C), and endogenous control 18S. The relative fold change expression of the Numb+E9 isoform relative to total Numb transcript expression (expressed as the splicing index) was calculated as a means of identifying change in Numb E9 inclusion, as previously described (Langer et al., 2010). At the transcript level, there was a strong trend towards E9 exclusion during the time course of differentiation, with a dramatic decrease occurring at around day 7, after cells had been re-plated, and coinciding with a reduction of p72 protein expression (Figure 3.1D).

3.2 Construction and Validating the Expression of an Alternative Splicing Reporter

In order to investigate the mechanisms that regulate alternative splicing of Numb E9, we constructed a splicing reporter by sub-cloning a human genomic fragment of Numb corresponding to chr14:72811671-72818966 into a pcDNA3.1+ vector containing an N-terminal double-HA (2XHA) tag, a cytomegalovirus promoter and a bovine growth hormone poly-adenylation signal. The genomic fragment corresponds to human Numb E9, its flanking introns (2934nt upstream, 1987nt downstream, and constitutive exons 8 and 10 (Figure 3.2A). When transfected into cells, the reporter was expected to produce two isoforms of Numb (Numb+E9 and NumbΔE9) that are detectable by PCR. In order to detect these two splicing reporter products but not endogenous Numb, we designed a PCR primer that overlapped the 2XHA tag and exon 8. The other PCR primer targeted exon 10 (Figure 3.2B). Primers were designed such that both isoforms were detectable within a single PCR reaction.

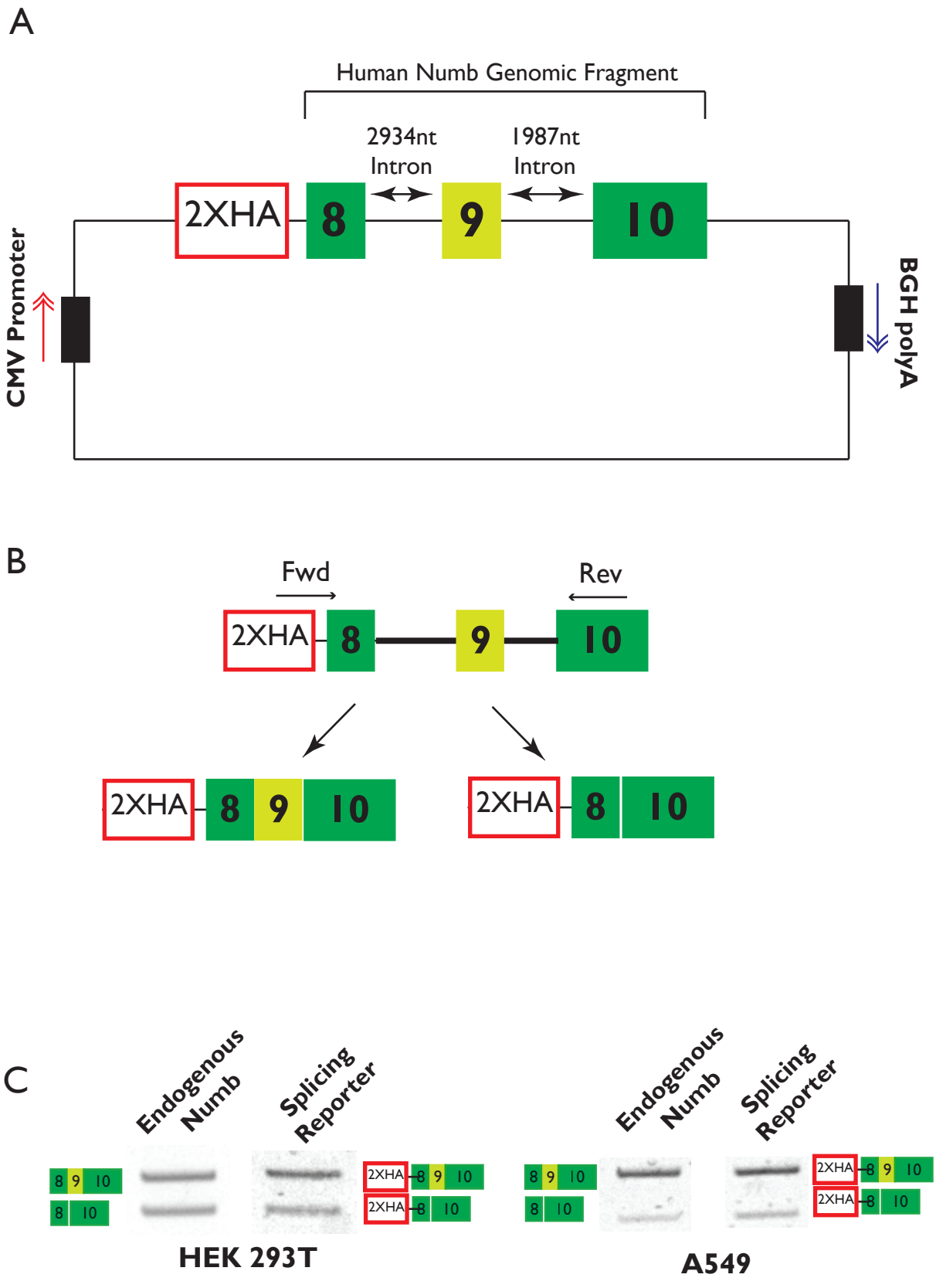
A
Human Numb Genomic Fragment
2934nt Intron
1987nt Intron
2XHA
8
9
10
CMV Promoter
BGH polyA
B
Fwd
Rev
2XHA
8
9
10
2XHA
8
9
10
2XHA
8
10
C
Endogenous Numb
Splicing Reporter
Endogenous Numb
Splicing Reporter
8 9 10
8 10
2XHA 8 9 10
2XHA 8 10
HEK 293T
A549

Figure 3.2

Figure 3.2. Construction and expression of an alternative splicing reporter for human Numb exon 9.

(A) Schematic of an alternative splicing reporter for Numb E9. The backbone is a pcdna3.1+ vector with an amino-terminal double-HA tag, a cytomegalovirus (CMV) promoter and a bovine growth hormone (BGH) poly-adenylation signal. A fragment of human Numb genomic DNA containing the entire region from exons 8 through 10, including introns, was cloned into the multiple cloning site of this vector (chr14:72811671-72818966, hg18). The total length of the insert is 7296nt.

(B) Schematic of primer design to detect expression of the Numb+E9 and NumbΔE9 mRNA isoforms by semi-quantitative PCR. The primers were designed such that both isoforms could be captured in the same PCR reaction. The forward primer was designed to overlap the junction between the double-HA tag and exon 8, while the reverse primer was designed against exon 10. This was to ensure that only isoforms produced by the splicing reporter and not endogenous isoforms, could be detected.

(C) The splicing reporter was expressed in both HEK 293T and A549 cells. 24 hours post-transfection, cells were lysed and total RNA was collected and reverse-transcribed. cDNA was subject to PCR using the primers described in Figure 2B, and resolved in a 1.5% agarose gel. Endogenous cDNA from HEK 293T and A549 cells was also collected, subject to PCR with the same primers, and resolved in a 1.5% agarose gel. ImageJ was used to analyze the expression of the Numb+E9 and NumbΔE9 isoforms. We confirmed that expression of the Numb isoforms when over-expressing the splicing reporter recapitulated endogenous Numb isoform expression in the same cell line.

To validate that the reporter recapitulated the endogenous Numb E9 alternative splicing event, we transfected the reporter in HEK 293T and A549 cells. These cell lines were selected because they show different expression patterns for the Numb splicing event: A549 cells express more of the Numb+E9 isoform compared to HEK 293T cells. After 24 hours of expression, RNA was extracted and reverse transcribed (RT), and the resulting cDNA underwent PCR using primers that specifically amplify the reporter transcripts. cDNA from parental HEK 293T and A549 cells was also collected, and Numb+E9 and NumbΔE9 isoforms were detected by PCR. We found that, in both cell lines, the Numb splicing pattern produced by the splicing reporter recapitulated the endogenous splicing pattern (Figure 3.2C).

3.3 PTBP1 and ASF/SF2 Regulate Numb Exon 9 Alternative Splicing *in vitro*

In order to investigate the splicing factors that regulate alternative splicing of Numb E9, we utilized the online computational program SFmap (http://sfmap.technion.ac.il) (Paz, Akerman, Dror, Kosti, & Mandel-Gutfreund, 2010), which scans an inputted DNA sequence for known splicing factor binding sites, while taking human-mouse conservation into consideration. The human Numb genomic sequence corresponding to chr14:72813900-72818579 (NCBI build 36.1, containing Numb E9 and most of its flanking introns) was searched for motifs with medium stringency. The splicing factors whose motifs identified are listed in Figure 3.3A. We selected the splicing factors ASF/SF2, MBNL1, NOVA1, PTBP1, PTBP2, YBX1, and FOX2 as candidate splicing factors for further investigation. These factors were selected based on their frequency of motif occurrence in the Numb genomic fragment, evidence in literature pointing to their roles in tumour alternative splicing events and differentiation, and previously reported involvement in Numb alternative splicing. The

other splicing factors listed in Figure 3.3A were largely omitted due to their predominant role in constitutive splicing.

The splicing factors FOX2, NOVA1, MBNL1, YBX1, ASF/SF2, PTBP1, and PTBP2 have previously been identified as regulating a wide range of alternative splicing events in tumour development and cell differentiation. FOX2 and NOVA1 have previously been implicated as regulators of Numb E9 alternative splicing to promote E9 exclusion (C. Zhang et al., 2010). Using the UCSC genome browser (genome.ucsc.edu), we utilized SFMap to locate the positions of the predicted motifs for the panel of splicing factors in the inputted Numb fragment (Figure 3.3B).

cDNAs for these selected splicing factors were obtained from the SPARC BioCenter (Hospital for Sick Children, Toronto) and were sub-cloned into a 2XHA-tagged pcDNA3.1+ mammalian expression vector. The 2XHA-tagged splicing factors were co-transfected with the Numb splicing reporter in HEK 293T cells for 24 hours, to assay their effects on alternative splicing of E9. Using RT-PCR, the alternative splicing pattern of the splicing reporter in response to over-expression of each splicing factor was detected using primers specific to the reporter (as described in Figure 3.2B). After resolving the PCR reactions in an agarose gel, the gel image was analyzed using ImageJ, and the percent E9 inclusion value was calculated for each condition (see chapter 2 for details regarding analysis methods). The change in percent E9 inclusion was calculated by comparing the percent E9 inclusion of the splicing reporter when over-expressing a splicing factor against the reporter splicing profile when co-overexpressed with an empty 2XHA-pcDNA3.1+ vector.

Expression of either tagged FOX2, NOVA1, MBNL1 or YBX1 resulted in a significant but modest increase in reporter E9 exclusion (Figure 3.4A, below). Co-transfection of ASF/SF2 with the reporter resulted in nearly exclusive expression of the

A

SPLICING FACTOR	MOTIF	FREQUENCY
ASF/SF2	crsmsgw	4
	ugrwgvh	14
9G8	acgagagay	5
	wggacra	16
SC35	gryymcyr	4
	ugcygyy	24
Tra2alpha	gaagaggaag	7
Tra2beta	gaagaa	8
	ghvvganr	3
	aaguguu	36
SRp20	cuckucy	21
	wcwwc	16
SRp40	yywcwsg	2
SRp55	yrcrkm	3
hnRNPA1	guaguagu	8
	rgnyag	8
hnRNPA2B1	gguaguag	4
	aggwuhgr	11
hnRNPF	gukgykg	9
	gugkau	5
	gggug	4
hnRNPH1	gargag	13
hnRNPM	gguugguu	1
hnRNPU	uguauug	22
MBNL	ygcuky	15
NOVA1	ycay	23
PTB	cucucu	5
	ucuu	8
CUG-BP	ugcug	39
YBX1	caaccacaa	14
FOX1	ugcaug	11
QK1	acuaay	11

Figure 3.3

B

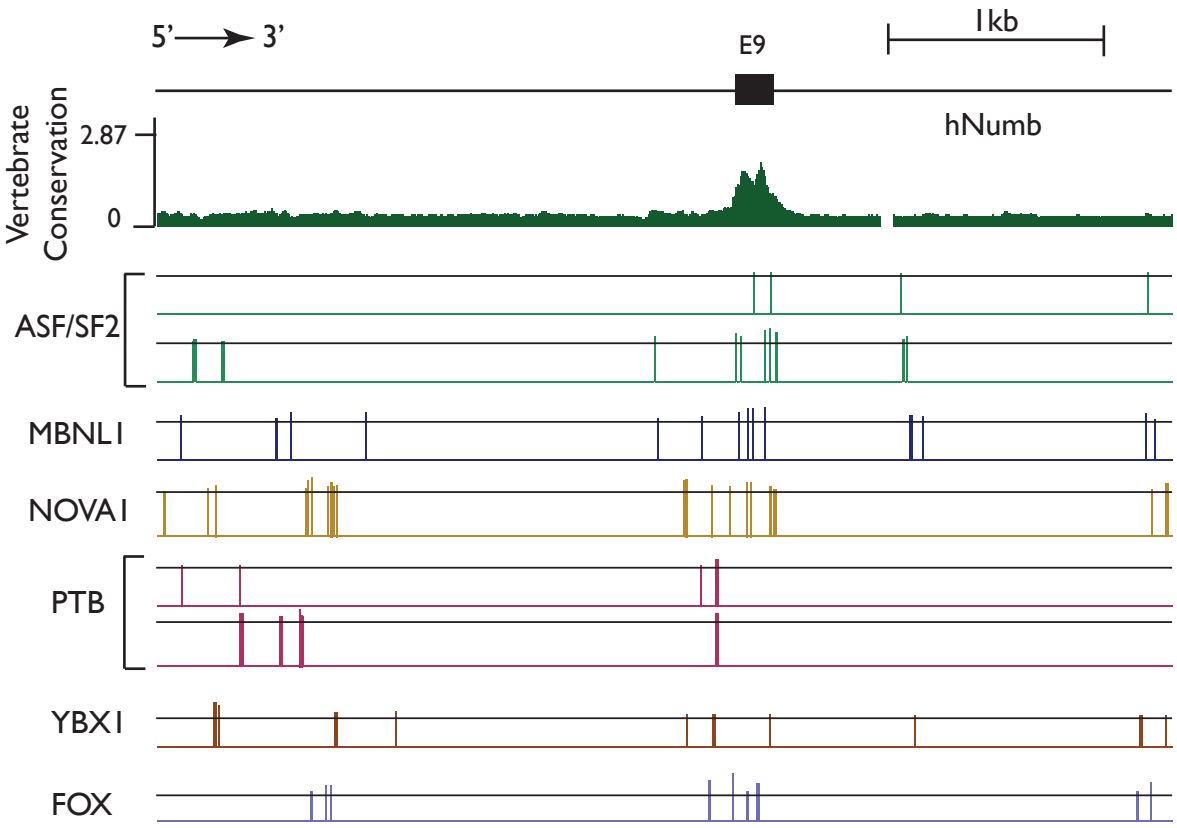

Figure 3.3 (cont'd)

Figure 3.3. Use of the online computational program SFMap to identify putative splicing factors that may regulate alternative splicing of Numb exon 9.

(A) SFMap (http://sfmap.technion.ac.il/) is an online computational program that scans any inputted DNA sequence for known splicing factor binding sites, while taking motif grouping and human-mouse conservation into consideration. The human Numb genomic sequence corresponding to chr14:72813900-72818579 was inputted into the program and the search threshold was set to medium stringency. Predicted splicing factors that may interact with the sequence are listed, alongside their motif binding sequence and the frequency of occurrence on the Numb genomic fragment. The boxed splicing factors are the ones selected as part of of a panel of splicing factors that we believe most likely regulate Numb E9 alternative splicing.

(B) SFMap mapping of the locations of the binding sites of the splicing factors boxed in Figure 3.3A on the human Numb genomic fragment corresponding to chr14:72813900-72818579. The predicted sites were mapped onto the UCSC genome browser as independent tracts for each motif sequence. Note that the splicing factors ASF/SF2 and PTB (PTBP1) have two binding motifs and thus have two tracts. The vertebrate conservation plot was constructed from the UCSC genome browser using the PhyloP vertebrate 28-way basewise conservation track (Miller et al., 2007).

NumbΔE9 isoform (Figure 3.4B, below). In contrast, co-transfection of PTBP1 with the splicing reporter resulted in a strong but not significant increase in E9 inclusion (Figure 3.4B). Co-transfection with PTBP2, a brain-specific orthologue of PTBP1 (Cheung et al., 2009), did not alter E9 splicing (Figure 3.4B), though this may be due to poor expression of our PTBP2 construct (Figure 3.4B, above right).

Since ASF/SF2 and PTBP1 appeared to have opposing effects on Numb E9 splicing, we examined the nature of the relationship between ASF/SF2 and PTBP1. ASF/SF2 was co-expressed with the splicing reporter and increasing amounts of PTBP1 in HEK 293T cells for 24 hours. Changes in Numb E9 inclusion was measured using RT-PCR using the reporter-specific primers described in Figure 3.2B, to detect expression of the Numb reporter isoforms. We found that expression of the Numb+E9 isoform, which is nearly completely lost when ASF/SF2 is expressed, can be recovered with increasing expression of PTBP1, to the point that the change in percent E9 inclusion is no different from control (Figure 3.4C, below). This suggests that ASF/SF2 and PTBP1 work antagonistically in regulating Numb E9 alternative splicing. However, further work needs to be done to establish if this relationship is direct or indirect.

3.4 PTBP1 and ASF/SF2 Expression Regulates Endogenous Numb Exon 9 Alternative Splicing

To determine whether these splicing factors regulated alternative splicing of endogenous Numb exon 9, we over-expressed each in HEK 293T for 24 hours. Post-transfection, we utilized RT-qPCR to determine the endogenous Numb+E9 splicing index, as previously described. The primers used to detect the Numb+E9 transcript and total Numb transcript were the human orthologs of those depicted in Figure 3.1C; however, GAPDH was

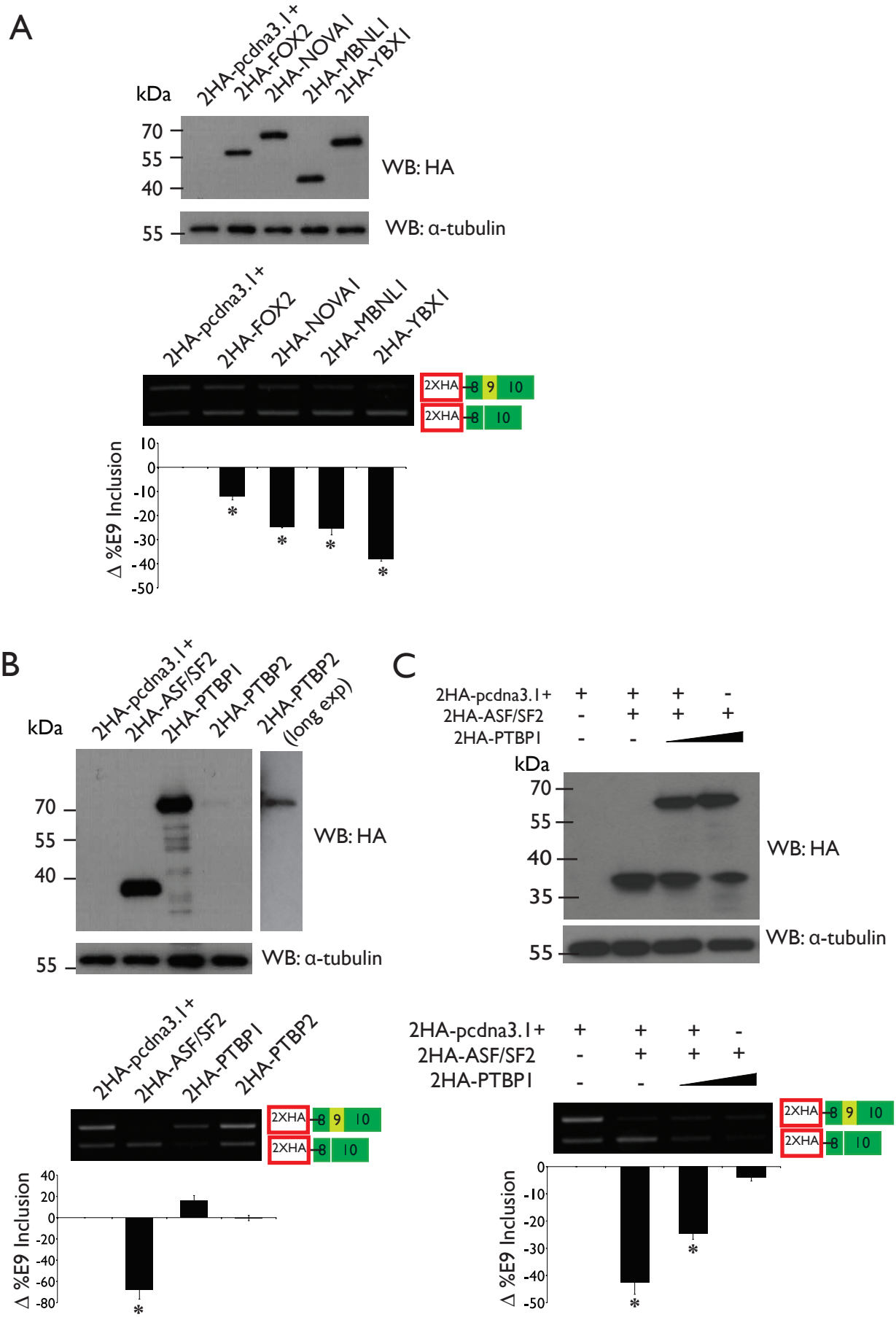
A
2HA-pcdna3.1+
2HA-FOX2
2HA-NOVA1
2HA-MBNL1
2HA-YBX1
kDa
70
55
40
WB: HA
55
WB: α-tubulin
2XHA
8 9 10
2XHA
8 10
Δ %E9 Inclusion
B
2HA-pcdna3.1+
2HA-ASF/SF2
2HA-PTBP1
2HA-PTBP2
2HA-PTBP2 (long exp)
kDa
70
55
40
WB: HA
55
WB: α-tubulin
C
2HA-pcdna3.1+
2HA-ASF/SF2
2HA-PTBP1
kDa
70
55
40
35
WB: HA
55
WB: α-tubulin
Δ %E9 Inclusion

Figure 3.4

Figure 3.4. Over-expression of a panel of splicing factors with a splicing reporter identifies several splicing factors as putative regulators of Numb exon 9 alternative splicing.

(A) Over-expression of the splicing factors FOX2, NOVA1, MBNL1, and YBX1 with the splicing reporter results in Numb E9 exclusion in HEK 293T cells. Cells were transfected with 1μg of either an empty double-HA-tagged pcDNA3.1+ vector or double-HA-tagged full-length constructs of either human FOX2, NOVA1, MBNL1, or YBX1. Each was co-overexpressed with the Numb splicing reporter described in Figure 3.2. 24 hours post-transfection, cells were lysed and both whole-cell protein lysate and total RNA was extracted from the samples. Above, representative Western blot confirming over-expression of the four splicing factors, which were double HA-tagged. Protein lysates were resolved in a 10% SDS-PAGE gel and expression of the splicing factors were confirmed by Western blotting with αHA (HA.11) and the loading control α-tubulin. Middle, a representative RT-PCR depicting the trend towards Numb exon 9 exclusion in the splicing reporter when over-expressing each factor. Total RNA was reverse transcribed to cDNA and subjected to semi-quantitative PCR using the primers described in Figure 3.2B. The PCR reactions were resolved in a 1.5% agarose gel. Below, change in % exon inclusion (n=3, mean+SEM), based on image analysis with ImageJ. A star (*) indicates statistical significance compared to 2HA-pcDNA3.1+ control ($p<0.05$).

(B) Over-expression of the splicing factors ASF/SF2 promotes exon exclusion while over-expression of PTBP1 promotes exon inclusion. Above, a representative Western blot confirming over-expression of 1μg of the three double-HA tagged splicing factors ASF/SF2, PTBP1, and PTBP2 in HEK 293T cells. The Western blot was conducted in a similar manner

to that described in Figure 3.4A. Middle, a representative RT-PCR (1.5% agarose), produced in a similar manner to that described in Figure 3.4A. Below, change in % exon inclusion (n=3, mean+SEM), calculated based on measurements with ImageJ. A star (*) indicates statistical significance compared to 2HA-pcDNA3.1+ control ($p<0.05$).

(C) ASF/SF2 and PTBP1 work antagonistically to regulate Numb alternative splicing. Above, a representative Western blot confirming over-expression of double-HA tagged PTBP1 and ASF/SF2. The Western blot was conducted in a similar manner to that described in Figure 3.4A. Middle, representative RT-PCR (1.5% agarose), produced in a similar manner to that described in Figure 3.4A. Below, change in % exon inclusion (n=3, mean+SEM), calculated based on measurements with ImageJ. A star (*) indicates statistical significance compared to 2HA-pcDNA3.1+ control ($p<0.05$).

used as an endogenous control instead of 18S.

Similar to the effects on the splicing reporter, over-expression of tissue-specific splicing factors YBX1 and MBNL1 produced a modest increase in endogenous Numb exon exclusion, while over-expression of either FOX2 or NOVA1 did not have a significant effect on alternative splicing of endogenous Numb (Figure 3.5A, right). In addition, over-expression of ASF/SF2 and PTBP1 had significant opposing effects on endogenous E9 exclusion and inclusion, respectively, whereas PTBP2 had no effect (Figure 3.5B, right), though this can be attributed to its poor expression (Figure 3.5B, left). We decided to focus on ASF/SF2 and PTBP1 since ASF/SF2 over-expression produced the most dramatic trend towards exon exclusion, and PTBP1 was the only factor in our panel to significantly promote E9 inclusion.

To confirm the roles of ASF/SF2 and PTBP1 in regulating Numb alternative splicing, we also depleted both HEK 293T cells and A549 cells of either ASF/SF2 or PTBP1 using siRNAs for 48 hours. Knockdown of either ASF/SF2 or PTBP1 was confirmed by Western blotting (Figure 3.5C). We then examined the effect of splicing factor depletion on endogenous Numb alternative splicing by using semi-quantitative PCR to measure the changes in expression of endogenous Numb transcript isoforms with primers that target exons 8 and 10. Compared to the Numb splicing pattern in cells treated with a negative control siRNA, knockdown of PTBP1 resulted in increased exon exclusion in both cell types (Figure 3.5D, left). In contrast, depletion of ASF/SF2 in either HEK 293T cells or A549 cells resulted in a trend towards E9 inclusion, though this was not significant (Figure 3.5D, below right). This could be attributed to the poor knock-down efficiency of the ASF/SF2 siRNA (Figure 3.5C). The difference in the observed knockdown efficiency between the two cell lines may be attributed to the increased transfection efficiency in HEK 293T cells compared

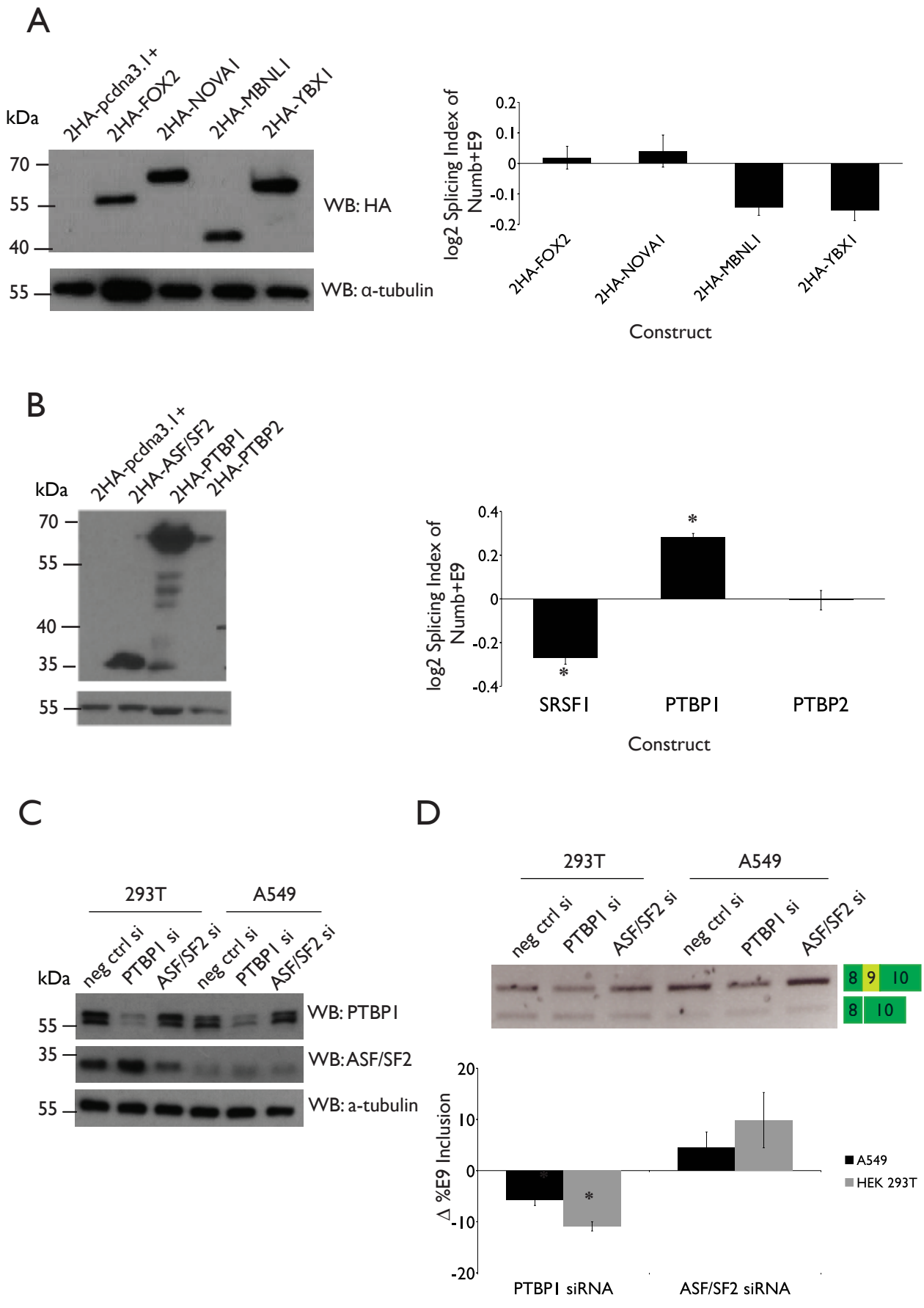
A
kDa
2HA-pcdna3.1+
2HA-FOX2
2HA-NOVA1
2HA-MBNL1
2HA-YBX1
70
55
40
55
WB: HA
WB: α-tubulin
log2 Splicing Index of Numb+E9
0.2
0.1
0
-0.1
-0.2
2HA-FOX2
2HA-NOVA1
2HA-MBNL1
2HA-YBX1
Construct
B
kDa
2HA-pcdna3.1+
2HA-ASF/SF2
2HA-PTBP1
2HA-PTBP2
70
55
40
35
55
log2 Splicing Index of Numb+E9
0.4
0.2
0
-0.2
-0.4
*
*
SRSF1
PTBP1
PTBP2
Construct
C
293T
A549
neg ctrl si
PTBP1 si
ASF/SF2 si
neg ctrl si
PTBP1 si
ASF/SF2 si
kDa
55
35
55
WB: PTBP1
WB: ASF/SF2
WB: a-tubulin
D
293T
A549
neg ctrl si
PTBP1 si
ASF/SF2 si
neg ctrl si
PTBP1 si
ASF/SF2 si
8 9 10
8 10
Δ %E9 Inclusion
20
10
0
-10
-20
*
*
A549
HEK 293T
PTBP1 siRNA
ASF/SF2 siRNA

Figure 3.5

Figure 3.5. Regulation of endogenous Numb exon 9 alternative splicing by panel of splicing factors.

(A) Left: representative Western blot depicting over-expression of 1μg of the double HA-tagged constructs FOX2, NOVA1, MBNL1, and YBX1 in HEK 293T cells. Blots were probed for either αHA or α-tubulin. Right: log2 splicing index of endogenous Numb+E9 isoform expression relative to total Numb expression (n=3, mean+SEM). A star (*) indicates statistical significance relative to 2HA-pcDNA3.1+ control ($p<0.05$).

(B) Left: representative Western blot depicting over-expression of 1μg of the double HA-tagged constructs ASF/SF2, PTBP1, and PTBP2 in HEK 293T cells. Right: log2 splicing index of endogenous Numb+E9 isoform expression relative to total Numb expression (n=3, mean+SEM). A star (*) indicates statistical significance relative to 2HA-pcDNA3.1+ control ($p<0.05$).

(C) Representative Western blot confirming knockdown of either PTBP1 or ASF/SF2 protein expression as a result of knockdown with 150 pmol siRNA for 48 hours in either HEK 293T or A549 cells. Blots were probed for either PTBP1, ASF/SF2 or the loading control α-tubulin**.**

(D) Change in Numb exon 9 inclusion as measured by RT-PCR (n=3), in response to treatment of HEK 293T or A549 cells with either PTBP1 or ASF/SF2 siRNAs. RNA was reverse-transcribed, and the resulting cDNA was subjected to semi-quantitative PCR using primers that target human Numb exons 8 and 10, respectively, in order to detect endogenous Numb+E9 and NumbΔE9 transcripts. The PCR reactions were resolved in a 1.5% agarose gel. Below, change in % exon inclusion (n=3, mean+SEM), based on image analysis with ImageJ. A star (*) indicates statistical significance relative to negative control siRNA ($p<0.05$).

to A549 cells.

These observations provide evidence that splicing factors ASF/SF2 and PTBP1 regulate alternative splicing of Numb E9 in both HEK 293T cells and the A549 lung adenocarcinoma cell line. ASF/SF2 appears to act as a splicing silencing regulator that promotes E9 exclusion, whereas PTBP1 acts as an enhancing regulator that promotes E9 inclusion.

3.5 MAPK/ERK Signalling Regulates Numb Exon 9 Alternative Splicing

Several studies have demonstrated that Numb E9 alternative splicing is misregulated in lung, breast and colon adenocarcinoma, resulting in increased E9 inclusion compared to matched normal tissue (Langer et al., 2010; Misquitta-Ali et al., 2011). Since MAPK/ERK and PI3K/Akt signal transduction pathways are constitutively active in non small-cell lung cancer (Brognard, Clark, Ni, & Dennis, 2001; Roberts & Der, 2007), we examined whether these pathways played a role in regulating Numb E9 alternative splicing.

A549 lung adenocarcinoma cells were treated with either DMSO vehicle control, U0126 (a selective MEK inhibitor), or LY 294002 (a selective PI3K inhibitor) for 48 hours. Effective inhibition of MEK and PI3K signalling was confirmed by immunoblotting lysates of both control and treated cells with anti-pERK and anti-pAkt antibodies (Figure 3.6A). Following treatment, total RNA was extracted and RT-qPCR was used to measure the expression levels of endogenous Numb transcripts and calculate the log2 splicing index of exon inclusion, using the human orthologs of the primers described in Figure 3.1C and GAPDH as an endogenous control. There was a strong trend towards Numb E9 exclusion in response to MEK inhibition compared to DMSO control, while LY 294002 treatment had little effect on the alternative splicing event (Figure 3.6B). At the transcript level, MEK

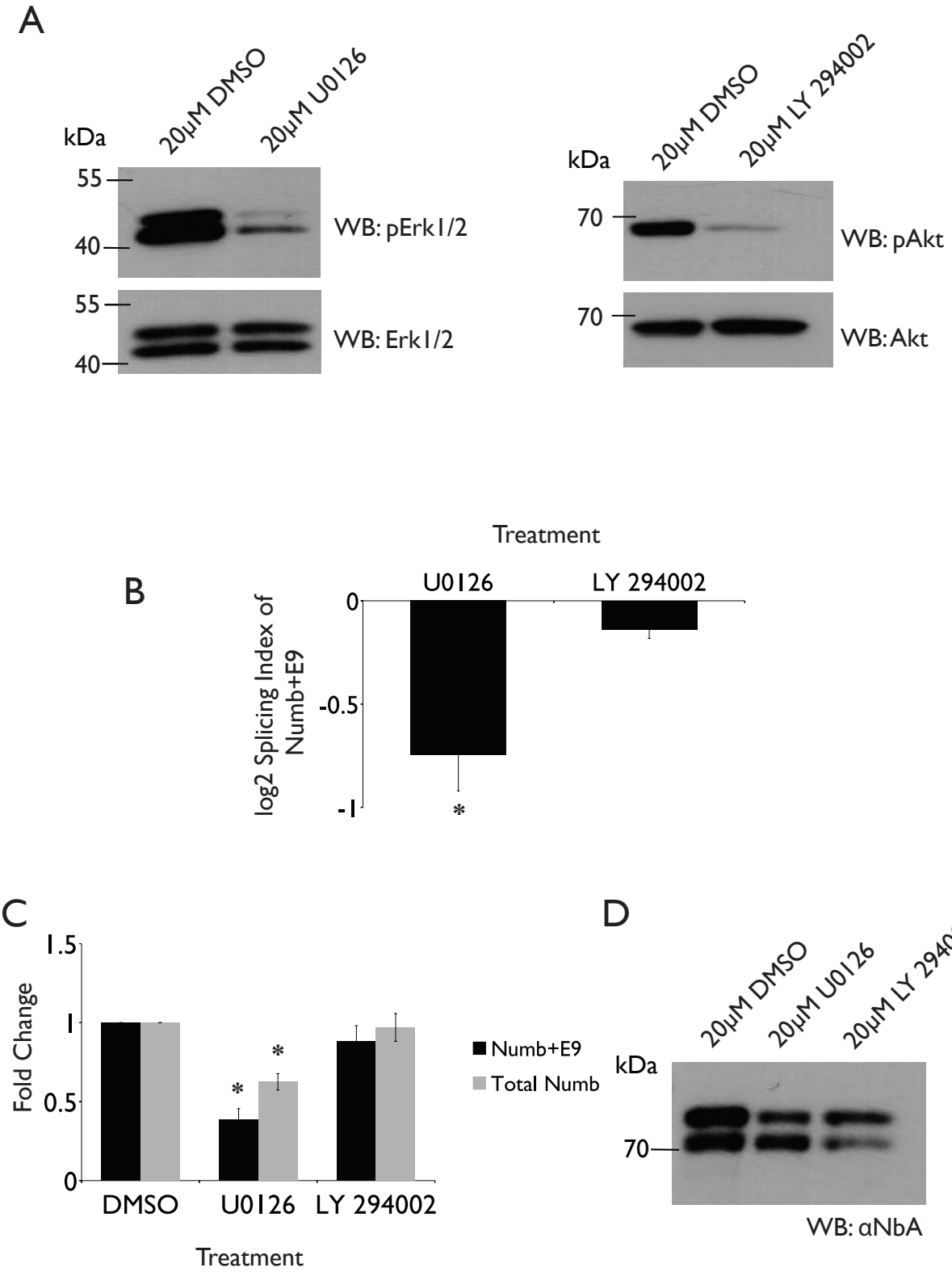
A
kDa
20μM DMSO
20μM U0126
55
40
WB: pErk1/2
55
40
WB: Erk1/2
kDa
20μM DMSO
20μM LY 294002
70
WB: pAkt
70
WB: Akt
B
Treatment
U0126
LY 294002
log2 Splicing Index of Numb+E9
0
-0.5
-1
*
C
Fold Change
1.5
1
0.5
0
*
*
DMSO
U0126
LY 294002
Treatment
Numb+E9
Total Numb
D
20μM DMSO
20μM U0126
20μM LY 294002
kDa
70
WB: αNbA

Figure 3.6

Figure 3.6. Inhibition of MAPK/ERK and PI3K/Akt signalling pathways to identify their role in Numb exon 9 alternative splicing.

(A) Representative Western blots confirming inhibition of MAPK/ERK and PI3K/Akt signalling after treatment of A549 lung adenocarcinoma cells with U0126 and LY 294002, respectively. A549 lung adenocarcinoma cells were treated for 48 hours with 20μM of either DMSO, MEK inhibitor U0126, or PI3K inhibitor LY 294002. Post-treatment, whole-cell protein lysate was extracted and resolved in a 10% SDS-PAGE gel. Western blots were probed for either phosphorylated or total ERK1/2 (for cell lysates treated with U0126; left), or either phosphorylated or total Akt (for cell lysates treated with LY 294002; right).

(B) log2 splicing index of endogenous Numb+E9 transcript expression relative to total Numb transcript expression (n=3, mean+SEM). A star (*) indicates statistical significance relative to DMSO vehicle control ($p<0.05$).

(C) Fold change of Numb+E9 and total Numb transcript expression after treatment of A549 cells with 20μM of either U0126 or LY 294002 for 48 hours (n=3, mean+SEM). Fold change was calculated relative to Numb+E9 and total Numb transcript expression in A549 cells treated with 20μM DMSO. A star (*) indicates statistical significance relative to DMSO ($p<0.05$).

(D) Representative Western blot depicting human Numb p72 and p66 protein isoform expression when A549 cells were treated with 20μM of either U0126 or LY 294002 for 48 hours. Lysates obtained for Figure 3.6A were resolved in a 10% SDS-PAGE gel. Western blots were probed for either αNumbA or α-tubulin.

inhibition also decreased total Numb transcript expression, while PI3K inhibition did not (Figure 3.6C). Finally, using a Numb-specific antibody that detects both the p72 and p66 isoforms, we confirmed that treatment of A549 cells with U0126 also resulted in decreased p72 isoform expression in agreement with the observed decrease in E9 inclusion (Figure 3.6D).

As an alternative approach to determine whether upregulation of either MAPK/ERK or PI3K/Akt signalling altered the Numb alternative splicing pattern, HEK 293T cells were transfected with constitutively active mutants V12HRAS, MEK kinase (MEKK), or MEK for 24 hours. Expression of activated Ras, MEKK or MEK all effectively led to phosphorylation of ERK (Figure 3.7A). We also found that expression of these activated constructs resulted in a strong trend towards increased Numb E9 inclusion at the transcript level (Figure 3.7B). Notably, activated MEK expression resulted in a much weaker effect on both ERK phosphorylation and Numb E9 inclusion at the transcript level (Figure 3.7A and Figure 3.7B, right). In addition, there was a trend towards increased total Numb transcript expression upon expression of either activated MEKK or activated Ras (Figure 3.7C). These results correlated with our observations of the effect of MEK inhibition on Numb E9 alternative splicing.

We also wanted to determine whether activation of PI3K/Akt signalling was capable of altering Numb E9 alternative splicing. We expressed either a constitutively active Akt (Akt-DD) or kinase-dead Akt (Akt-AAA) in HEK 293T cells for 24 hours and observed that over-expression of Akt-DD resulted in increased phosphorylation of Akt, whereas over-expression of Akt-AAA had no effect on Akt phosphorylation (Figure 3.8A). The Numb E9 alternative splicing event at the transcript level was not altered by over-expression of either construct (Figure 3.8B). In addition, there was no effect on total Numb transcript expression (Figure 3.8C).

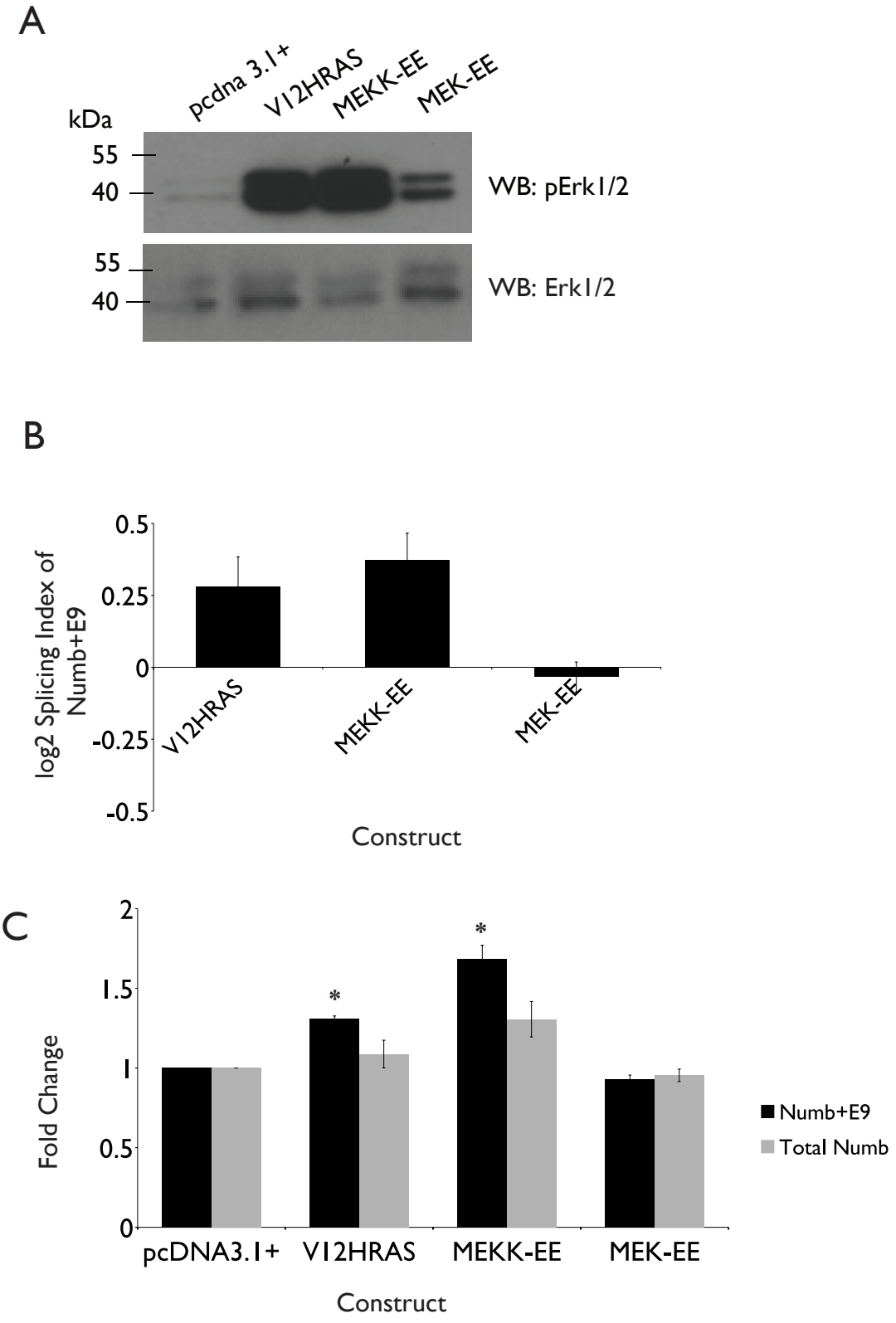
A
pcdna 3.1+
V12HRAS
MEKK-EE
MEK-EE
kDa
55
40
WB: pErk1/2
55
40
WB: Erk1/2
B
log2 Splicing Index of Numb+E9
0.5
0.25
0
-0.25
-0.5
V12HRAS
MEKK-EE
MEK-EE
Construct
C
Fold Change
2
1.5
1
0.5
0
*
*
pcDNA3.1+
V12HRAS
MEKK-EE
MEK-EE
Construct
Numb+E9
Total Numb

Figure 3.7

Figure 3.7. Upregulation of MAPK/ERK signalling pathway components results in Numb exon 9 inclusion.

(A) Representative Western blot confirming over-expression in HEK 293T cells of 1µg of either untagged pcDNA3.1+ empty vector, or constitutively active components of ERK signalling: V12HRAS, MEKK-EE, or MEK-EE. 24 hours post-transfection, whole-cell protein lysate was extracted and resolved in a 10% SDS-PAGE gel. Western blots were probed for either phosphorylated or total ERK1/2, to confirm increased expression of phosphorylated ERK1/2.

(B) log2 splicing index of endogenous Numb+E9 transcript expression relative to total Numb expression after over-expressing either untagged pcDNA3.1+ empty vector or constitutively active V12HRAS, MEKK-EE, or MEK-EE in HEK 293T cells for 24 hours (n=3, mean+SEM).

(C) Fold change of Numb+E9 and total Numb transcript expression after transfection of HEK 293T cells with 1µg of constitutively active V12HRAS, MEKK-EE or MEK-EE, for 24 hours (n=3, mean+SEM). Fold change was calculated relative to Numb+E9 and total Numb transcript expression in HEK 293T cells transfected with untagged pcDNA3.1+ empty vector. A star (*) indicates statistical significance relative to pcDNA3.1+ vector ($p<0.05$).

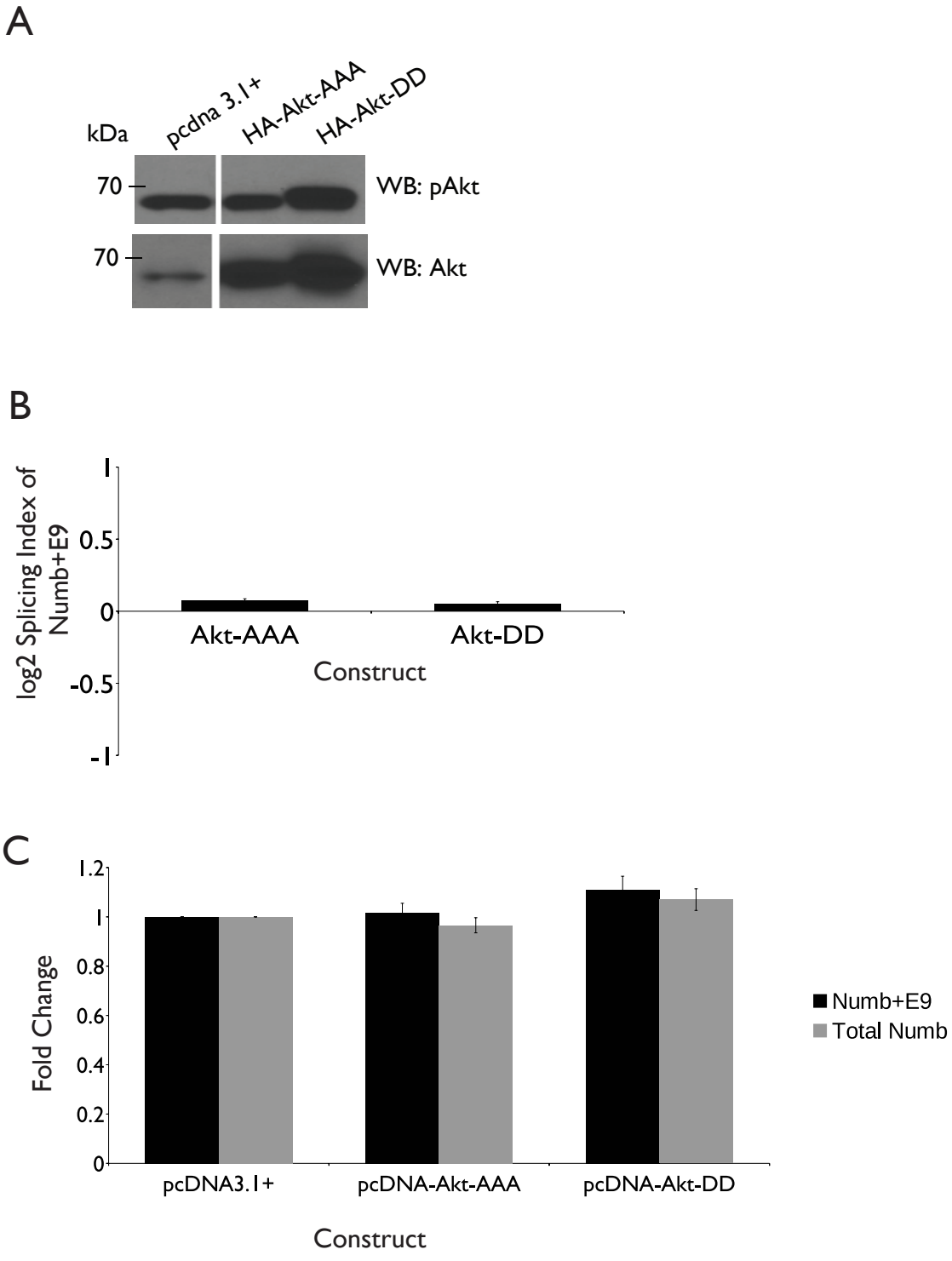
A
kDa
pcdna 3.1+
HA-Akt-AAA
HA-Akt-DD
70
WB: pAkt
70
WB: Akt
B
log2 Splicing Index of Numb+E9
1
0.5
0
-0.5
-1
Akt-AAA
Akt-DD
Construct
C
Fold Change
1.2
1
0.8
0.6
0.4
0.2
0
pcDNA3.1+
pcDNA-Akt-AAA
pcDNA-Akt-DD
Construct
Numb+E9
Total Numb

Figure 3.8

Figure 3.8. Regulation off the alternative splicing pattern of Numb exon 9 is not PI3K/Akt signalling-dependent in A549 lung adenocarcinoma cells.

(A) Representative Western blot confirming over-expression in HEK 293T cells of 1μg of either untagged pcDNA3.1+ empty vector, HA-tagged kinase-dead Akt (Akt-AAA), or HA-tagged constitutively active Akt (Akt-DD). 24 hours post-transfection, whole-cell protein lysate was extracted and resolved in a 10% SDS-PAGE gel. Western blots were probed for either phosphorylated or total Akt, to confirm increased Akt phosphorylation in the case of HA-Akt-DD.

(B) log2 splicing index of endogenous Numb+E9 transcript expression relative to total Numb expression after over-expressing either untagged pcDNA3.1+ empty vector, HA-tagged kinase-dead Akt (Akt-AAA), or HA-tagged constitutively active Akt (Akt-DD) in HEK 293T cells for 24 hours (n=3, mean+SEM).

(C) Fold change of Numb+E9 and total Numb transcript expression after transfection of HEK 293T cells with HA-tagged kinase-dead Akt (Akt-AAA) or HA-tagged constitutively active Akt (Akt-DD), for 24 hours (n=3, mean+SEM). Fold change was calculated relative to Numb+E9 and total Numb transcript expression in HEK 293T cells transfected with untagged pcDNA3.1+ empty vector.

Overall, our observations revealed that activated MAPK/ERK signalling likely plays a role in the increased expression of the Numb+E9 isoform observed in lung adenocarcinoma, while activated PI3K/Akt signalling may not play any role in regulating this alternative splicing event in lung cancer.

3.6 MAPK/ERK Signalling Does Not Regulate Numb Exon 9 Alternative Splicing in Breast Adenocarcinoma Cells

A previous study by Misquitta-Ali et al. (2011) found that increased Numb E9 inclusion in breast adenocarcinoma, in addition to lung adenocarcinoma. As both MAPK/ERK and PI3K/Akt signalling pathways are highly active in breast cancer, we wanted to determine whether either pathway was responsible for the regulation of Numb E9 alternative splicing in breast cancer.

We treated MCF-7 breast adenocarcinoma cells with either DMSO vehicle control, U0126, or LY 294002 for 48 hours, to inhibit MEK and PI3K signalling. Effective inhibition of MEK and PI3K signalling was confirmed by immunoblotting lysates of both control and treated cells with anti-pERK and anti-pAkt antibodies (Figure 3.9A). The Numb splicing index and total Numb transcript expression was measured by RT-qPCR. In contrast to A549 cells, inhibition of either the MAPK/ERK or PI3K/Akt pathways had no effect on Numb E9 splicing (Figure 3.9B), or on total Numb transcript expression (Figure 3.9C). We conclude that the ERK-dependent regulation of Numb E9 alternative splicing may be unique to lung adenocarcinoma. However, to confirm this, other tumour cell lines with increased MAPK/ERK or PI3K/Akt signalling activity should be tested.

3.7 MAPK/ERK-Dependent Regulation of Numb Exon 9 Splicing Alters Notch

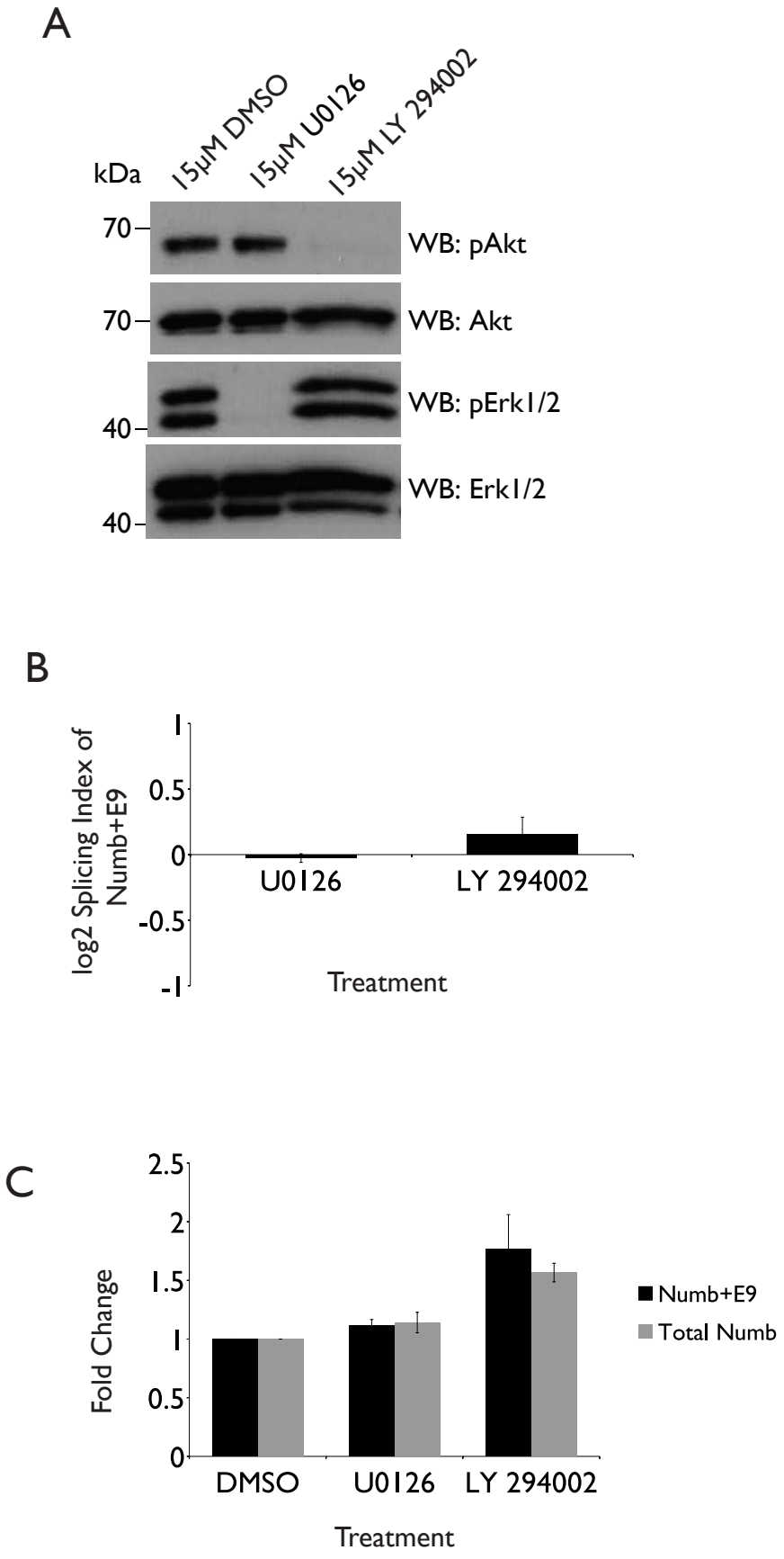
A
15μM DMSO
15μM U0126
15μM LY 294002
kDa
70
70
40
40
WB: pAkt
WB: Akt
WB: pErk1/2
WB: Erk1/2
B
log2 Splicing Index of Numb+E9
1
0.5
0
-0.5
-1
U0126
LY 294002
Treatment
C
Fold Change
2.5
2
1.5
1
0.5
0
DMSO
U0126
LY 294002
Treatment
Numb+E9
Total Numb

Figure 3.9

Figure 3.9. Regulation off the alternative splicing pattern of Numb exon 9 is not ERK or PI3K/Akt signalling-dependent in MCF-7 breast adenocarcinoma cells.

(A) Representative Western blot confirming inhibition of MAPK/ERK and PI3K/Akt signalling after treatment of MCF-7 breast adenocarcinoma cells with U0126 and LY 294002, respectively. MCF-7 cells were treated for 48 hours with 15μM of either DMSO, MEK inhibitor U0126, or PI3K inhibitor LY 294002. Post-treatment, whole-cell protein lysate was extracted and resolved in a 10% SDS-PAGE gel. Western blots were probed for either phosphorylated or total ERK1/2 (for cell lysates treated with U0126; left), or either phosphorylated or total Akt (for cell lysates treated with LY 294002; right).

(B) log2 splicing index of endogenous Numb+E9 transcript expression relative to total Numb transcript expression (n=2, mean+SEM).

(C) Fold change of Numb+E9 and total Numb transcript expression after treatment of MCF-7 cells with 15μM of either U0126 or LY 294002 for 48 hours (n=2, mean+SEM). Fold change was calculated relative to Numb+E9 and total Numb transcript expression in MCF-7 cells treated with 15μM DMSO.

Signalling in Lung Adenocarcinoma

In order to identify the downstream effects of MAPK/ERK signalling on Numb E9 alternative splicing, we decided to focus our efforts on observing the effects on the Notch developmental signalling pathway, on which Numb acts as a negative regulator. The Notch pathway is known to play a role in cell fate decision-making, and is activated in both lung and breast adenocarcinoma (Maraver et al., 2012; Pece et al., 2004; Stylianou et al., 2006; Westhoff et al., 2009), which correlates with downregulated expression of Numb (Pece et al., 2004; Stylianou et al., 2006; Westhoff et al., 2009).

There is evidence that the Numb p66 and p72 isoforms differentially regulate Notch signalling. While the p66 isoform is capable of suppressing Notch signalling through decreased Notch target gene expression, the p72 isoform is capable of activating Notch signalling through increased Notch target gene expression, but only in the presence of p66, suggesting that p72 disinhibits the suppressive ability of p66 (Misquitta-Ali et al., 2011).

We wanted to determine whether MAPK/ERK signalling-dependent splicing regulation of Numb E9 correlated with changes in Notch signalling activity. The RNA isolated from the kinase inhibition experiments depicted in Figure 3.6 was used to detect expression of Notch signalling targets HEY1, HEY2, and HES1 by RT-qPCR. We observed a significant decrease in HEY1 and HEY2 transcript expression in response to MEK inhibition, correlating with the reduced E9 inclusion observed in Figure 3.6B. However, there was no significant change in HES1 transcript expression (Figure 3.10A), similar to previously published evidence of Notch target gene expression in response to p66 isoform overexpression in A549 cells (Misquitta-Ali et al., 2011). Therefore, inhibition of MAPK signalling, which correlates with decreased expression of the E9-included isoform, results in suppression of Notch signalling. Based on our evidence it is possible that the differential

effect of the Numb isoforms on Notch may only occur through specific gene targets, which was similarly observed by Misquitta et al. (2011). Further experimentation is also required to determine whether the relationship between MAPK/ERK signalling and Notch target gene expression is Numb-dependent.

We also treated A549 cells with either DMSO vehicle control or PI3K inhibitor LY 294002 for 48 hours, and mRNA expression of Notch signalling targets HES1 and HEY2 between the two conditions were detected by RT-qPCR. We saw a significant decrease in HES1 transcript expression compared to vehicle control, but no significant change in HEY2 expression (Figure 3.10B). This points to the possibility of additional factors that may be regulating Notch activity directly through PI3K signalling.

We also investigated whether changes in Notch target gene expression occurred over the course of p19 differentiation. We found that, during retinoic acid-induced differentiation, transcript expression of both HEY1 and HEY2 initially increases, then decreases upon completion of differentiation (Figure 3.10C). In this case, changes in Numb expression during differentiation did not correlate with expression of the Notch targets similar to what was observed upon MEK inhibition in A549 cells. Our results therefore indicate a more complex model involving MAPK/ERK signalling and Notch signalling. Further experimentation is required to determine whether the relationship between MAPK/ERK signalling and Notch target gene expression is Numb-dependent during differentiation.

3.8 Identifying the relationship between PTBP1 and ASF/SF2 expression and MAPK/ERK Signalling Activation

In order to test whether MAPK/ERK activation regulates Numb E9 alternative splicing through either ASF/SF2 or PTBP1, we first wanted to determine whether there was

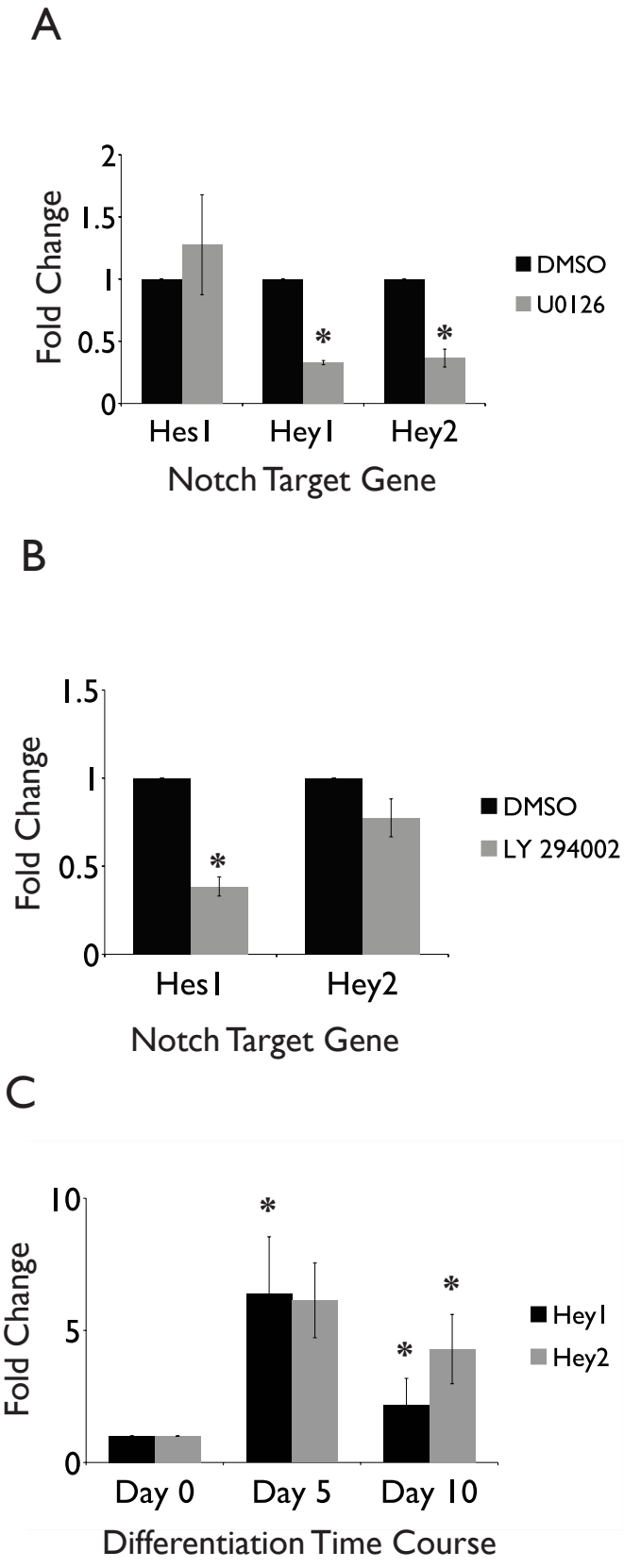
A
Fold Change
2
1.5
1
0.5
0
*
*
DMSO
U0126
Hes1
Hey1
Hey2
Notch Target Gene
B
Fold Change
1.5
1
0.5
0
*
DMSO
LY 294002
Hes1
Hey2
Notch Target Gene
C
Fold Change
10
5
0
*
*
*
Hey1
Hey2
Day 0
Day 5
Day 10
Differentiation Time Course

Figure 3.10

Figure 3.10. Manipulation of Numb exon 9 alternative splicing by ERK signalling is correlated with changes in expression of Notch target genes.

(A) Fold change expression of Notch target genes Hes1, Hey1 and Hey2 after treatment of A549 cells with 20μM MEK inhibitor U0126 for 48 hours, relative to expression in DMSO vehicle control (the samples used were the same as those from Figure 3.6) (n=3, mean+SEM). A star (*) indicates statistical significance relative to DMSO ($p<0.05$).

(B) Fold change expression of Notch target genes Hes1 and Hey2 after treatment of A549 cells with 20μM PI3K inhibitor LY 294002 for 48 hours, relative to DMSO vehicle control (the samples used were the same as those from Figure 3.6) (n=3, mean+SEM). A star (*) indicates statistical significance relative to DMSO ($p<0.05$).

(C) Fold change expression of Notch target genes Hey1 and Hey2 over the course of p19 embryonal carcinoma differentiation into neurons (n=3, mean+SEM). The samples were the same as those used in Figure 3.1D. Fold change was calculated relative to transcript expression in undifferentiated p19 cells. A star (*) indicates statistical significance relative to expression in undifferentiated cells ($p<0.05$).

an additive relationship between MAPK/ERK signalling activation and the activities of these splicing factors. We co-transfected both constitutively active MEKK and each splicing factor along with our splicing reporter in HEK 293T cells for 24 hours. Interestingly, expression of PTBP1 with activated MEKK led to an increase in PTBP1 protein expression, though expression of MEKK alone did not elicit increased expression of endogenous PTBP1 protein (Figure 3.11A, left). As expected, we found that expression of PTBP1 or activated MEKK alone led to an increase in E9 inclusion. However, no additive effect was observed when PTBP1 and activated MEKK were co-overexpressed (Figure 3.7A, above right). This indicates that the effect of MAPK/ERK signalling and PTBP1 over-expression on promoting Numb E9 inclusion may occur through independent mechanisms.

We also co-over-expressed MEKK with ASF/SF2 IN HEK 293T cells (Figure 3.11B, left) for 24 hours. By RT-PCR, we again observed that expression of ASF/SF2 alone led to Numb E9 exclusion, while expression of activated MEKK alone led to Numb E9 inclusion. However, exon inclusion was not increased when co-over-expressing MEKK with ASF/SF2 (Figure 3.11B, above right). This suggests that MEKK and ASF/SF2 likely acted on different pathways to regulate Numb alternative splicing.

In order to further test whether MAPK/ERK activation regulates Numb E9 alternative splicing through either PTBP1 or ASF/SF2, we examined whether inhibition of MAPK/ERK signalling led to an effect on mRNA transcript and protein levels of either ASF/SF2 and PTPB1. Using the same RNA samples from the experiments described in Figure 3.6, we used RT-qPCR to measure expression of both PTBP1 and ASF/SF2 transcripts in A549 cells when treated for 48 hours with MEK inhibitor U0126, compared to DMSO vehicle control. We found that inhibition of MAPK/ERK signalling resulted in decreased transcript expression of both factors, though only the change in PTBP1 transcript expression was significant (Figure

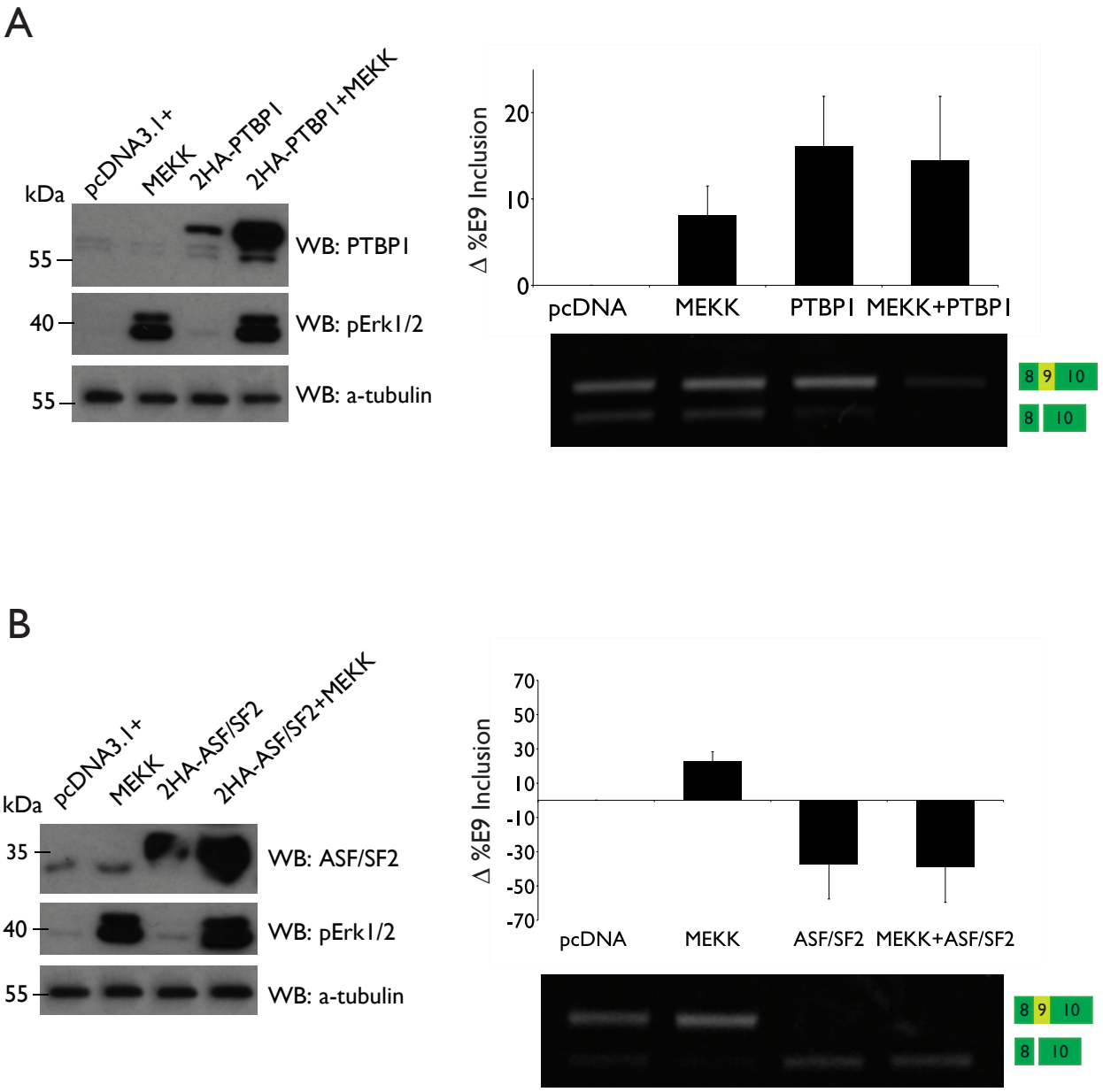
A
pcDNA3.1+
MEKK
2HA-PTBP1
2HA-PTBP1+MEKK
kDa
55
WB: PTBP1
40
WB: pErk1/2
55
WB: a-tubulin
Δ %E9 Inclusion
20
10
0
pcDNA
MEKK
PTBP1
MEKK+PTBP1
8 9 10
8 10
B
pcDNA3.1+
MEKK
2HA-ASF/SF2
2HA-ASF/SF2+MEKK
kDa
35
WB: ASF/SF2
40
WB: pErk1/2
55
WB: a-tubulin
Δ %E9 Inclusion
70
50
30
10
-10
-30
-50
-70
pcDNA
MEKK
ASF/SF2
MEKK+ASF/SF2
8 9 10
8 10

Figure 3.11

Figure 3.11. Relationship between MAPK/ERK signalling pathway activation and function of splicing factors ASF/SF2 and PTBP1 on Numb E9 alternative splicing.

(A) Left: Representative Western blot confirming over-expression of either untagged pcDNA3.1+ vector, 1μg MEKK-EE, 1μg 2HA-PTBP1, or 0.5μg each of PTBP1 and MEKK-EE after transfection in HEK 293T cells for 24 hours. The constructs were co-transfected with the Numb splicing reporter described in Figure 3.2A. Post-transfection, whole-cell lysate was collected and resolved in a 10% acrylamide gel. The Western blot was probed for either PTBP1, phosphorylated ERK, or α-tubulin. Right: RNA samples were reverse transcribed and the resulting cDNA was subject to PCR using the primers described in Figure 3.2B. The PCR reactions were resolved in a 1.5% agarose gel (below). Change in % Numb exon 9 inclusion compared to untagged pcDNA3.1+ control (above) was calculated based on analysis of PCR images with ImageJ (n=2, mean+SEM).

(B) Left: Representative Western blot confirming over-expression of either untagged pcDNA3.1+ vector, 1μg MEKK-EE, 1μg 2HA-ASF/SF2, or 0.5μg each of ASF/SF2 and MEKK-EE after transfection in HEK 293T cells for 24 hours. The constructs were co-transfected with the Numb splicing reporter described in Figure 3.2A. Post-transfection, whole-cell lystate was collected and resolved in a 10% acrylamide gel. The Western blot was probed for either ASF/SF2, phosphorylated ERK, or α-tubulin. Right: RNA samples were reverse transcribed and the resulting cDNA was subject to PCR using the primers described in Figure 3.2B. The PCR reactions were resolved in a 1.5% agarose gel (below). Change in % Numb exon 9 inclusion compared to untagged pcDNA3.1+ control (above) was calculated based on analysis of PCR images with ImageJ.

3.12A). This suggests to us that upregulation of MAPK/ERK signalling may promote upregulated expression of both factors.

We also used Western blotting to detect potential changes in expression of both PTBP1 and ASF/SF2 proteins in A549 cells when treated for 48 hours with MEK inhibitor U0126, compared to DMSO vehicle control. We found that expression of PTBP1 and ASF/SF2 protein in whole-cell lysate of A549 cells treated with either vehicle or U0126 was unchanged (Figure 3.12B).

The function of PTBP1 has previously been shown in other contexts to be regulated through its localization in the cell. For example, phosphorylation of PTBP1 at a serine site was found to promote transport of PTBP1 from the nucleus to the cytoplasm in PC12 cells (Xie, Lee, Kress, Mowry, & Black, 2003). Therefore we tested whether MAPK/ERK signalling may regulate PTBP1 function by altering its cellular localization. A549 cells were treated with either vehicle control DMSO or the MEK inhibitor U0126 for 48 hours before cells were fixed and fluorescently stained for either PTBP1 or the nuclear marker DAPI. We observed that PTBP1 localized predominantly in the nucleus in untreated cells. However, this localization pattern was not altered in cells treated with U0126 (Figure 3.12C). These results show that MAPK/ERK signalling does not regulate PTBP1 activity by altering its localization. However, there are likely other possible mechanisms of ERK-dependent PTBP1 or ASF/SF2 regulation of Numb alternative splicing. Further testing needs to be done to determine whether there are other possible mechanisms, such as the alteration of PTBP1 phosphorylation in response to activated MAPK/ERK signalling.

3.9 Identifying of Potential Cis-Acting regulators of Numb Exon 9 Alternative Splicing

In addition to identifying the signalling pathways and the splicing factors that may

A

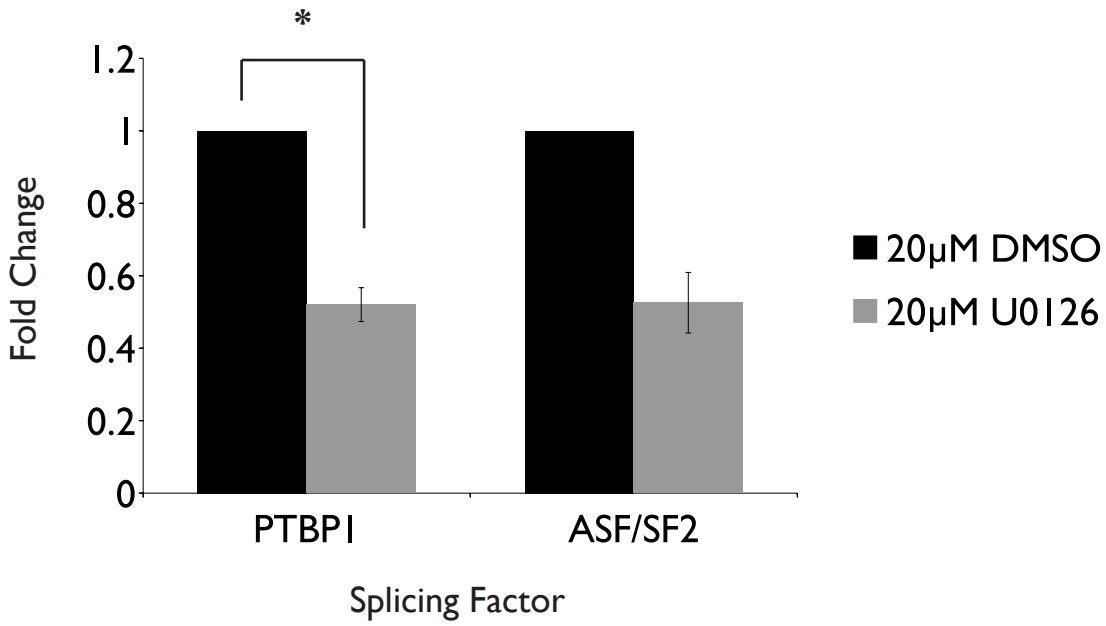

B

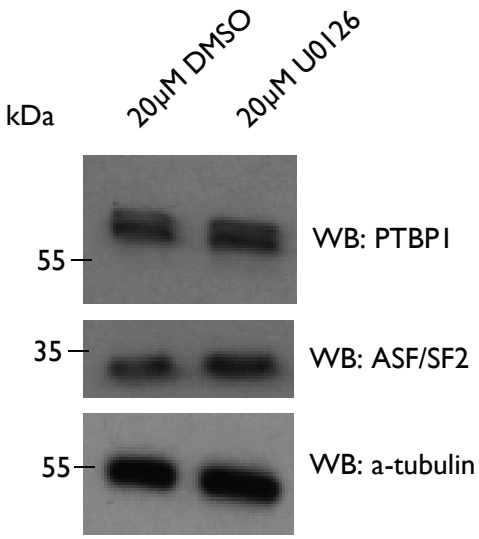

C

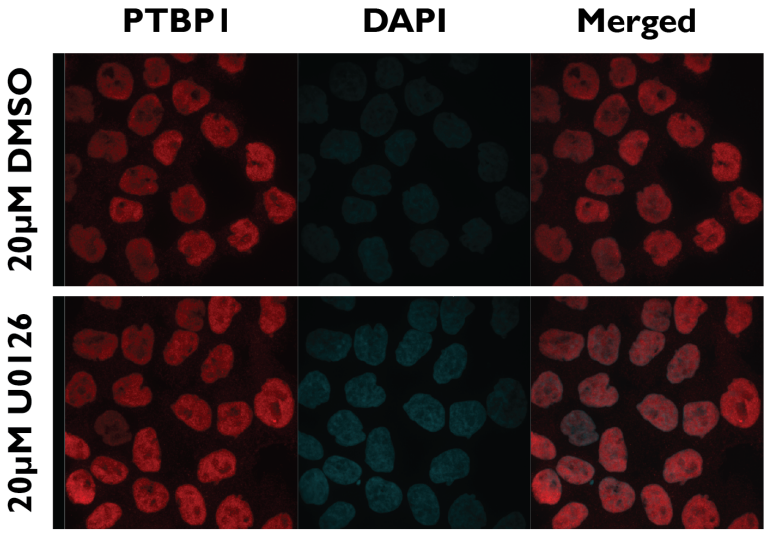

Figure 3.12

Figure 3.12. Relationship between MAPK/ERK and expression of splicing factors ASF/SF2 and PTBP1 on Numb E9 alternative splicing.

(A) Fold change expression of PTBP1 and ASF/SF2 transcripts after treatment of A549 cells with 20μM MEK inhibitor U0126 for 48 hours, relative to DMSO vehicle control (the samples used were the same as those from Figure 3.6) (n=3, mean+SEM). A star (*) indicates statistical significance relative to DMSO ($p<0.05$).

(B) Representative Western blot determining protein expression of PTBP1 or ASF/SF2 in response to MEK inhibition in A549 cells for 48 hours. The lysates used were the same as those from Figure 3.6A, and were resolved in a 10% acrylamide gel prior to Western blotting (n=3).

(C) Localization of PTBP1 protein in A549 cells treated with MEK inhibitor U0126 in A549 cells for 48 hours. Cells were seeded onto glass plates and treated 20 hours later with either 20μM DMSO or U0126. Post-treatment, cells were fixed in 2% paraformaldehyde and permeabilized with 0.2% triton X-100. Cells were incubated with monoclonal PTBP1 overnight. Before mounting, plates were briefly treated with the nucleotide-binding marker DAPI, to use as a nuclear marker. Slides were then observed under a confocal microscope. The image is representative of two independent experiments.

regulate Numb E9 alternative splicing, we also wanted to identify putative motifs on the Numb pre-mRNA that are important for regulation of Numb E9 alternative splicing.

Upon analysis of the human Numb genomic region surrounding E9, we found that the genomic region including approximately 500nt of directly upstream and downstream intron was highly conserved. To confirm this, we analyzed the human genomic region included in Chr14:72815133-72816424 (NCBI Build 36.1) in the UCSC genome browser and produced both mammalian and vertebrate conservation plots. This region was highly conserved, not only in mammals (PhyloP range of 3.378, with a range of 2 considered to be highly significant (Pickrell, Pai, Gilad, & Pritchard, 2010)), but also across vertebrates (PhyloP range of 2.154) (Figure 3.13A). This told us that the ~500nt intronic region both upstream and downstream of E9 likely contained sequences that were very important for the regulation of E9 alternative splicing.

We therefore constructed a smaller splicing reporter (Numb1kb) by inserting the human genomic region included in Chr14:72815237-72816420 (corresponding to human E9, a 540nt intron directly upstream of E9, and a 507nt intron directly downstream of E9) into an ExonTrap vector. This vector contains a Rous sarcoma virus long terminal repeat promoter, as well as two constitutive exons that flank the genomic region and that have the potential to act as constitutive exons that flank an alternative exon. The genomic fragment was inserted between these constitutive exons (Figure 3.13B). In order to detect E9 splicing events from this reporter, we designed primers that targeted the two constitutive exons (Figure 3.13C, above), allowing detection of both E9-included and E9-excluded transcripts in the same reaction.

To determine if the splicing profile produced when expressing this reporter recapitulated the endogenous Numb splicing pattern, we reverse-transcribed parental HEK

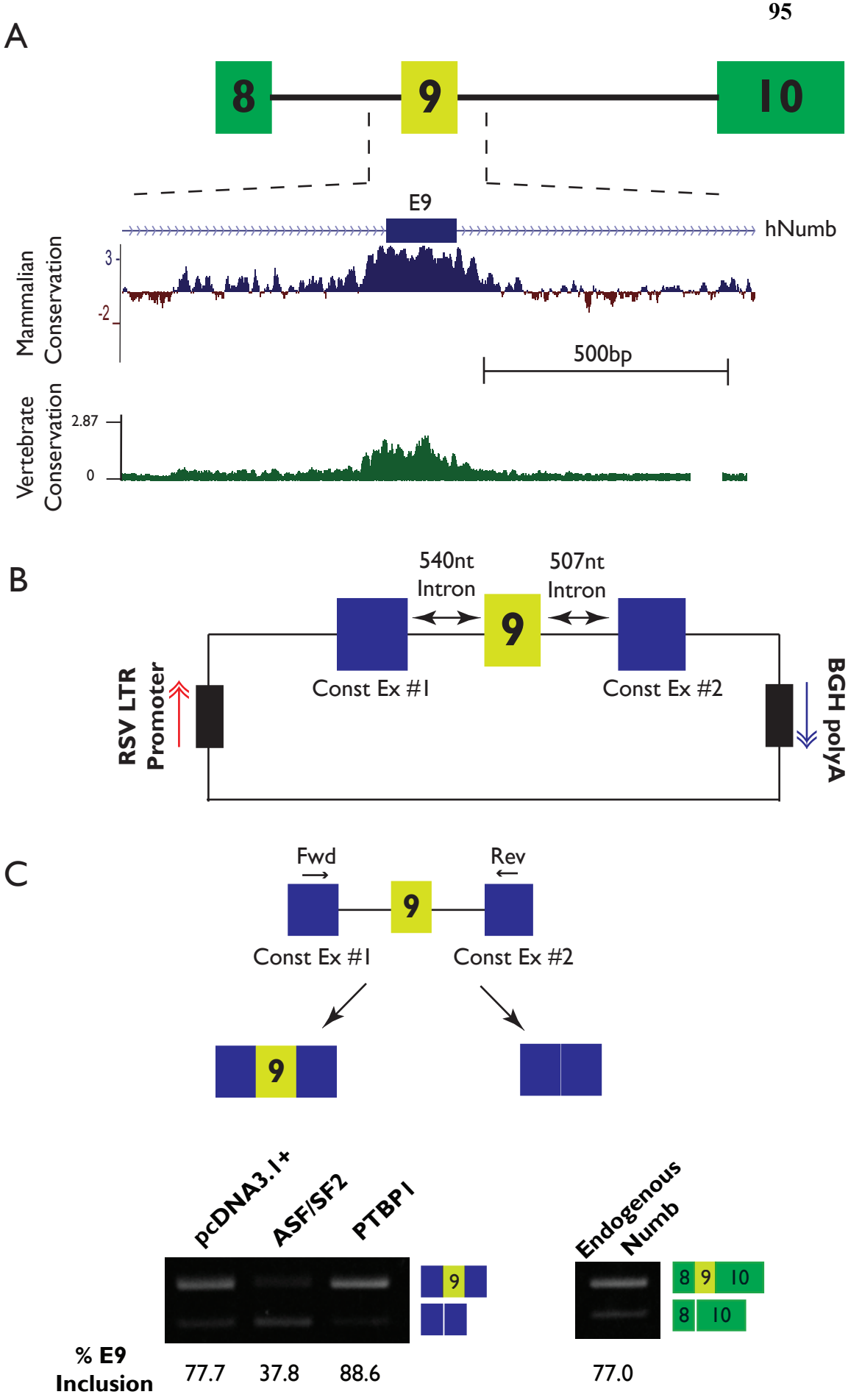
A
8
9
10
E9
hNumb
Mammalian Conservation
3
-2
500bp
Vertebrate Conservation
2.87
0
B
540nt Intron
507nt Intron
9
Const Ex #1
Const Ex #2
RSV LTR Promoter
BGH polyA
C
Fwd
Rev
9
Const Ex #1
Const Ex #2
9
pcDNA3.1+
ASF/SF2
PTBP1
9
Endogenous Numb
8 9 10
8 10
% E9 Inclusion
77.7
37.8
88.6
77.0

Figure 3.13

Figure 3.13. Construction and expression of a truncated alternative splicing reporter for Numb exon 9.

(A) Mammalian and vertebrate conservation plots for Numb E9 and its flanking intronic regions (539nt upstream, 609nt downstream), corresponding to the genomic region in chromosome 14 from 72,815,133-72,816,424 nucleotide positions (NCBI build 36.1). The mammalian conservation plot (above) was constructed from the UCSC genome browser (genome.ucsc.edu), using the PhyloP placental mammalian basewise conservation track (*H. sapiens*, *M. musculus*, *R. norvegicus, C. lupus familiaris, M. mulatta, P. Troglodytes*). The vertebrate conservation plot (below) was constructed from the UCSC genome browser using the PhyloP vertebrate 28-way basewise conservation track (Miller et al., 2007).

(B) Schematic of a truncated alternative splicing reporter for Numb E9. The backbone is a ExonTrap pet01 vector, which contains built-in constitutive exons, a Rous sarcoma virus long terminal repeat (RSV LTR) promoter, and a BGH poly-adenylation signal. A fragment of human Numb genomic DNA containing exon 9, as well as intronic regions directly 540nt upstream and 507nt downstream of the exon, was cloned into this vector between the constitutive exons.

(C) Above: Schematic of primer design to detect expression of the Numb+E9 and NumbΔE9 mRNA isoforms by semi-quantitative PCR. The primers were designed such that both isoforms could be captured in the same PCR reaction. The forward primer was designed against the 5' constitutive exon, while the reverse primer was designed against the 3' constitutive exon. Below: The splicing reporter was co-expressed in HEK 293T cells with 1μg of either double-HA-tagged empty pcDNA3.1+ vector, double-HA-tagged ASF/SF2, or double-HA-tagged PTBP1 in a single experiment. 24 hours post-transfection, cells were

lysed and total RNA was collected and reverse-transcribed. cDNA was subject to PCR using the primers described in Figure 3.13C (above), and resolved in a 1.5% agarose gel. Endogenous cDNA from HEK 293T cells was also collected, subject to PCR with primers targeting exons 8 and 10, respectively, and resolved in a 1.5% agarose gel. ImageJ was used to analyze the expression of the Numb+E9 and NumbΔE9 isoforms. We confirmed that expression of the Numb isoforms when over-expressing the splicing reporter recapitulated endogenous Numb isoform expression in the same cell line. In addition, over-expression of ASF/SF2 and PTBP1 promoted exon exclusion and inclusion in the splicing reporter, respectively, which was the expected trend.

293T RNA to cDNA, which then underwent PCR using primers that target exons 8 and 10, in order to detect endogenous Numb. We found that the expression profile of the E9-included and excluded isoforms when over-expressing the Numb1kb reporter was comparable to endogenous expression of the E9-included and -excluded transcripts in HEK 293T cells (Figure 3.13C, below right).

In order to determine whether the splicing activity of this Numb1kb reporter recapitulated endogenous alternative splicing, we co-overexpressed the reporter in HEK 293T cells with either ASF/SF2 or PTBP1. Similar to what was observed both endogenously and with the full-length splicing reporter, we found that ASF/SF2 promoted E9 exclusion while PTBP1 promoted E9 inclusion (Figure 3.13C, below left).

Based on the conservation plot in Figure 3.13A, we strategically constructed a series of truncations and deletions within the Numb1kb reporter, to determine the splicing factor binding sites important for regulation of E9 alternative splicing (Figure 3.14A). Deletion sites were determined based on level of conservation, at random in order to easily identify the regions required for regulating E9 alternative splicing. We also ensured that the predicted sites for PTBP1 binding, as shown in Figure 3.3B, that were located in the receptor were not altered.

The wildtype Numb1kb and mutant reporters were each expressed in HEK 293T cells for 24 hours. Total RNA was extracted and the resulting cDNA was made to undergo PCR using the reporter-specific primers depicted in Figure 3.13C (above). Expression of nearly all mutant constructs in HEK 293T cells showed increased E9 inclusion compared to the wildtype Numb1kb construct, though the increase in inclusion for constructs F1R2 and Del2 were not significant (Figure 3.14B, above). Interestingly, over-expression of the construct Del1 showed exon exclusion compared to the full-length vector, though this was also not

A

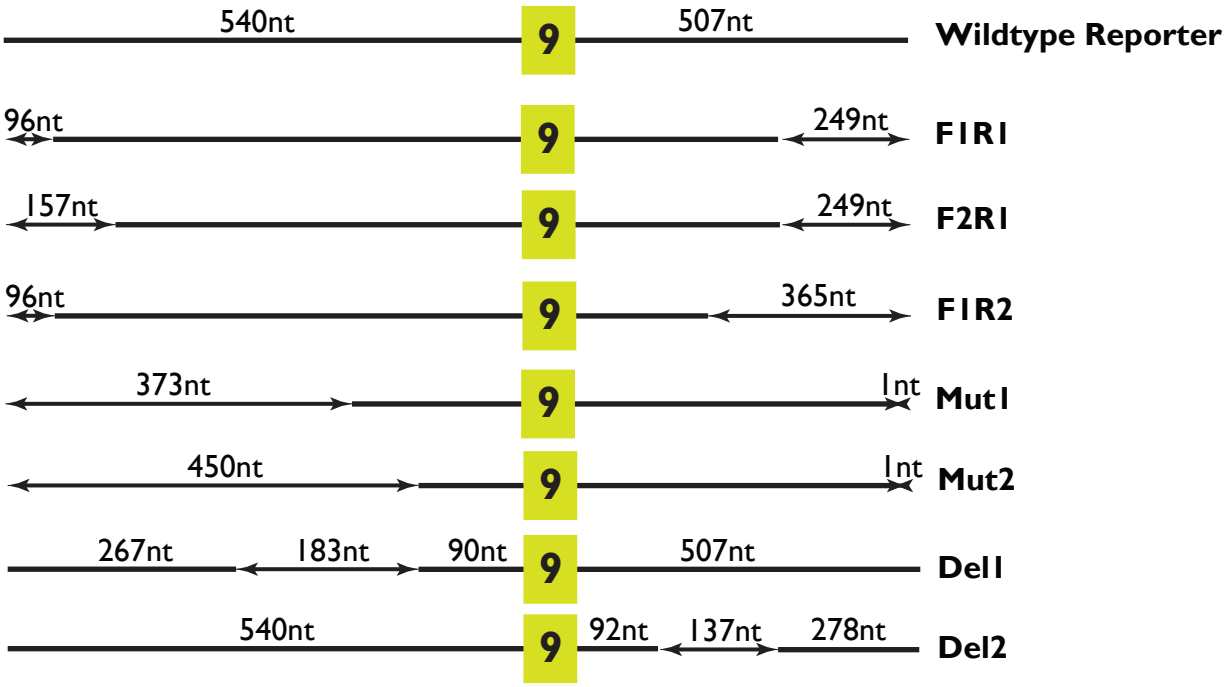

B

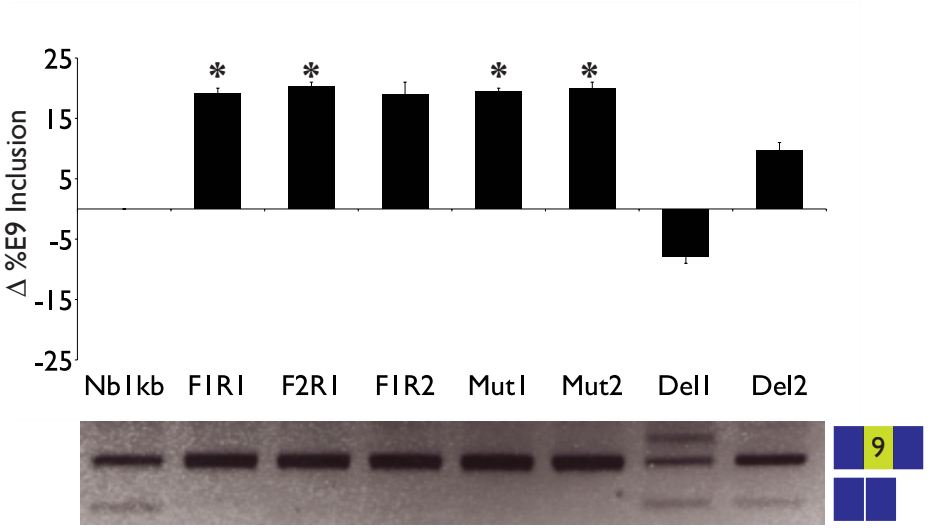

Figure 3.14

Figure 3.14. Manipulation of cis-acting sequences in Numb pre-mRNA to determine regulation of Numb Exon 9 alternative splicing.

(A) Schematic of mutation strategy for splicing reporter described in Figure 3.13. The deletions made in F1R1 were done to remove regions that were not highly conserved in human and mouse. Subsequent deletions of less conserved regions were conducted at random in order to better understand regions that are required for regulation of Numb E9 splicing. We did, however, ensure that the predicted sites for PTBP1 binding (Figure 3.3B) that are located in the reporter were not altered.

(B) HEK 293T cells were transfected with either wild-type Numb1kb reporter or one of the seven mutant reporters. After 24 hours, cells were lysed and RNA was extracted. After reverse transcription of the RNA to cDNA, the cDNA underwent PCR using the primers described in Figure 3.13C, to detect the exon 9-included and -excluded isoforms produced by the reporter. The PCR reactions were resolved in a 1.5% agarose gel (below). Change in E9 inclusion relative to isoform expression with the Numb1kb reporter (above, n=2, mean+SEM) was calculated from measurements of the PCR images by ImageJ. A star (*) indicates statistical significance relative to Numb1kb wild type ($p<0.05$). Note the aberrant splice product that is formed when over-expressing the Del1 construct.

significant (Figure 3.14B). In addition, expression of this construct produced an aberrant splice variant (Figure 3.14B), possibly through the production of an unrecognized splice site when producing the construct. This result shows that the 183nt region deleted in the intron upstream of E9 may contain splicing factor motifs vital for maintaining E9 inclusion. However, it should be noted that this same region is deleted in both the Mut1 and Mut2 reporters, though expression of either reporter resulted in E9 inclusion. These results show that the intronic regions approximately 500nt upstream and downstream of E9 likely regulate E9 inclusion or exclusion through a large number of splicing motifs and factors that bind them. More work involving direct binding assays would be required to identify the significance of the deleted region in Del1 on regulating Numb E9 alternative splicing.

CHAPTER 4: DISCUSSION AND FUTURE DIRECTIONS

4.1 Summary

The aim of this study was to characterize the alternative splicing (AS) program that regulates splicing of Numb exon 9 (E9), an exon whose inclusion and exclusion in the Numb pre-mRNA is correlated with the production of protein isoforms that are differentially expressed during differentiation and in cancer. Using the lung adenocarcinoma cell line A549, we found that AS of Numb E9 is regulated by MAPK/ERK signalling: activation of the pathway promotes the enhancement of E9 AS while inhibition of the pathway promotes silencing of E9 AS. In addition, we found some evidence that the regulation of Numb splicing by MAPK/ERK signalling is correlated with the expression of Notch target genes. We also identified several splicing factors capable of regulating Numb E9 AS, of which ASF/SF2 (which promotes E9 exclusion) and PTBP1 (which promotes E9 inclusion) had the greatest effect. In addition, PTBP1 mRNA expression was found to be positively correlated with MAPK/ERK signalling in A549 cells. The results of our study has outlined a splicing program that may play an important role in regulating Numb AS in cancer.

4.2 Stability of Numb mRNA Isoforms

Though we established that MAPK/ERK signalling regulated Numb E9 alternative splicing, we wanted to ensure that our observations were not as a result of differences in Numb mRNA isoform stability or isoform transport. Very little is understood regarding the localization and stability of the Numb+E9 and NumbΔE9 mRNA isoforms, and how this may affect the protein product expression levels. To assess whether such differences could also regulate isoform expression levels, we therefore conducted preliminary experiments to

compare the nuclear versus cytoplasmic localization of the Numb+E9 and NumbΔE9 mRNAs in A549 cells. Cells were also treated with either the MEK inhibitor U0126 or DMSO vehicle control to test whether MEK inhibition alters nuclear versus cytoplasmic distribution of the Numb mRNA isoforms. After treatment with U0126, nuclear and cytoplasmic RNA was isolated and RT-PCR with primers specific for exons 8 and 10, respectively, was conducted to determine whether the two endogenous Numb isoforms differed in expression levels between the two cellular compartments. In addition, cells were treated with U0126 to test whether MEK inhibition altered nuclear versus cytoplasmic distribution of Numb mRNA isoforms. We found that the expression of the two endogenous Numb isoforms was similar between the nucleus and cytoplasm. In addition, the trend in E9 exclusion as a result of MEK inhibition was consistent between the nuclear and cytoplasmic compartments (Figure 4.1A). This suggests that the changes we see in Numb alternative splicing in response to MEK inhibition are not a result of changes in nuclear transport of the Numb mRNA isoforms.

We also treated A549 cells with the transcription inhibitor actinomycin D to determine whether the Numb mRNA isoforms have a similar half-life. Cells were treated with actinomycin D for 3.5, 6.5, 8.5 or 26.5 hours prior to isolation of cytoplasmic RNA. Using RT-PCR, the expression of c-jun and β-actin mRNA was detected over the same time period. c-jun mRNA has a half-life of about 20 minutes (Kayahara, Wang, & Tournier, 2005), so it was used as a positive control to confirm that actinomycin D was successfully inhibiting transcription (Rosenberger, De-Castro Arce, Langbein, Steenbergen, & Rösl, 2010) (Figure 4.1B, above). We then detected expression of the endogenous Numb+E9 and NumbΔE9 mRNA isoforms using primers that target exons 8 and 10. β-actin was used as a loading control.

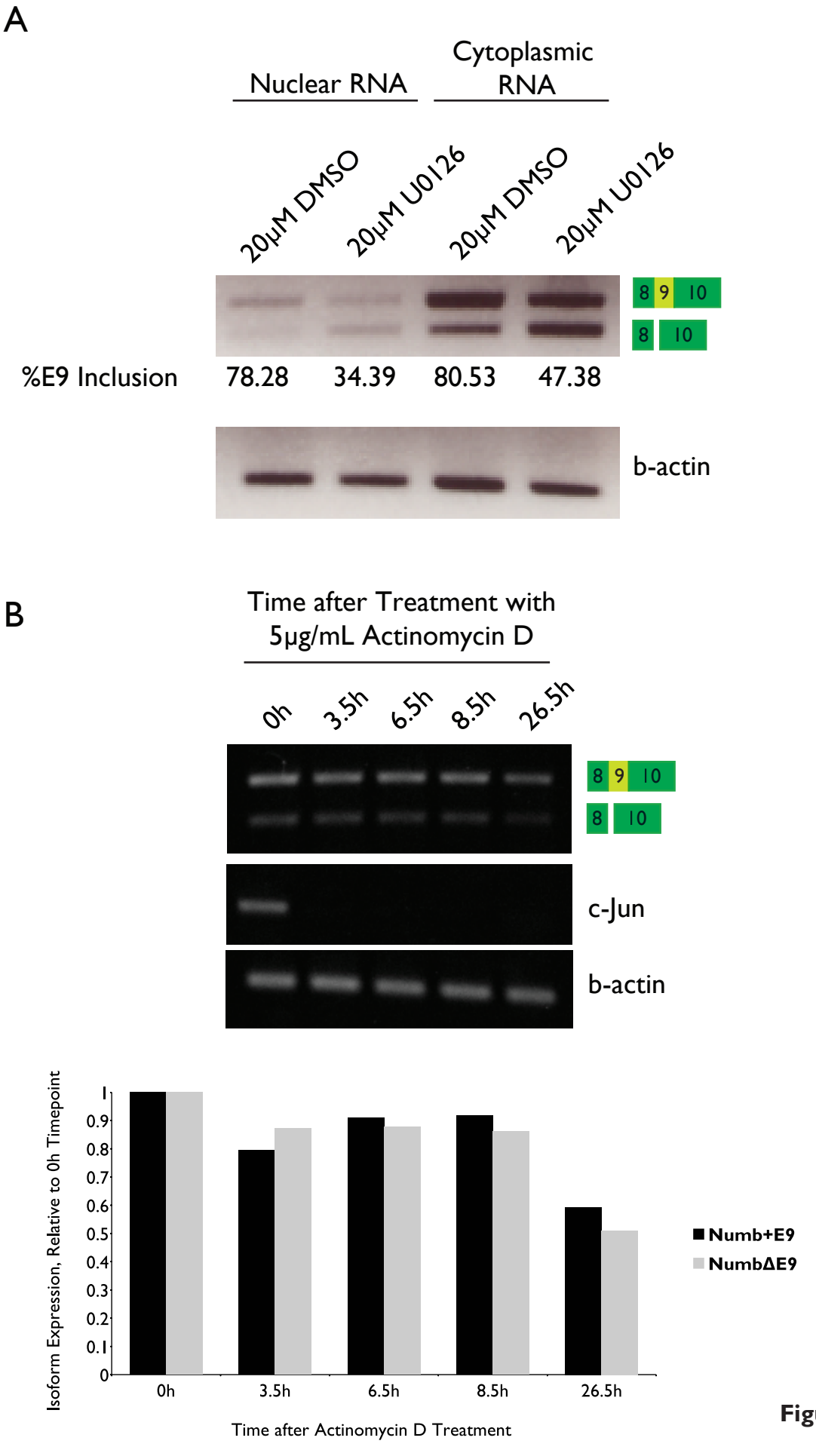
A
Nuclear RNA
Cytoplasmic RNA
20μM DMSO
20μM U0126
20μM DMSO
20μM U0126
8 9 10
8 10
%E9 Inclusion
78.28
34.39
80.53
47.38
b-actin
B
Time after Treatment with 5μg/mL Actinomycin D
0h
3.5h
6.5h
8.5h
26.5h
8 9 10
8 10
c-Jun
b-actin
Isoform Expression, Relative to 0h Timepoint
0
0.1
0.2
0.3
0.4
0.5
0.6
0.7
0.8
0.9
1
0h
3.5h
6.5h
8.5h
26.5h
Time after Actinomycin D Treatment
Numb+E9
NumbΔE9

Figure 4.1

Figure 4.1. Determination of Numb mRNA isoform cellular localization and stability.

(A) A549 lung adenocarcinoma cells at 70% confluence were treated with 20μM of either DMSO vehicle control or MEK inhibitor U0126 for 48 hours. Cells were trypsinized after treatment and centrifuge to isolate the nucleus and cytoplasm, before isolating mRNA from each compartment. The RNA was then reverse transcribed and the resulting cDNA underwent semi-quantitative PCR using primers that target exons 8 and 10, respectively. The PCR reactions were then resolved in a 1.5% agarose gel. Percent exon 9 inclusion was calculated based on figure analysis with ImageJ. β-actin was used as a loading control.

(B) A549 cells at 70% confluence were treated with 5μg/mL actinomycin D. Cells were trypsinized after treatment for 3.5, 6.5, 8.5, and 26.5 hours, after which cytoplasmic RNA was isolated. The RNA was then reverse transcribed and the resulting cDNA underwent semi-quantitative PCR using primers that target exons 8 and 10, respectively. Above: the PCR reactions were then resolved in a 1.5% agarose gel. β-actin transcript detection was used as a loading control, while c-Jun transcript detection was used as a positive control. Below: using ImageJ, the relative expression of each Numb isoform was calculated compared to isoform expression at 0h, and normalized to β-actin expression.

Using ImageJ to detect relative expression of each isoform normalized to β-actin, we observed that, while c-jun degraded very quickly, the two Numb isoforms were similarly stable over the entire time course (Figure 4.1B, below). Therefore, differential half-lives of the Numb mRNA isoforms does not contribute to their differential expression.

4.3 Regulation of Numb E9 Alternative Splicing in Neuronal Differentiation

Previous studies showed that the expression of the Numb protein isoforms p66 and p72 varied during neuronal differentiation. For example, during all-trans retinoic acid (atRA)-induced neuronal differentiation of p19 embryonal carcinoma cells, there is a switch in expression from predominantly the Numb E9-included p72 isoform to the Numb E9-excluded p66 isoform (Dho et al., 1999). My studies demonstrated that this change in protein expression reflects a switch from predominantly E9 inclusion to E9 exclusion at the transcript level. These observations suggest that the Numb splicing machinery is regulated during neuronal differentiation to promote Numb E9 silencing, thus resulting in an increase in p66 and decrease in p72 protein expression. However, the signalling mechanism by which this splicing event is regulated by atRA is currently unclear.

Over the course of this project, evidence has accumulated that suggests that Numb AS may be regulated during differentiation by a complex network. A study by Kim et al. (2013) outlined a mechanism by which a novel splicing factor, Rbfox3, a paralog of the hnRNP-like proteins Fox1 and Fox2, plays a vital role in Numb AS during neuronal development. Rbfox3 protein expression was shown to be required for late neuronal development, as demonstrated in both p19 cells and in chicken neural tube progenitor cells. Rbfox3 also recognizes a motif element in the Numb pre-mRNA, upstream of the chicken homolog of human Numb E9, resulting in the promotion of exon exclusion. The authors showed that the Numb alternative

splicing event seen in neuronal differentiation, which is regulated by Rbfox3 protein up-regulation, was a required event for late-stage neuronal differentiation.

There is also increasing evidence that PTBP1 plays a major role in regulating neuronal differentiation. During differentiation, expression of the nervous system-specific miRNA miR-124 is upregulated, resulting in miRNA-124 targeting the 3' untranslated region of the PTBP1 mRNA for degradation and subsequent downregulation of PTBP1 protein expression (Makeyev, Zhang, Carrasco, & Maniatis, 2007). Based on our evidence of PTBP1 promoting Numb E9 inclusion, it is possible that PTBP1 downregulation during neuronal differentiation may play a role in promoting Numb E9 AS silencing. In order to better understand the splicing mechanisms that regulate Numb E9 AS during neuronal differentiation, an siRNA screen targeting known splicing factors in undifferentiated p19 cells could be used to identify factors that regulate the Numb splicing profile.

We also attempted to establish whether the switch in Numb isoform expression observed in differentiating embryonal carcinoma cells was maintained in tumour cells. Both the SH-SH5Y and IMR-32 human neuroblastoma cell lines differentiate into neurons in response to atRA, and the NB4 human promyelotic leukemia cell line differentiates into granulocytes following treatment with atRA. Upon differentiating each cell line, whole-cell protein lysate was collected from both undifferentiated and differentiated cells, resolved in an acrylamide gel, and Western blotted using a Numb-specific antibody that detects both the p72 and p66 protein isoforms. We did not detect a switch in Numb protein isoform expression in in any of the cancer cell lines in response to atRA-induced differentiation. One possible explanation as to why the regulation of Numb splicing in response to atRA is not preserved in cancer lines is that, unlike p19 cells, these cancer cell lines are not pluripotent. Pluripotent cell lines, such as p19 cells, are capable of differentiating into all three germ layers (Soprano,

Teets, & Soprano, 2007; Takahashi & Yamanaka, 2006). In contrast, multipotent cells such as SH-SY5Y cells are progenitors that have more specific and limited differentiation lineages (Encinas et al., 2000). In addition, a recent study by Yeo et al. (2007) found that many alternative splicing events differ widely between pluripotent stem cells and multipotent neural progenitors, possibly due to genetic differences between the cell types, in how they are cultured, and in the expression levels of post-transcriptional and post-translational proteins between the two cell lines that may alter the activity of splicing regulatory networks (Nelles & Yeo, 2010; Yeo et al., 2007). This highlights that the Numb E9 AS silencing event in differentiating embryonic stem cells may be regulated by the activity of specific signalling pathways or splicing factors that may not be as active in tumour cells. Determining whether atRA-induced neuronal differentiation of other embryonal carcinoma cell lines such as mouse F9 cells and human NT2/D1 cells causes a switch in Numb isoform expression similar to that seen in differentiating p19 cells may provide us with a better understanding of the general mechanisms involved in regulating Numb E9 AS during neuronal differentiation.

4.4 The Role of PTBP1 in the Regulation of Alternative Splicing of Numb in Cancer

In this study, we identified the splicing factor PTBP1 as a regulator of Numb E9 AS in both HEK 293T and A549 cells, where PTBP1 played a role in promoting E9 splicing enhancement. PTBP1 is an ubiquitously expressed hnRNP protein that has been implicated in the regulation of AS events across a wide range of cancers (Christofk et al., 2008; Izaguirre et al., 2012). PTBP1 is aberrantly overexpressed in several cancers, such as breast adenocarcinoma (He et al., 2014), ovarian cancer (He et al., 2007) and glioma (Cheung et al., 2006; McCutcheon, Hentschel, Fuller, Jin, & Cote, 2004), and is believed to contribute to tumour growth and migration. In contrast, a recent study authored by Lin, Wang, and Tseng

(2013) found that, in the non-small cell lung cancer cell line H1299, over-expression of PTBP1 inhibited cell growth by promoting the expression of the cyclin-dependent kinase inhibitor p19INK4d (Lin, Wang, & Tseng, 2013). Though these observations are based on a single cell line, their results highlight the potentially complex role that PTBP1 plays in different cancer types. To further understand the role of PTBP1 in promoting or inhibiting tumour growth, the effects of PTBP1 knockdown in a panel of cancer cell lines on cell growth and colony formation needs to be assessed.

In Chapter 3, we attempted to identify whether there was a relationship between the MAPK/ERK signalling pathway and the effects on E9 AS by PTBP1. Our reasoning was based on observations that: (1) MAPK/ERK signalling is frequently activated in cancer cells, (2) PTBP1 promotes Numb E9 inclusion, and (3) Numb E9 inclusion is a frequently observed event in several cancers. We found that inhibition of MAPK/ERK signalling in A549 lung adenocarcinoma cells with U0126 resulted in significant downregulation of PTBP1 mRNA expression, which points to PTBP1 as a potential mediator of MAPK/ERK-regulated AS of Numb E9. However, no decrease of PTBP1 at the protein level was detected.

There are several possible reasons why the change in PTBP1 mRNA expression in response to MAPK/ERK pathway inhibition was not reflected at the protein level. One possible explanation is the experimental design: for the time period that cells are treated with U0126, changes in PTBP1 protein expression levels may be difficult to detect, especially if the protein or transcript is unstable. A time-course MEK inhibition assay is suggested to determine whether changes in PTBP1 protein expression levels may be detected within time periods shorter than what was used in this study. Post-transcriptional modifications that alter the ability of the PTBP1 mRNA to be translated may affect the ability for changes in transcript expression to be reflected at the protein level.

Finally, MAPK/ERK signalling may alter PTBP1 function through post-translational modification, which would not be detectable simply by observing mRNA or protein expression. To determine whether post-translational events such as phosphorylation of PTBP1 is altered in response to MAPK/ERK signalling inhibition, affinity purification followed by mass spectrometry could be utilized. A potential experiment would be to compare PTBP1 immunoprecipitated from untreated A549 cells or from cells treated with the MEK inhibitor U0126, using mass spectrometry.

4.5 Direct Binding of Splicing Factors to the Numb pre-mRNA

Understanding whether the relationship between a splicing factor and the pre-mRNA it interacts with is direct or indirect is useful for determining the mechanism by which pre-mRNA splicing events occur. To address whether PTBP1 interacts with the Numb pre-mRNA, we conducted an RNA-binding protein immunoprecipitation (RIP) assay, which involves the immunoprecipitation of RNA-binding proteins followed by detection of RNA bound to the protein by PCR (Jain et al., 2011).

PTBP1 complexed to RNA was immunoprecipitated from whole-cell HEK 293T lysate using an anti-mouse PTBP1 antibody; Mouse IgG was used as a negative control (Figure 4.2A). Mature mRNA was then separated from the complex and underwent reverse transcription to produce cDNA. The presence of Numb mRNA was detected by RT-PCR, using primers that targeted exons 8 and 10, respectively, so that both Numb+E9 and NumbΔE9 isoforms can be detected within a single PCR reaction. β-actin was used as a loading control for the PCR reaction. We found that, while the mouse IgG antibody did not complex with either Numb isoform, PTBP1 appeared to complex with only the NumbΔE9 isoform, even though both Numb isoforms were present in the pre-IP input samples (Figure

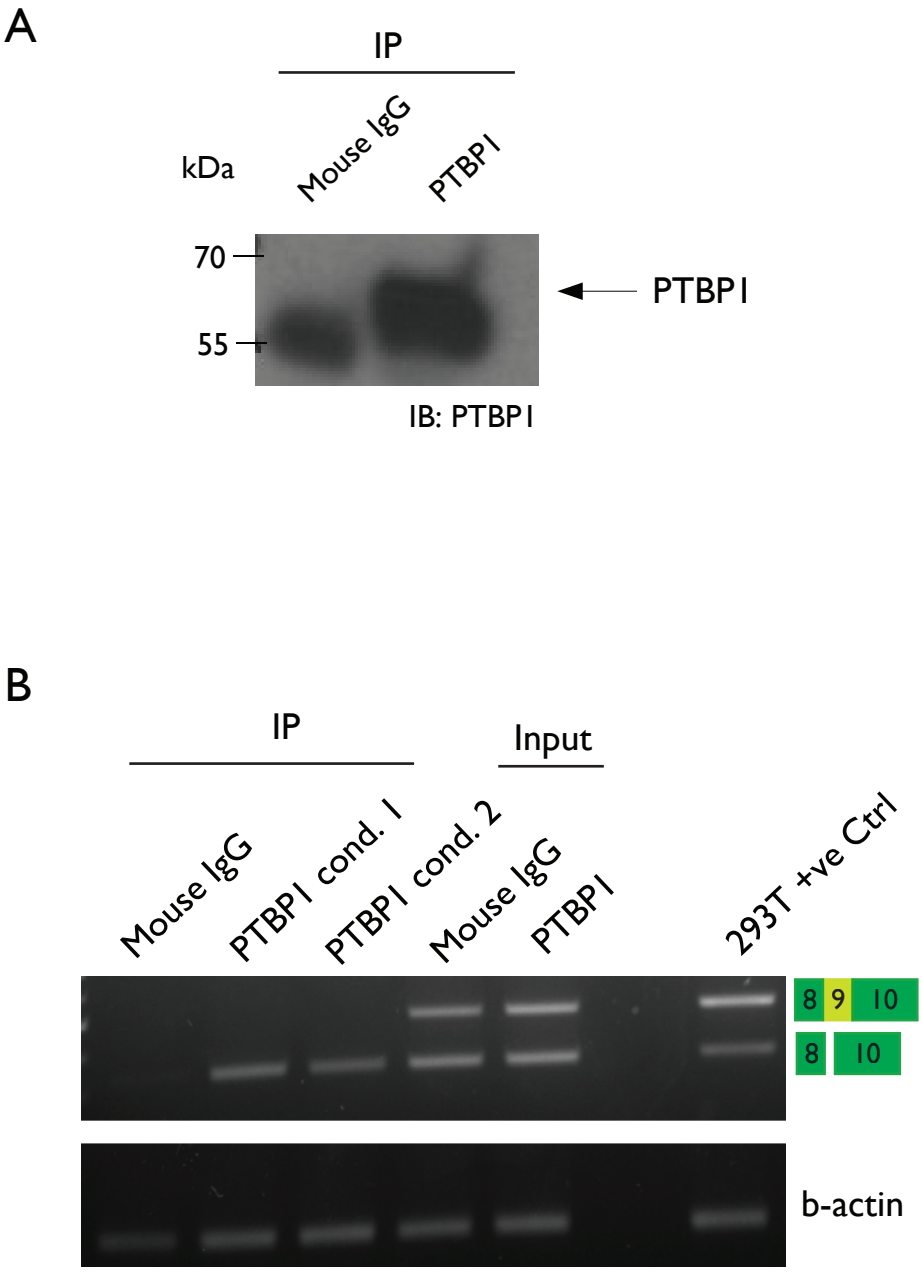
A
IP
kDa
Mouse IgG
PTBP1
70
55
PTBP1
IB: PTBP1
B
IP
Input
Mouse IgG
PTBP1 cond. 1
PTBP1 cond. 2
Mouse IgG
PTBP1
293T +ve Ctrl
8 9 10
8 10
b-actin

Figure 4.2

Figure 4.2. RNA immunoprecipitation of PTBP1 to detect interaction with Numb mRNA isoforms Numb+E9 and NumbΔE9.

(A) Confluent HEK 293T cells were lysed in a polysome lysis buffer and incubated with mouse IgG beads and 5μg of either PTBP1 or mouse IgG antibody for two hours. Beads were either boiled in 2X Laemmli buffer or incubated in Buffer RLT (Qiagen) at room temperature for 5 minutes. Boiled samples were then resolved in a 10% acrylamide gel and Western blotted using a PTBP1 antibody.

(B) RNA was then reverse transcribed and the resulting cDNA underwent semi-quantitative PCR using primers that target exons 8 and 10, respectively. The PCR reactions were then resolved in a 1.5% agarose gel. β-actin was used as a loading control. RNA extracted from pre-IP lysate and parental HEK 293T cells underwent RT-PCR using the same conditions. These reactions were run in the same agarose gel as a positive control.

4.2B). As PTBP1 has been shown to interact with mRNAs to regulate mRNA metabolism and activity (Romanelli, Diani, & Lievens, 2013), our preliminary experiment pointed towards a potential alternative function of PTBP1 in regulating expression of the Numb isoforms independent of AS. Future experiments should further investigate the relationship between PTBP1 and the Numb mRNA isoforms in the context of cancer.

This experiment did not reveal whether PTBP1 interacted with the Numb pre-mRNA to regulate Numb alternative splicing. A future experiment to address this issue would be to immunoprecipitate PTBP1 from whole-cell lysate, and reverse transcribe pre-mRNA bound to PTBP1, followed by PCR using primers that target E9 and an intron flanking E9, respectively. To determine whether any potential interaction between PTBP1 and Numb pre-mRNA is MAPK/ERK signalling-dependent, cells would be treated with either MEK inhibitor U0126 or DMSO vehicle control prior to conducting the RIP assay.

As another approach to investigate splicing factor interaction with the Numb pre-mRNA, we constructed a splicing reporter containing Numb E9 and approximately 500 nucleotides of flanking intron on either side, and then made deletions within the intronic regions of this reporter. We found that deletion of a conserved 183-nucleotide sequence 90 nucleotides upstream of E9 resulted in E9 exclusion (Figure 3.14B, Figure 4.3A). To predict cis-acting motif elements present in the sequence, the sequence was analyzed by the motif prediction programs SFmap (http://sfmap.technion.ac.il) and SpliceAid (http://www.introni.it/splicing.html). The splicing factors predicted to contain putative binding motifs according to both programs are boxed, in Figure 4.3B. Notably, two clusters of PTBP1 binding motifs were identified in the sequence (Figure 4.3C). These data suggest that this specific sequence may be important for promoting E9 inclusion, and further experimentation involving RIP assays and each of the predicted splicing factors would

A

B

Factors Listed by SpliceAid	Factors Listed by Sfmap
NOVA1	NOVA1
HuB	YBX1
TIA-1	PTB
TIAL1	SRp20
hnRNP E2	Tra2Beta
hnRNP K	SRp55
SRp30c	hnRNPU
DAZAP1	MBNL1
HNRNP A1	FOX1
HNRNP A2B1	
YBX1	
HNRNP A0	
HNRNP C	
HNRNP D	
HuR	
Sam68	
PTBP1	
MBNL1	
ETR-3	
SRp20	
HNRNP K	
NOVA2	
Tra2Beta1	
RBM5	

Figure 4.3

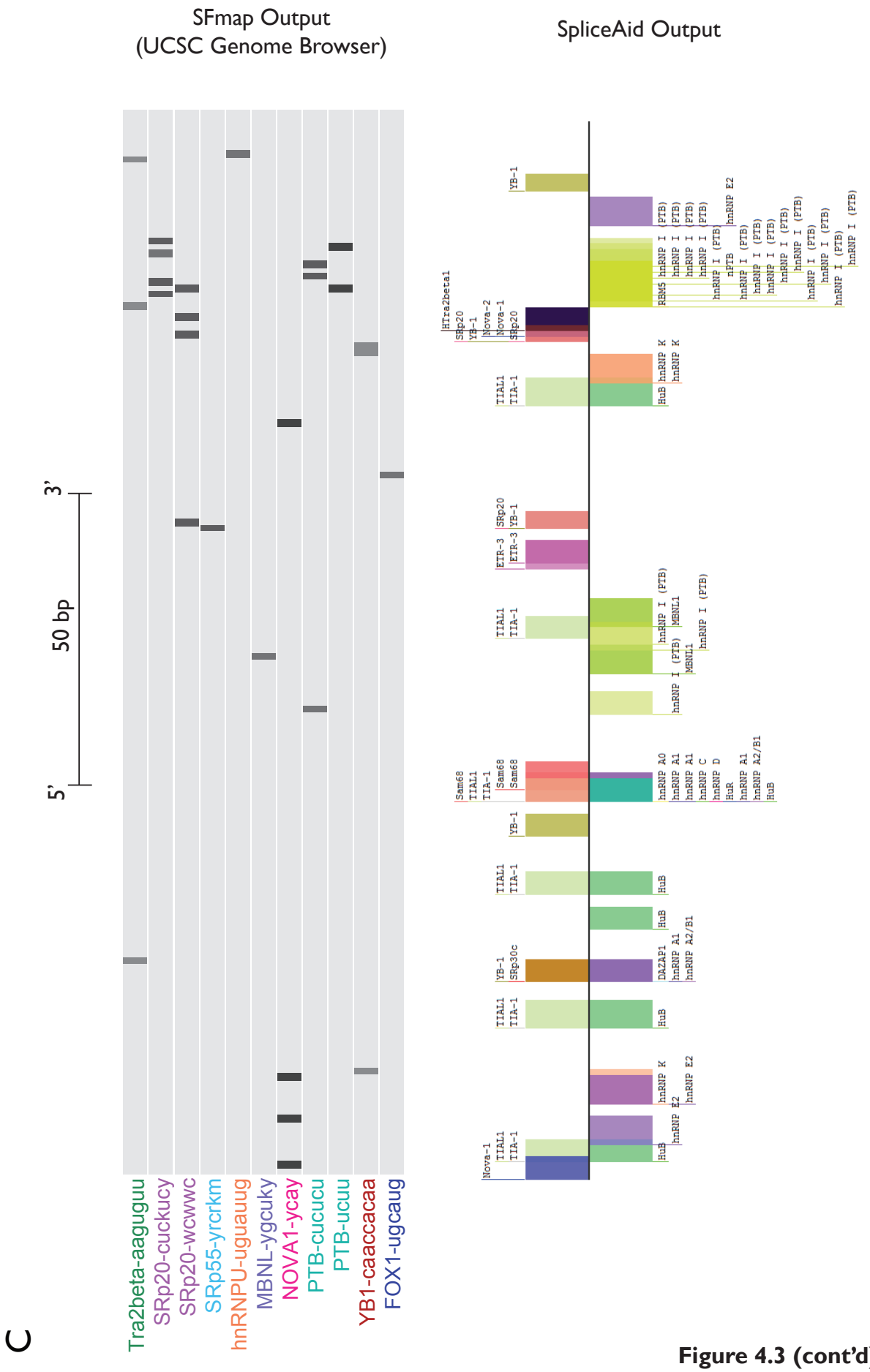

Figure 4.3 (cont'd)

Figure 4.3. Analysis of an 183-nucleotide sequence in the Numb pre-mRNA to identify potential splicing factor regulators of Numb E9 alternative splicing.

(A) A schematic derived from Figure 3.14 describing the 183-nucleotide deletion made in the mutant splicing reporter Del1.

(B) The 183-nucleotide sequence was inputted in both SFmap (http://sfmap.technion.ac.il/) and SpliceAid2 (http://193.206.120.249/splicing_tissue.html), which are freely available computational programs that predict the location of splicing factor motif sequences in a given DNA sequence. Predicted splicing factors that may interact with the sequence are listed according to the program used. The boxed splicing factors are ones that were predicted in both databases.

(C) SFmap and SpliceAid2 mapping of the locations of the binding sites of the splicing factors listed in Figure 4.3B on the human Numb genomic fragment corresponding to the 183-nucleotide sequence. The predicted sites from SFmap were mapped onto the UCSC genome browser as independent tracts for each motif sequence. The predicted sites for SpliceAid2 was mapped in a bar chart format, with positive bars corresponding to positive regulators of exon splicing enhancement, and negative bars corresponding to negative regulators of exon splicing enhancement.

provide us with a better understanding of the specific dynamics between splicing factors and their direct or indirect interactions with the Numb pre-mRNA.

4.6 A Role for ASF/SF2 in the Regulation of Numb E9 Alternative Splicing in Cancer

Our investigations also identified ASF/SF2 as a regulator of Numb E9 alternative splicing, where ASF/SF2 over-expression resulted in near-complete E9 splicing suppression. We found that inhibition of MAPK/ERK signalling in A549 cells resulted in decreased expression of ASF/SF2 transcript expression. ASF/SF2, which functions as an oncoprotein (Karni et al., 2007), is known to be over-expressed in lung adenocarcinoma (Das, Anczuków, Akerman, & Krainer, 2012; R. Guo et al., 2013). Since previous studies show that there are abnormal levels of Numb E9 inclusion in lung adenocarcinoma, and we established that ASF/SF2 over-expression promoted E9 exclusion, we inferred that ASF/SF2 may therefore not play a direct role in regulating E9 AS in cancer. Further work must be done to determine whether ASF/SF2 indirectly plays a role in Numb AS by interacting with other splicing or signalling factors.

4.7 A Role for MAPK/ERK Signalling in Regulating Numb Splicing Networks in Cancer

We identified a novel function for the MAPK/ERK signal transduction pathway as a splicing enhancer of Numb E9 in the lung cancer cell line A549. This finding was in agreement with the fact that MAPK/ERK signalling is highly active in lung adenocarcinoma, as a consequence of activating mutations in EGFR and KRAS that occur in 34% and 20% of tumours, respectively (COSMIC Database). Since there is growing evidence that abnormally increased Numb E9 inclusion is a frequent event in cancer (Langer et al., 2010; Misquitta-Ali et al., 2011; S. Zhang et al., 2014), our results reveal that, *in vivo*, there is likely a positive

relationship between MAPK/ERK pathway activation in cancer and increased Numb E9 inclusion. However, in order to ensure that this observation can be applied broadly to cancer as a whole, analysis of other cancer cell lines that display altered E9 splicing to determine whether MAPK/ERK pathway activation or suppression regulates Numb splicing in other cancer contexts. In addition, primary tumour samples could be used to determine whether there is a correlation between MAPK/ERK signalling and the extent of Numb E9 AS, compared to matched normal control tissue.

Based on our kinase inhibition experiments discussed in Figure 3.6, we were able to establish that inhibition of MEK by the selective inhibitor U0126 suppressed Numb E9 splicing. To specifically identify the players in the MAPK/ERK signalling network that regulate this splicing event, additional kinase inhibition and siRNA experiments could be used to identify what MEK targets are responsible for this effect on Numb splicing.

4.8 Does the MAPK/ERK signalling pathway regulate the activity of Notch signalling in cancer through Numb E9 alternative splicing?

We also identified a relationship between MAPK/ERK signalling pathway activation, Numb E9 AS, and activation of the Notch signalling pathway. The Notch signalling pathway is a highly conserved developmental network that regulates a wide range of cellular functions in multicellular organisms, including the determination of cell fate and the formation of distinct cell populations, cell survival, and proliferation (Bray, 2006; S. Guo, Liu, & Gonzalez-Perez, 2012). Abnormal activation of Notch signalling and upregulation of Notch target genes has been observed in colon (Reedijk et al., 2008), breast (Pece et al., 2004; Stylianou et al., 2006), and lung adenocarcinomas (Maraver et al., 2012; Westhoff et al., 2009). In breast and lung cancer, there is cross-talk between the Notch and MAPK/ERK

signalling pathways, resulting in the promotion of tumour growth and progression, and correlates with a poorer prognosis (Al-Hussaini, Subramanyam, Reedijk, & Sridhar, 2011; Izrailit, Berman, Datti, Wrana, & Reedijk, 2013; Maraver et al., 2012).

The Numb p66 and p72 isoforms have also been shown to differentially regulate Notch signalling in lung adenocarcinoma (Misquitta-Ali et al., 2011). It was shown that, while the p66 isoform is capable of suppressing Notch signalling through decreased Notch target gene expression, the p72 isoform is capable of activating Notch signalling through increased Notch target gene expression, but only in the presence of p66, suggesting that p72 disinhibits the suppressive ability of p66 (Misquitta-Ali et al., 2011). We were able to establish that, when MAPK/ERK signalling was suppressed in A549 cells, Numb E9 splicing is silenced, and expression of Notch target genes Hey1 and Hey2 is downregulated, which agrees with this model. However, we did not determine whether the correlation between MAPK/ERK signalling inhibition and the downregulation of Hey1 and Hey2 expression was dependent on Numb E9 AS. To further understand this relationship, one approach would be to ectopically express the p72 isoform after inhibition of MAPK/ERK signalling to determine whether over-expression of p72 rescues the effect of MEK inhibition on Notch signalling inhibition.

Though it has been established that Notch signalling is activated in lung adenocarcinomas and contributes to tumour development, conflicting evidence suggests that Notch signalling activation may inhibit tumour growth in A549 cells (Zheng et al., 2007). Our studies did not directly assess Notch signalling activity in A549 cells. Therefore, further experiments are required to demonstrate that Hes and Hey expression is under the control of Notch signalling within these cells. One way to assess this would be to treat A549 cells with the γ-secretase inhibitor DAPT to suppress Notch signalling, to determine the effects of

Notch signalling inhibition on Hes and Hey transcript expression. In addition, to identify whether Notch signalling and MAPK/ERK signalling were components of the same pathway, we would also treat cells with DAPT in addition to U0126, and detect whether there was an additive effect on decreased Notch target gene expression compared to treating cells with each compound alone.

4.9 Identifying other Splicing Factors and Signalling Pathways that Regulate Numb E9 AS in Cancer

Several recent studies have identified additional splicing factors that regulate Numb E9 alternative splicing. Bechara et al. (2013) identified the homologs RBM5, RBM6 and RBM10 as regulators of Numb E9 AS. These three splicing factors are members of a family of SR-like proteins that, when over-expressed, promote cell apoptosis and act as inhibitors of tumour growth (Bechara, Sebestyén, Bernardis, Eyras, & Valcárcel, 2013; Shu et al., 2007). The genes that code for these programs are also frequently mutated in a variety of cancers, resulting in downregulated protein expression (Bechara et al., 2013). The study found that over-expression of each of the three splicing factors resulted in Numb E9 exclusion. In addition, RBM10 was found to contain an inactivating mutation in both lung and breast adenocarcinoma tumour samples. Inactivation of RBM10 function either by over-expression of an inactive mutant or by knock-down of the wild-type protein in lung and breast cancer cell lines promoted E9 exclusion, increased Notch pathway activity, and suppressed cell proliferation. They proposed that inhibited expression and function of these three splicing factors resulted in increased Numb E9 inclusion, resulting in activation of Notch target signalling and the promotion of tumour progression.

Another study by Zong et al. (2014) identified the RNA-binding protein QK-1, a

member of the STAR family of splicing factors, as a promoter of E9 exclusion. They also found that QK-1 expression was downregulated in lung adenocarcinoma, resulting in Numb E9 splicing enhancement, activation of Notch signalling, and increased proliferation of tumour cells (Zong et al., 2014).

We have been interested in studying other splicing factors that may regulate Numb E9 AS, particularly those that have a clear link to MAPK/ERK signalling. The oncoprotein Sam68 (Vogel and Richard, 2012), another member of the STAR family of proteins, is one such candidate. Sam68 is frequently over-expressed in breast and prostate carcinomas, and its expression is generally correlated with a poorer prognosis for these cancers (Busà et al., 2007; Song et al., 2010; Vogel & Richard, 2012). In addition, Sam68 plays a very important role in neuronal development, through the regulation of several pro-neuronal alternative splicing events (Vogel & Richard, 2012). Finally, the mechanism of Sam68 activation by signalling pathways is well-documented: it is phosphorylated on a serine site (S20) by the CaMK pathway in response to neuronal depolarization (Iijima et al., 2011), on S58, T71, and T84 by MAPK/ERK signalling in activated T-cells (Matter et al., 2002), and on Y20 by Fyn in HEK 293T cells (Paronetto et al., 2007). Future studies in the lab will investigate the role of Sam68 in mediating MAPK/ERK signalling effects on Numb E9 AS.

In our study, we tested whether two common signalling pathways activated in both lung and breast adenocarcinoma, MAPK/ERK signalling and PI3K/Akt signalling, regulate Numb E9 alternative splicing. However, it is likely that other signalling pathways might regulate AS of Numb. For example, the Wnt/β-catenin signalling pathway has been shown to be highly active in a large number of cancers (Anastas & Moon, 2013). To test if Wnt signalling affects Numb AS, we treated HEK 293T cells with exogenous Wnt3a ligand to activate the Wnt/β-catenin signalling pathway. However, our results were inconclusive, partly

due to inconsistencies between experiments and an inability to confirm that Wnt3a ligand treatment promoted Wnt signalling. To identify additional pathways that regulate Numb E9 AS, a screen based on a panel of kinase inhibitors could be performed using A549 lung adenocarcinoma cells, followed by qRT-PCR, in order to identify whether inhibiting a pathway alters the endogenous Numb E9 AS profile. Alternatively, cells can be stably transfected with our full-length Numb alternative splicing reporter prior to performing the screen, in order to identify whether inhibiting a pathway alters the reporter Numb E9 AS profile.

4.10 Conclusion

There is substantial evidence that misregulation of AS is a frequent event that can contribute to the development of cancer. Previous studies have identified abnormal levels of Numb exon 9 (E9) inclusion in lung, breast and colon cancer, resulting in increased production of the Numb+E9 transcript and the p72 protein isoform in tumours. However, the mechanism by which this occurs and the consequences to lung cancer development had not been elucidated. We have shown that Numb E9 splicing is regulated by MAPK/ERK signalling, consistent with MAPK/ERK signalling activation and increased Numb E9 inclusion in cancer. In addition, we identified PTBP1 as a splicing enhancer of Numb E9, though we could not clearly establish whether PTBP1 function was regulated by MAPK/ERK signalling. Finally, we identified a correlative relationship between MAPK/ERK signalling inhibition, Numb E9 exclusion, and Notch target gene expression. Based on these results we propose a model in which, in cancer cells, activating mutations that result in increased MAPK/ERK signalling results in phosphorylation events that increase the activity of PTBP1, leading to its direct or indirect interaction with the Numb pre-mRNA,

resulting in E9 inclusion. One consequence of increased E9 inclusion and p72 protein expression is the upregulation of Notch signalling, resulting in increased tumour growth and invasiveness (Figure 4.4). Further evidence that PTBP1 is the mediating factor between MAPK/ERK signalling and Numb E9 AS is required in order to support this model.

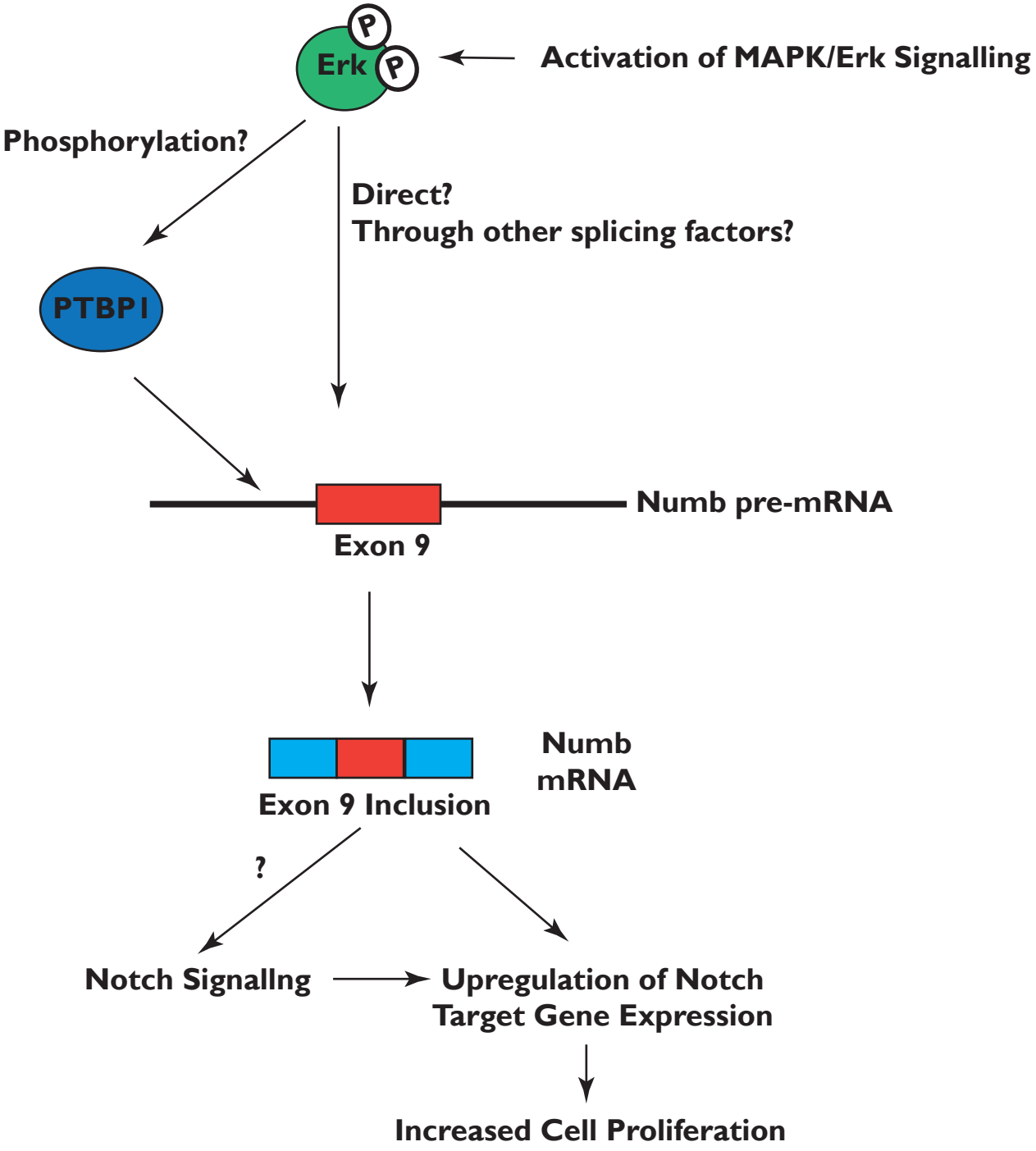
P
Erk
P
Activation of MAPK/Erk Signalling
Phosphorylation?
Direct?
Through other splicing factors?
PTBP1
Numb pre-mRNA
Exon 9
Numb
mRNA
Exon 9 Inclusion
?
Notch Signalling
Upregulation of Notch
Target Gene Expression
Increased Cell Proliferation

Figure 4.4

Figure 4.4. A proposed model for Numb E9 alternative splicing by the MAPK/ERK signalling in cancer.

Activation of MAPK/ERK signalling, resulting in the phosphorylation of ERK1/2, can either regulate Numb E9 alternative splicing either by activating PTBP1 (possibly by a post-translational event such as phosphorylation) or by promoting the activity of other unidentified splicing factors. The resulting increase in exon inclusion results in upregulation of Notch target genes Hes and Hey, which may occur due to the activation of the Notch signalling pathway. This can result in increased cell proliferation.

BIBLIOGRAPHY

Al-Hussaini, H., Subramanyam, D., Reedijk, M., & Sridhar, S. S. (2011). Notch signaling pathway as a therapeutic target in breast cancer. *Molecular Cancer Therapeutics*, *10*(1), 9–15. doi:10.1158/1535-7163.MCT-10-0677

Altomare, D. A., & Testa, J. R. (2005). Perturbations of the AKT signaling pathway in human cancer. *Oncogene*, *24*(50), 7455–64. doi:10.1038/sj.onc.1209085

Anastas, J. N., & Moon, R. T. (2013). WNT signalling pathways as therapeutic targets in cancer. *Nature Reviews Cancer*, *13*(1), 11–26. doi:10.1038/nrc3419

Bani-Yaghoub, M., Kubu, C. J., Cowling, R., Rochira, J., Nikopoulos, G. N., Bellum, S., & Verdi, J. M. (2007). A switch in numb isoforms is a critical step in cortical development. *Developmental Dynamics*, *236*(3), 696–705. doi:10.1002/dvdy.21072

Bechara, E. G., Sebestyén, E., Bernardis, I., Eyras, E., & Valcárcel, J. (2013). RBM5, 6, and 10 differentially regulate NUMB alternative splicing to control cancer cell proliferation. *Molecular Cell*, *52*(5), 720–33. doi:10.1016/j.molcel.2013.11.010

Bielli, P., Busà, R., Paronetto, M. P., & Sette, C. (2011). The RNA-binding protein Sam68 is a multifunctional player in human cancer. *Endocrine-Related Cancer*, *18*(4), R91–R102. doi:10.1530/ERC-11-0041

Bissell, M. J., & Labarge, M. A. (2005). Context, tissue plasticity, and cancer: are tumor stem cells also regulated by the microenvironment? *Cancer Cell*, *7*(1), 17–23. doi:10.1016/j.ccr.2004.12.013

Blaustein, M., Pelisch, F., & Srebrow, A. (2007). Signals, pathways and splicing regulation. *The International Journal of Biochemistry & Cell Biology*, *39*(11), 2031–48. doi:10.1016/j.biocel.2007.04.004

Bray, S. J. (2006). Notch signalling: a simple pathway becomes complex. *Nature Reviews Molecular Cell Biology*, *7*(9), 678–89. doi:10.1038/nrm2009

Brognard, J., Clark, A. S., Ni, Y., & Dennis, P. A. (2001). Akt/Protein Kinase B is constitutively active in non-small cell lung cancer and promotes cellular survival and resistance to chemotherapy and radiation. *Cancer Research*, *61*, 3986–3997.

Busà, R., Paronetto, M. P., Farini, D., Pierantozzi, E., Botti, F., Angelini, D. F., Attisani, F., Vespasiani, G., & Sette, C. (2007). The RNA-binding protein Sam68 contributes to proliferation and survival of human prostate cancer cells. *Oncogene*, *26*(30), 4372–82. doi:10.1038/sj.onc.1210224

Busch, A., & Hertel, K. J. (2012). Evolution of SR protein and hnRNP splicing regulatory factors. *Wiley Interdisciplinary Reviews RNA*, *3*(1), 1–12. doi:10.1002/wrna.100

Carpenter, B., MacKay, C., Alnabulsi, A., MacKay, M., Telfer, C., Melvin, W. T., & Murray, G. I. (2006). The roles of heterogeneous nuclear ribonucleoproteins in tumour development and progression. *Biochimica et Biophysica Acta*, *1765*(2), 85–100. doi:10.1016/j.bbcan.2005.10.002

Carter, S., & Vousden, K. H. (2008). A role for Numb in p53 stabilization. *Genome Biology*,

9(5), 221. doi:10.1186/gb-2008-9-5-221

Casanova, J. E. (2007). PARtitioning Numb. *EMBO Reports*, *8*(3), 233–235.

Chen, M., & Manley, J. L. (2009). Mechanisms of alternative splicing regulation: insights from molecular and genomics approaches. *Nature Reviews Molecular Cell Biology*, *10*(11), 741–754. doi:10.1038/nrm2777.Mechanisms

Cheung, H. C., Corley, L. J., Fuller, G. N., McCutcheon, I. E., & Cote, G. J. (2006). Polypyrimidine tract binding protein and Notch1 are independently re-expressed in glioma. *Modern Pathology*, *19*(8), 1034–41. doi:10.1038/modpathol.3800635

Cheung, H. C., Hai, T., Zhu, W., Baggerly, K. a, Tsavachidis, S., Krahe, R., & Cote, G. J. (2009). Splicing factors PTBP1 and PTBP2 promote proliferation and migration of glioma cell lines. *Brain*, *132*, 2277–88. doi:10.1093/brain/awp153

Christofk, H. R., Vander Heiden, M. G., Harris, M. H., Ramanathan, A., Gerszten, R. E., Wei, R., Fleming, M. D., Schreiber, S. L., & Cantley, L. C. (2008). The M2 splice isoform of pyruvate kinase is important for cancer metabolism and tumour growth. *Nature*, *452*(7184), 230–3. doi:10.1038/nature06734

Colaluca, I. N., Tosoni, D., Nuciforo, P., Senic-Matuglia, F., Galimberti, V., Viale, G., Pece, S., & Di Fiore, P. P. (2008). NUMB controls p53 tumour suppressor activity. *Nature*, *451*(7174), 76–80. doi:10.1038/nature06412

Cooper, T. A., Wan, L., & Dreyfuss, G. (2009). RNA and disease. *Cell*, *136*(4), 777–793.

Das, S., Anczuków, O., Akerman, M., & Krainer, A. R. (2012). Oncogenic splicing factor SRSF1 is a critical transcriptional target of MYC. *Cell Reports*, *1*(2), 110–7. doi:10.1016/j.celrep.2011.12.001

David, C. J., & Manley, J. L. (2010). Alternative pre-mRNA splicing regulation in cancer: pathways and programs unhinged. *Genes & Development*, *24*(21), 2343–64. doi:10.1101/gad.1973010

Dhami, G. K., Liu, H., Galka, M., Voss, C., Wei, R., Muranko, K., Kaneko, T., Cregan, S. P., Li, L., & Li, S. S.-C. (2013). Dynamic methylation of Numb by Set8 regulates its binding to p53 and apoptosis. *Molecular Cell*, *50*(4), 565–76. doi:10.1016/j.molcel.2013.04.028

Dhillon, A S., Hagan, S., Rath, O., & Kolch, W. (2007). MAP kinase signalling pathways in cancer. *Oncogene*, *26*(22), 3279–90. doi:10.1038/sj.onc.1210421

Dho, S. E., French, M. B., Woods, S. A., & McGlade, C. J. (1999). Characterization of four mammalian Numb protein isoforms. *The Journal of Biological Chemistry*, *274*(46), 33097–33104.

Dho, S. E., Trejo, J., Siderovski, D. P., & McGlade, C. J. (2006). Dynamic regulation of mammalian Numb by G protein-coupled receptors and protein kinase C activation: Structural determinants of Numb association with the cortical membrane. *Molecular Biology of the Cell*, *17*, 4142–4155. doi:10.1091/mbc.E06

Di Marcotullio, L., Ferretti, E., Greco, A., De Smaele, E., Po, A., Sico, M. A., Alimandi, M., Giannini, G., Maroder, M., Screpanti, I., & Gulino, A. (2006). Numb is a suppressor of Hedgehog signalling and targets Gli1 for Itch-dependent ubiquitination. *Nature Cell*

Biology, *8*(12), 1415–23. doi:10.1038/ncb1510

Dooley, C. M., James, J., McGlade, C. J., & Ahmad, I. (2003). Involvement of numb in vertebrate retinal development: evidence for multiple roles of numb in neural differentiation and maturation. *Journal of Neurobiology*, *54*(2), 313–25. doi:10.1002/neu.10176

Encinas, M., Iglesias, M., Liu, Y., Wang, H., Muhaisen, A., Ceña, V., Gallego, C., & Comella, J. X. (2000). Sequential treatment of SH-SY5Y cells with retinoic acid and brain-derived neurotrophic factor gives rise to fully differentiated, neurotrophic factor-dependent, human neuron-like cells. *Journal of Neurochemistry*, *75*(3), 991–1003. Retrieved from http://www.ncbi.nlm.nih.gov/pubmed/10936180

Engelman, J. A. (2009). Targeting PI3K signalling in cancer: opportunities, challenges and limitations. *Nature Reviews Cancer*, *9*(8), 550–62. doi:10.1038/nrc2664

Farnebo, M., Bykov, V. J. N., & Wiman, K. G. (2010). The p53 tumor suppressor: a master regulator of diverse cellular processes and therapeutic target in cancer. *Biochemical and Biophysical Research Communications*, *396*(1), 85–9. doi:10.1016/j.bbrc.2010.02.152

Friday, B. B., & Adjei, A. A. (2008). Advances in targeting the Ras/Raf/MEK/Erk mitogen-activated protein kinase cascade with MEK inhibitors for cancer therapy. *Clinical Cancer Research*, *14*(2), 342–6. doi:10.1158/1078-0432.CCR-07-4790

Gazel, A., Nijhawan, R. I., Walsh, R., & Blumenberg, M. (2008). Transcriptional profiling defines the roles of ERK and p38 kinases in epidermal keratinocytes. *Journal of Cellular Physiology*, *215*(2), 292–308. doi:10.1002/jcp.21394

Ghigna, C., Valacca, C., & Biamonti, G. (2008). Alternative splicing and tumor progression. *Current Genomics*, *9*(8), 556–70. doi:10.2174/138920208786847971

Gonçalves, V., Henriques, A., Pereira, J., Costa, A. N., Moyer, M. P., Moita, L. F., Gama-Carvalho, M., Matos, P., & Jordan, P. (2014). Phosphorylation of SRSF1 by SRPK1 regulates alternative splicing of tumor-related Rac1b in colorectal cells. *RNA*, *20*(4), 474–482. doi:10.1261/rna.041376.113.6

Gonçalves, V., Matos, P., & Jordan, P. (2009). Antagonistic SR proteins regulate alternative splicing of tumor-related Rac1b downstream of the PI3-kinase and Wnt pathways. *Human Molecular Genetics*, *18*(19), 3696–707. doi:10.1093/hmg/ddp317

Grosso, A. R., Gomes, A. Q., Barbosa-Morais, N. L., Caldeira, S., Thorne, N. P., Grech, G., von Lindern, M., & Carmo-Fonseca, M. (2008). Tissue-specific splicing factor gene expression signatures. *Nucleic Acids Research*, *36*(15), 4823–32. doi:10.1093/nar/gkn463

Grosso, A. R., Martins, S., & Carmo-Fonseca, M. (2008). The emerging role of splicing factors in cancer. *EMBO Reports*, *9*(11), 1087–93. doi:10.1038/embor.2008.189

Guo, R., Li, Y., Ning, J., Sun, D., Lin, L., & Liu, X. (2013). HnRNP A1/A2 and SF2/ASF regulate alternative splicing of interferon regulatory factor-3 and affect immunomodulatory functions in human non-small cell lung cancer cells. *PloS ONE*, *8*(4), e62729. doi:10.1371/journal.pone.0062729

Guo, S., Liu, M., & Gonzalez-Perez, R. (2012). Role of Notch and its oncogenic signaling

crosstalk in breast cancer. *Biochimica et Biophysica Acta*, *1815*(2), 197–213. doi:10.1016/j.bbcan.2010.12.002.Role

He, X., Arslan, A. D., Ho, T.-T., Yuan, C., Stampfer, M. R., & Beck, W. T. (2014). Involvement of polypyrimidine tract-binding protein (PTBP1) in maintaining breast cancer cell growth and malignant properties. *Oncogenesis*, *3*(August 2013), e84. doi:10.1038/oncsis.2013.47

He, X., Pool, M., Darcy, K. M., Lim, S. B., Auersperg, N., Coon, J. S., & Beck, W. T. (2007). Knockdown of polypyrimidine tract-binding protein suppresses ovarian tumor cell growth and invasiveness in vitro. *Oncogene*, *26*(34), 4961–8. doi:10.1038/sj.onc.1210307

Henrique, D., & Schweisguth, F. (2003). Cell polarity: the ups and downs of the Par6/aPKC complex. *Current Opinion in Genetics & Development*, *13*(4), 341–350. doi:10.1016/S0959-437X(03)00077-7

Iijima, T., Wu, K., Witte, H., Hanno-Iijima, Y., Glatter, T., Richard, S., & Scheiffele, P. (2011). Sam68 regulates neuronal activity-dependent alternative splicing of neurexin-1. *Cell*, *147*(7), 1601–1614. doi:10.1016/j.cell.2011.11.028.SAM68

Izaguirre, D. I., Zhu, W., Hai, T., Cheung, H. C., Krahe, R., & Cote, G. J. (2012). PTBP1-dependent regulation of USP5 alternative RNA splicing plays a role in glioblastoma tumorigenesis. *Molecular Carcinogenesis*, *51*(11), 895–906. doi:10.1002/mc.20859

Izrailit, J., Berman, H. K., Datti, A., Wrana, J. L., & Reedijk, M. (2013). High throughput kinase inhibitor screens reveal TRB3 and MAPK-ERK/TGFβ pathways as fundamental Notch regulators in breast cancer. *Proceedings of the National Academy of Sciences of the United States of America*, *110*(5), 1714–1719. doi:10.1073/pnas.1214014110/-/DCSupplemental.www.pnas.org/cgi/doi/10.1073/pnas.1214014110

Jain, R., Devine, T., George, A. D., Chittur, S. V, Baroni, T. E., Penalva, L. O., & Tenenbaum, S. A. (2011). RIP-Chip Analysis : RNA-Binding Protein Immunoprecipitation-Microarray (Chip) Profiling. In H. Nielsen (Ed.), *Methods in Molecular Biology* (pp. 247–263). Springer Science+Business Media. doi:10.1007/978-1-59745-248-9

Jiang, X., Xing, H., Kim, T.-M., Jung, Y., Huang, W., Yang, H. W., Song, S., Park, P. J., Carroll, R. S., & Johnson, M. D. (2012). Numb regulates glioma stem cell fate and growth by altering epidermal growth factor receptor and Skp1-Cullin-F-box ubiquitin ligase activity. *Stem Cells*, *30*(7), 1313–26. doi:10.1002/stem.1120

Jones-Villeneuve, E. M., Rudnicki, M. A., Harris, J. F., & McBurney, M. W. (1983). Retinoic acid-induced neural differentiation of embryonal Retinoic Acid-Induced Neural Differentiation of Embryonal Carcinoma Cells. *Molecular and Cellular Biology*, *3*(12), 2271–2279. doi:10.1128/MCB.3.12.2271.Updated

Karaczyn, A., Bani-Yaghoub, M., Tremblay, R., Kubu, C., Cowling, R., Adams, T. L., Prudovsky, I., Spicer, D., Friesel, R., Vary, C., & Verdi, J. M. (2010). Two novel human NUMB isoforms provide a potential link between development and cancer. *Neural Development*, *5*(1), 31. doi:10.1186/1749-8104-5-31

Karni, R., de Stanchina, E., Lowe, S. W., Sinha, R., Mu, D., & Krainer, A. R. (2007). The

gene encoding the splicing factor SF2/ASF is a proto-oncogene. *Nature Structural & Molecular Biology*, *14*(3), 185–93. doi:10.1038/nsmb1209

Kayahara, M., Wang, X., & Tournier, C. (2005). Selective regulation of c-jun gene expression by mitogen-activated protein kinases via the 12-O-tetradecanoylphorbol-13-acetate-responsive element and myocyte enhancer factor 2 binding sites. *Molecular and Cellular Biology*, *25*(9), 3784–3792. doi:10.1128/MCB.25.9.3784

Kim, K. K., Nam, J., Mukouyama, Y.-S., & Kawamoto, S. (2013). Rbfox3-regulated alternative splicing of Numb promotes neuronal differentiation during development. *The Journal of Cell Biology*, *200*(4), 443–58. doi:10.1083/jcb.201206146

Knoblich, J. A. (2008). Mechanisms of asymmetric stem cell division. *Cell*, *132*(4), 583–97. doi:10.1016/j.cell.2008.02.007

Komatsu, M., Kominami, E., Arahata, K., & Tsukahara, T. (1999). Cloning and characterization of two neural-salient serine/arginine-rich (NSSR) proteins involved in the regulation of alternative splicing in neurones. *Genes to Cells*, *4*(10), 593–606. Retrieved from http://www.ncbi.nlm.nih.gov/pubmed/10583508

Krieger, J. R., Taylor, P., Gajadhar, A. S., Guha, A., Moran, M. F., & McGlade, C. J. (2013). Identification and SRM quantification of endocytosis factors associated with Numb. *Molecular and Cellular Proteomics*, *12*(2), 499-514.

Kyriazis, G. A., Wei, Z., Vandermey, M., Jo, D.-G., Xin, O., Mattson, M. P., & Chan, S. L. (2008). Numb endocytic adapter proteins regulate the transport and processing of the amyloid precursor protein in an isoform-dependent manner: implications for Alzheimer disease pathogenesis. *The Journal of Biological Chemistry*, *283*(37), 25492–502. doi:10.1074/jbc.M802072200

Langer, W., Sohler, F., Leder, G., Beckmann, G., Seidel, H., Gröne, J., Hummel, M., & Sommer, A. (2010). Exon array analysis using re-defined probe sets results in reliable identification of alternatively spliced genes in non-small cell lung cancer. *BMC Genomics*, *11*(1), 676. doi:10.1186/1471-2164-11-676

Lau, K. M., & McGlade, C. J. (2011). Numb is a negative regulator of HGF dependent cell scattering and Rac1 activation. *Experimental Cell Research*, *317*(4), 539–51. doi:10.1016/j.yexcr.2010.12.005

Li, Q., Lee, J.-A., & Black, D. L. (2007). Neuronal regulation of alternative pre-mRNA splicing. *Nature Reviews Neuroscience*, *8*(11), 819–31. doi:10.1038/nrn2237

Licatalosi, D. D., Yano, M., Fak, J. J., Mele, A., Grabinski, S. E., Zhang, C., & Darnell, R. B. (2012). Ptbp2 represses adult-specific splicing to regulate the generation of neuronal precursors in the embryonic brain. *Genes & Development*, *26*(14), 1626–42. doi:10.1101/gad.191338.112

Lin, S., Wang, M. J., & Tseng, K.-Y. (2013). Polypyrimidine tract-binding protein induces p19(Ink4d) expression and inhibits the proliferation of H1299 cells. *PloS ONE*, *8*(3), e58227. doi:10.1371/journal.pone.0058227

Luo, J., Manning, B. D., & Cantley, L. C. (2003). Targeting the PI3K-Akt pathway in human cancer: Rationale and promise. *Cancer Cell*, *4*(October), 257–262.

Lynch, K. W. (2007). Regulation of Alternative Splicing by Signal Transduction Pathways. In B. Blencowe & B. Graveley (Eds.), *Advances in Experimental Medicine and Biology: Alternative Splicing in the Postgenomic Era* (Book 623., pp. 161–174). Landes Bioscience and Springer Science+Business Media.

Makeyev, E. V, Zhang, J., Carrasco, M. A., & Maniatis, T. (2007). The MicroRNA miR-124 promotes neuronal differentiation by triggering brain-specific alternative pre-mRNA splicing. *Molecular Cell*, *27*(3), 435–48. doi:10.1016/j.molcel.2007.07.015

Maraver, A., Fernandez-Marcos, P. J., Herranz, D., Cañamero, M., Muñoz-Martin, M., Gómez-López, G., Mulero, F., Megias, D., Sanchez-Carbayo, M., Shen, J., Sanchez-Cespedes, M., Palomero, T., Ferrando, A., & Serrano, M. (2012). Therapeutic effect of γ-secretase inhibition in KrasG12V-driven non-small cell lung carcinoma by derepression of DUSP1 and inhibition of ERK. *Cancer Cell*, *22*(2), 222–34. doi:10.1016/j.ccr.2012.06.014

Matter, N., Herrlich, P., & Konig, H. (2002). Signal-dependent regulation of splicing via phosphorylation of Sam68. *Nature*, *420*, 691–695.

McCutcheon, I. E., Hentschel, S. J., Fuller, G. N., Jin, W., & Cote, G. J. (2004). Expression of the splicing regulator polypyrimidine tract-binding protein in normal and neoplastic brain. *Neuro-Oncology*, *6*(1), 9–14. doi:10.1215/S1152

McGill, M. A., Dho, S. E., Weinmaster, G., & McGlade, C. J. (2009). Numb regulates post-endocytic trafficking and degradation of Notch1. *The Journal of Biological Chemistry*, *284*(39), 26427–26438. doi:10.1074/jbc.M109.014845

Michelle, L., Barbier, J., & Chabot, B. (2012). hnRNP and hnRNP-like proteins in splicing control: Molecular mechanisms and implication in human pathologies. In Z. J. Lorkovic (Ed.), *RNA Binding Proteins* (pp. 1–26).

Miller, W., Rosenbloom, K., Hardison, R. C., Hou, M., Taylor, J., Raney, B., … Kent, W. J. (2007). 28-way vertebrate alignment and conservation track in the UCSC Genome Browser. *Genome Research*, *17*, 1797–808. doi:10.1101/gr.6761107

Misquitta-Ali, C. M., Cheng, E., O'Hanlon, D., Liu, N., McGlade, C. J., Tsao, M. S., & Blencowe, B. J. (2011). Global Profiling and Molecular Characterization of Alternative Splicing Events Misregulated in Lung Cancer. *Molecular and Cellular Biology*, *31*(1), 138–150. doi:10.1128/MCB.00709-10

Naro, C., & Sette, C. (2013). Phosphorylation-Mediated Regulation of Alternative Splicing in Cancer. *International Journal of Cell Biology*, *2013*, 151839.

Nelles, D. A., & Yeo, G. W. (2010). Alternative splicing in stem cell self-renewal and differentiation. In E. Meshorer & K. Plath (Eds.), *The Cell Biology of Stem Cells* (pp. 92–104). Landes Bioscience and Springer Science+Business Media.

Nie, J., Li, S. S.-C., & McGlade, C. J. (2004). A novel PTB-PDZ domain interaction mediates isoform-specific ubiquitylation of mammalian Numb. *The Journal of Biological Chemistry*, *279*(20), 20807–15. doi:10.1074/jbc.M311396200

Nie, J., McGill, M. a, Dermer, M., Dho, S. E., Wolting, C. D., & McGlade, C. J. (2002). LNX functions as a RING type E3 ubiquitin ligase that targets the cell fate determinant Numb

for ubiquitin-dependent degradation. *The EMBO Journal*, *21*(1-2), 93–102. doi:10.1093/emboj/21.1.93

Nishimura, T., & Kaibuchi, K. (2007). Numb controls integrin endocytosis for directional cell migration with aPKC and PAR-3. *Developmental Cell*, *13*(1), 15–28. doi:10.1016/j.devcel.2007.05.003

Paronetto, M. P., Achsel, T., Massiello, A., Chalfant, C. E., & Sette, C. (2007). The RNA-binding protein Sam68 modulates the alternative splicing of Bcl-x. *The Journal of Cell Biology*, *176*(7), 929–939. doi:10.1083/jcb.200701005

Paz, I., Akerman, M., Dror, I., Kosti, I., & Mandel-Gutfreund, Y. (2010). SFmap: a web server for motif analysis and prediction of splicing factor binding sites. *Nucleic Acids Research*, *38*(Web Server issue), W281–5. doi:10.1093/nar/gkq444

Pece, S., Serresi, M., Santolini, E., Capra, M., Hulleman, E., Galimberti, V., Zurrida, S., Maisonneuve, P., Viale, G., & Di Fiore, P. P. (2004). Loss of negative regulation by Numb over Notch is relevant to human breast carcinogenesis. *The Journal of Cell Biology*, *167*(2), 215–21. doi:10.1083/jcb.200406140

Pickrell, J. K., Pai, A. A., Gilad, Y., & Pritchard, J. K. (2010). Noisy splicing drives mRNA isoform diversity in human cells. *PLoS Genetics*, *6*(12), e1001236. doi:10.1371/journal.pgen.1001236

Pino, I., Pio, R., Toledo, G., Zabelegui, N., Vicent, S., Rey, N., Lozano, M. D., Torre, W., Garcia-Foncillas, J., & Montuenga, L. M. (2003). Altered patterns of expression of members of the heterogeneous nuclear ribonucleoprotein (hnRNP) family in lung cancer. *Lung Cancer*, *41*(2), 131–143. doi:10.1016/S0169-5002(03)00193-4

Rasin, M.-R., Gazula, V.-R., Breunig, J. J., Kwan, K. Y., Johnson, M. B., Liu-Chen, S., … Sestan, N. (2007). Numb and Numbl are required for maintenance of cadherin-based adhesion and polarity of neural progenitors. *Nature Neuroscience*, *10*(7), 819–27. doi:10.1038/nn1924

Reedijk, M., Odorcic, S., Zhang, H., Chetty, R., Tennert, C., Dickson, B. C., Lockwood, G., Gallinger, S., & Egan, S. E. (2008). Activation of Notch signaling in human colon adenocarcinoma. *International Journal of Oncology*, *33*(6), 1223–1229. doi:10.3892/ijo

Revil, T., Gaffney, D., Dias, C., Majewski, J., & Jerome-Majewska, L. A. (2010). Alternative splicing is frequent during early embryonic development in mouse. *BMC Genomics*, *11*, 399.

Rhyu, M. S., Jan, L. Y., & Jan, Y. N. (1994). Asymmetric Distribution of Numb Protein during Division of the Sensory Organ Precursor Cell Confers Distinct Fates to Daughter Cells. *Cell*, *76*, 477–491.

Roberts, P. J., & Der, C. J. (2007). Targeting the Raf-MEK-ERK mitogen-activated protein kinase cascade for the treatment of cancer. *Oncogene*, *26*(22), 3291–310. doi:10.1038/sj.onc.1210422

Romanelli, M. G., Diani, E., & Lievens, P. M.-J. (2013). New insights into functional roles of the polypyrimidine tract-binding protein. *International Journal of Molecular Sciences*, *14*(11), 22906–22932. doi:10.3390/ijms141122906

Rosenberger, S., De-Castro Arce, J., Langbein, L., Steenbergen, R. D. M., & Rösl, F. (2010). Alternative splicing of human papillomavirus type-16 E6/E6* early mRNA is coupled to EGF signaling via Erk1/2 activation. *Proceedings of the National Academy of Sciences of the United States of America*, *107*(15), 7006–11. doi:10.1073/pnas.1002620107

Salcini, A. E., Confalonieri, S., Doria, M., Santolini, E., Tassi, E., Minenkova, O., Cesarini, G., Pelicci, P. G., & Di Fiore, P. P. (1997). Binding specificity and in vivo targets of the EH domain, a novel protein-protein interaction module. *Genes & Development*, *11*(17), 2239–2249. doi:10.1101/gad.11.17.2239

Sampath, J., Long, P. R., Shepard, R. L., Xia, X., Devanarayan, V., Sandusky, G. E., Perry, W. L., Dantzig, A. H., Williamson, M., Rolfe, M., & Moore, R. E. (2003). Human SPF45, a splicing factor, has limited expression in normal tissues, is overexpressed in many tumors, and can confer a multidrug-resistant phenotype to cells. *American Journal of Pathology*, *163*(5), 1781–90. doi:10.1016/S0002-9440(10)63538-9

Santarpia, L., Lippman, S. M., & El-Naggar, A. K. (2012). Targeting the MAPK-RAS-RAF signaling pathway in cancer therapy. *Expert Opinion on Therapeutic Targets*, *16*(1), 103–19. doi:10.1517/14728222.2011.645805

Santolini, E., Puri, C., Salcini, A. E., Gagliani, M. C., Pelicci, P. G., Tacchetti, C., & Di Fiore, P. P. (2000). Numb is an endocytic protein. *The Journal of Cell Biology*, *151*(6), 1345–52. Retrieved from http://www.pubmedcentral.nih.gov/articlerender.fcgi?artid=2533073&tool=pmcentrez&rendertype=abstract

Saulière, J., Sureau, A., Expert-Bezançon, A., & Marie, J. (2006). The polypyrimidine tract binding protein (PTB) represses splicing of exon 6B from the beta-tropomyosin pre-mRNA by directly interfering with the binding of the U2AF65 subunit. *Molecular and Cellular Biology*, *26*(23), 8755–69. doi:10.1128/MCB.00893-06

Schroeder, R., Barta, A., & Semrad, K. (2004). Strategies for RNA folding and assembly. *Nature Reviews Molecular Cell Biology*, *5*(11), 908–19. doi:10.1038/nrm1497

Shen, Q., Zhong, W., Jan, Y. N., & Temple, S. (2002). Asymmetric Numb distribution is critical for asymmetric cell division of mouse cerebral cortical stem cells and neuroblasts. *Development*, *129*(20), 4843–53. Retrieved from http://www.ncbi.nlm.nih.gov/pubmed/12361975

Sherman, L., Sleeman, J., Dall, P., Hekele, A., Moll, J., Ponta, H., & Herrlich, P. (1996). The CD44 proteins in embryonic development and cancer. *Current Topics in Microbiology and Immunology, 213*(1), 249-69.

Shin, C., & Manley, J. L. (2004). Cell signalling and the control of pre-mRNA splicing. *Nature Reviews Molecular Cell Biology*, *5*(9), 727–38. doi:10.1038/nrm1467

Shu, Y., Rintala-Maki, N. D., Wall, V. E., Wang, K., Goard, C. A., Langdon, C. E., & Sutherland, L. C. (2007). The apoptosis modulator and tumour suppressor protein RBM5 is a phosphoprotein. *Cell Biochemistry and Function*, *25*(6), 643–653. doi:10.1002/cbf

Siegfried, Z., Bonomi, S., Ghigna, C., & Karni, R. (2013). Regulation of the Ras-MAPK and PI3K-mTOR signalling pathways by alternative splicing in cancer. *International Journal of Cell Biology*, *2013*, 568931.

Smith, C. A., Lau, K. M., Rahmani, Z., Dho, S. E., Brothers, G., She, Y. M., Berry, D. M., Bonneil, E., Thibault, P., Schweisguth, F., Le Borgne, R., & McGlade, C. J. (2007). aPKC-mediated phosphorylation regulates asymmetric membrane localization of the cell fate determinant Numb. *EMBO Journal*, *26*(2), 468–480. doi:10.1038/sj.emboj.7601495

Song, L., Wang, L., Li, Y., Xiong, H., Wu, J., Li, J., & Li, M. (2010). Sam68 up-regulation correlates with, and its down-regulation inhibits, proliferation and tumourigenicity of breast cancer cells. *Journal of Pathology*, *222*(3), 227–37. doi:10.1002/path.2751

Soprano, D. R., Teets, B. W., & Soprano, K. J. (2007). Role of retinoic acid in the differentiation of embryonal carcinoma and embryonic stem cells. In G. Litwack (Ed.), *Vitamins and Hormones* (75th ed., Vol. 75, pp. 69–95). Elsevier Inc. doi:10.1016/S0083-6729(06)75003-8

Spellman, R., & Smith, C. W. J. (2006). Novel modes of splicing repression by PTB. *Trends in Biochemical Sciences*, *31*(2), 73–6. doi:10.1016/j.tibs.2005.12.003

Stylianou, S., Clarke, R. B., & Brennan, K. (2006). Aberrant activation of notch signaling in human breast cancer. *Cancer Research*, *66*(3), 1517–1525. doi:10.1158/0008-5472.CAN-05-3054

Takahashi, K., & Yamanaka, S. (2006). Induction of pluripotent stem cells from mouse embryonic and adult fibroblast cultures by defined factors. *Cell*, *126*(4), 663–76. doi:10.1016/j.cell.2006.07.024

Uemura, T., Shepherd, S., Ackerman, L., Jan, L. Y., & Jan, Y. N. (1989). Numb, a gene required in determination of cell fate during sensory organ formation in Drosophila embryos. *Cell, 58*(2), 349-60.

Ule, J., Stefani, G., Mele, A., Ruggiu, M., Wang, X., Taneri, B., Gaasterland, T., Blencowe, B. J., & Darnell, R. B. (2006). An RNA map predicting Nova-dependent splicing regulation. *Nature*, *444*(7119), 580–6. doi:10.1038/nature05304

Verdi, J. M., Bashirullah, A., Goldhawk, D. E., Kubu, C. J., Jamali, M., Meakin, S. O., & Lipshitz, H. D. (1999). Distinct human NUMB isoforms regulate differentiation vs. proliferation in the neuronal lineage. *Proceedings of the National Academy of Sciences of the United States of America*, *96*(18), 10472–10476.

Verdi, J. M., Schmandt, R., Bashirullah, A., Jacob, S., Salvino, R., Craig, C. G., Amgen EST Program, Lipshitz, H. D., & McGlade, C. J. (1996). Mammalian NUMB is an evolutionarily conserved signaling adapter protein that specifies cell fate. *Current Biology*, *6*(9), 1134–1145.

Vogel, G., & Richard, S. (2012). Emerging roles for Sam68 in adipogenesis and neuronal development. *RNA Biology*, *9*(9), 1129–1133.

Vu, N. T., Park, M. A., Shultz, J. C., Goehe, R. W., Hoeferlin, L. A., Shultz, M. D., Smith, S. A., Lynch, K. W., & Chalfant, C. E. (2013). hnRNP U enhances caspase-9 splicing and is modulated by AKT-dependent phosphorylation of hnRNP L. *The Journal of Biological Chemistry*, *288*(12), 8575–84. doi:10.1074/jbc.M112.443333

Wakamatsu, Y., Maynard, T. M., Jones, S. U., & Weston, J. A. (1999). NUMB localizes in the

basal cortex of mitotic avian neuroepithelial cells and modulates neuronal differentiation by binding to NOTCH-1. *Neuron*, *23*(1), 71–81. Retrieved from http://www.ncbi.nlm.nih.gov/pubmed/10402194

Wang, Z., Sandiford, S., Wu, C., & Li, S. S.-C. (2009). Numb regulates cell-cell adhesion and polarity in response to tyrosine kinase signalling. *The EMBO Journal*, *28*(16), 2360–73. doi:10.1038/emboj.2009.190

Ward, A. J., & Cooper, T. A. (2010). The pathobiology of splicing. *Journal of Pathology*, *220*(2), 152–163. doi:10.1002/path

Westhoff, B., Colaluca, I. N., D'Ario, G., Donzelli, M., Tosoni, D., Volorio, S., Pelosi, G., Spaggiari, L., Mazzarol, G., Viale, G., Pece, S., & Di Fiore, P. P. (2009). Alterations of the Notch pathway in lung cancer. *Proceedings of the National Academy of Sciences of the United States of America*, *106*(52), 22293–22298.

Xie, J., Lee, J.-A., Kress, T. L., Mowry, K. L., & Black, D. L. (2003). Protein kinase A phosphorylation modulates transport of the polypyrimidine tract-binding protein. *Proceedings of the National Academy of Sciences of the United States of America*, *100*(15), 8776–8781.

Yang, S.-H., Sharrocks, A. D., & Whitmarsh, A. J. (2013). MAP kinase signalling cascades and transcriptional regulation. *Gene*, *513*(1), 1–13. doi:10.1016/j.gene.2012.10.033

Yeo, G. W., Coufal, N. G., Liang, T. Y., Peng, G. E., Fu, X.-D., & Gage, F. H. (2009). An RNA code for the FOX2 splicing regulator revealed by mapping RNA-protein interactions in stem cells. *Nature Structural & Molecular Biology*, *16*(2), 130–137. doi:10.1038/nsmb.1545

Yeo, G. W., Xu, X., Liang, T. Y., Muotri, A. R., Carson, C. T., Coufal, N. G., & Gage, F. H. (2007). Alternative splicing events identified in human embryonic stem cells and neural progenitors. *PLoS Computational Biology*, *3*(10), e196. doi:10.1371/journal.pcbi.0030196

Yogosawa, S., Miyauchi, Y., Honda, R., Tanaka, H., & Yasuda, H. (2003). Mammalian Numb is a target protein of Mdm2, ubiquitin ligase. *Biochemical and Biophysical Research Communications*, *302*(4), 869–872. doi:10.1016/S0006-291X(03)00282-1

Yoshida, T., Tokunaga, A., Nakao, K., & Okano, H. (2003). Distinct expression patterns of splicing isoforms of mNumb in the endocrine lineage of developing pancreas. *Differentiation*, *71*(8), 486–95. doi:10.1046/j.1432-0436.2003.7108006.x

Zhang, C., Frias, M. A., Mele, A., Ruggiu, M., Eom, T., Marney, C. B., Wang, H., Licatalosi, D. D., Fak, J. J., & Darnell, R. B. (2010). Integrative modeling defines the Nova splicing-regulatory network and its combinatorial controls. *Science*, *329*(5990), 439–443. doi:10.1126/science.1191150

Zhang, S., Liu, Y., Liu, Z., Zhang, C., Cao, H., Ye, Y., Wang, S., Zhang, Y., Xiao, S., Yang, P., Li, J., & Bai, Z. (2014). Transcriptome profiling of a multiple recurrent muscle-invasive urothelial carcinoma of the bladder by deep sequencing. *PLoS ONE*, *9*(3), e91466. doi:10.1371/journal.pone.0091466

Zhang, Z., & Stamm, S. (2011). Analysis of mutations that influence pre-mRNA splicing. In

H. Nielsen (Ed.), *Methods in Molecular Biology* (703rd ed., Vol. 703, pp. 137–160). Totowa, NJ: Humana Press. doi:10.1007/978-1-59745-248-9

Zheng, Q., Qin, H., Zhang, H., Li, J., Hou, L., Wang, H., Zhang, X., Zhang, S., Feng, L., Liang, Y., Han, H., & Yi, D. (2007). Notch signaling inhibits growth of the human lung adenocarcinoma cell line A549. *Oncology Reports*, *17*(12), 847–852.

Zhong, W., Feder, J. N., Jiang, M.-M., Jan, L. Y., & Jan, Y. N. (1996). Asymmetric localization of a mammalian numb homolog during mouse cortical neurogenesis. *Neuron*, *17*(1), 43–53.

Zhong, W., Jiang, M. M., Schonemann, M. D., Meneses, J. J., Pedersen, R. A, Jan, L. Y., & Jan, Y. N. (2000). Mouse numb is an essential gene involved in cortical neurogenesis. *Proceedings of the National Academy of Sciences of the United States of America*, *97*(12), 6844–9. Retrieved from http://www.pubmedcentral.nih.gov/articlerender.fcgi?artid=18761&tool=pmcentrez&rendertype=abstract

Zilian, O., Saner, C., Hagedorn, L., Lee, H. Y., Säuberli, E., Suter, U., Sommer, L., & Aguet, M. (2001). Multiple roles of mouse Numb in tuning developmental cell fates. *Current Biology*, *11*(7), 494–501. Retrieved from http://www.ncbi.nlm.nih.gov/pubmed/11412999

Zong, F.-Y., Fu, X., Wei, W.-J., Luo, Y.-G., Heiner, M., Cao, L.-J., Fang, Z., Fang, R., Lu, D., Ji, H., & Hui, J. (2014). The RNA-binding protein QK1 suppresses cancer-associated aberrant splicing. *PLoS Genetics*, *10*(4), e1004289. doi:10.1371/journal.pgen.1004289